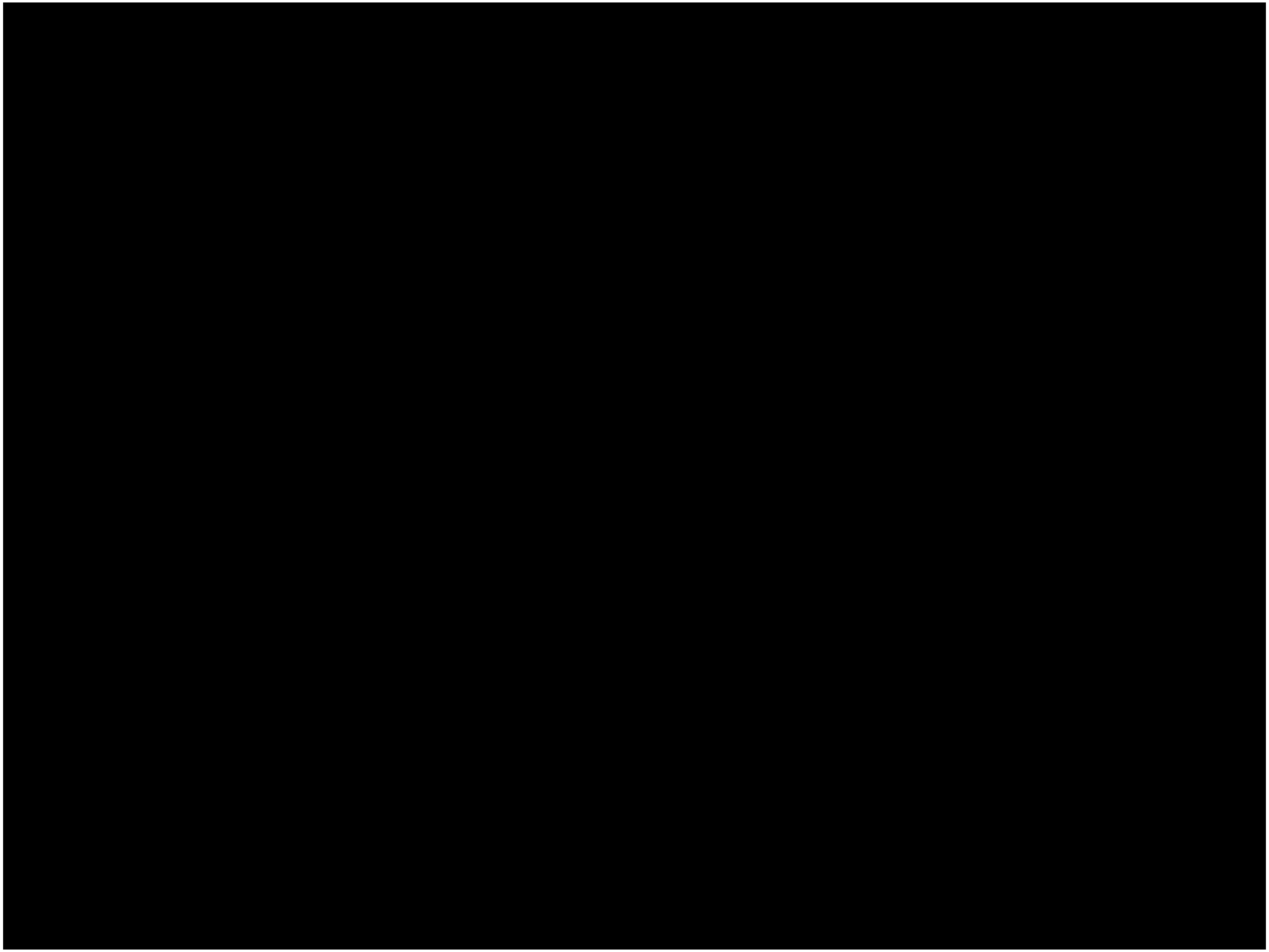




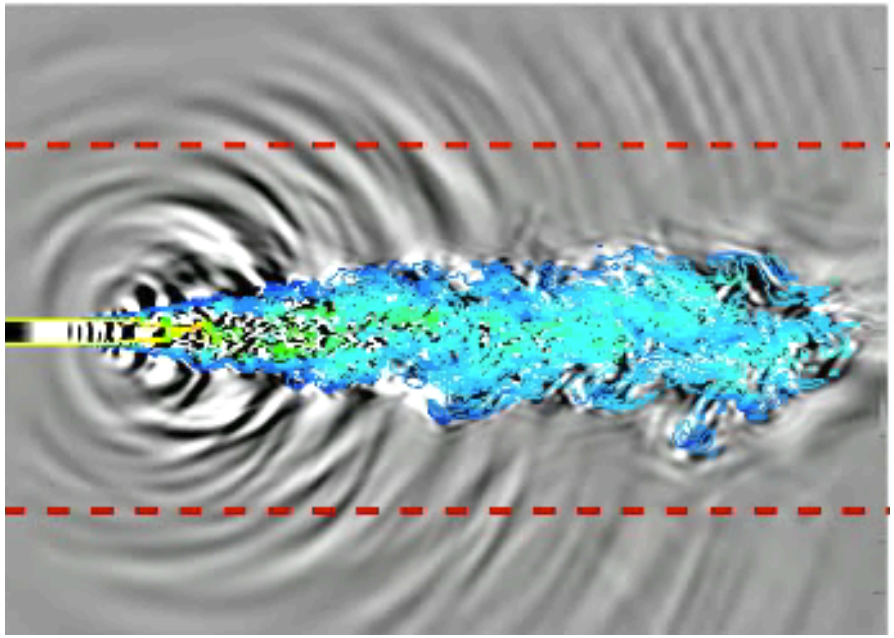
Advanced Modeling and Simulation (AMS) Seminar Series
NASA Ames Research Center, Dec 15, 2020



Active control strategies for compressible and multiphase flows

Mahesh Natarajan

High-Performance Algorithms and Complex Fluids (HPACF)
Computational Science Center
National Renewable Energy Laboratory
Golden, CO 80401

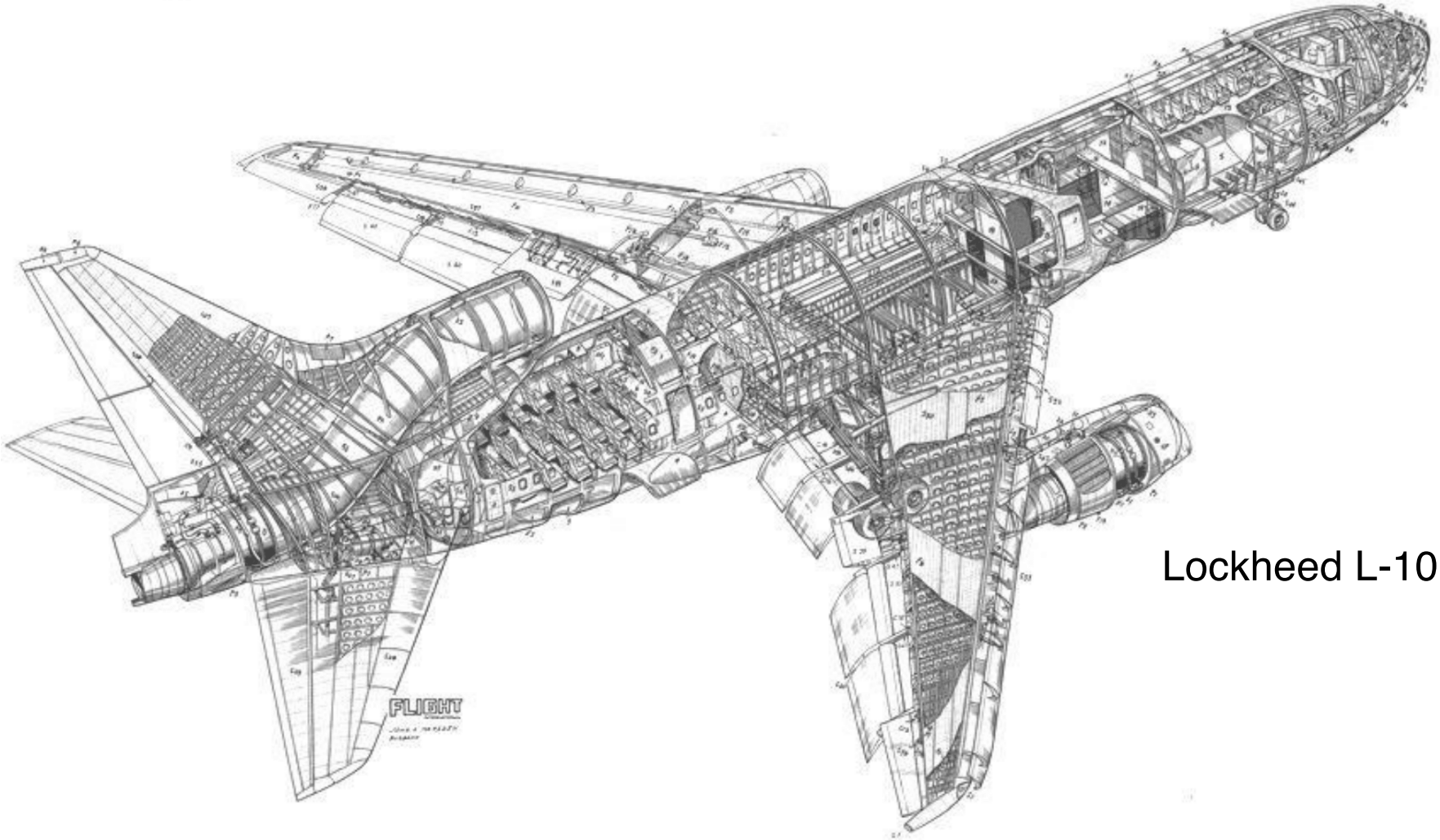


Biographical sketch



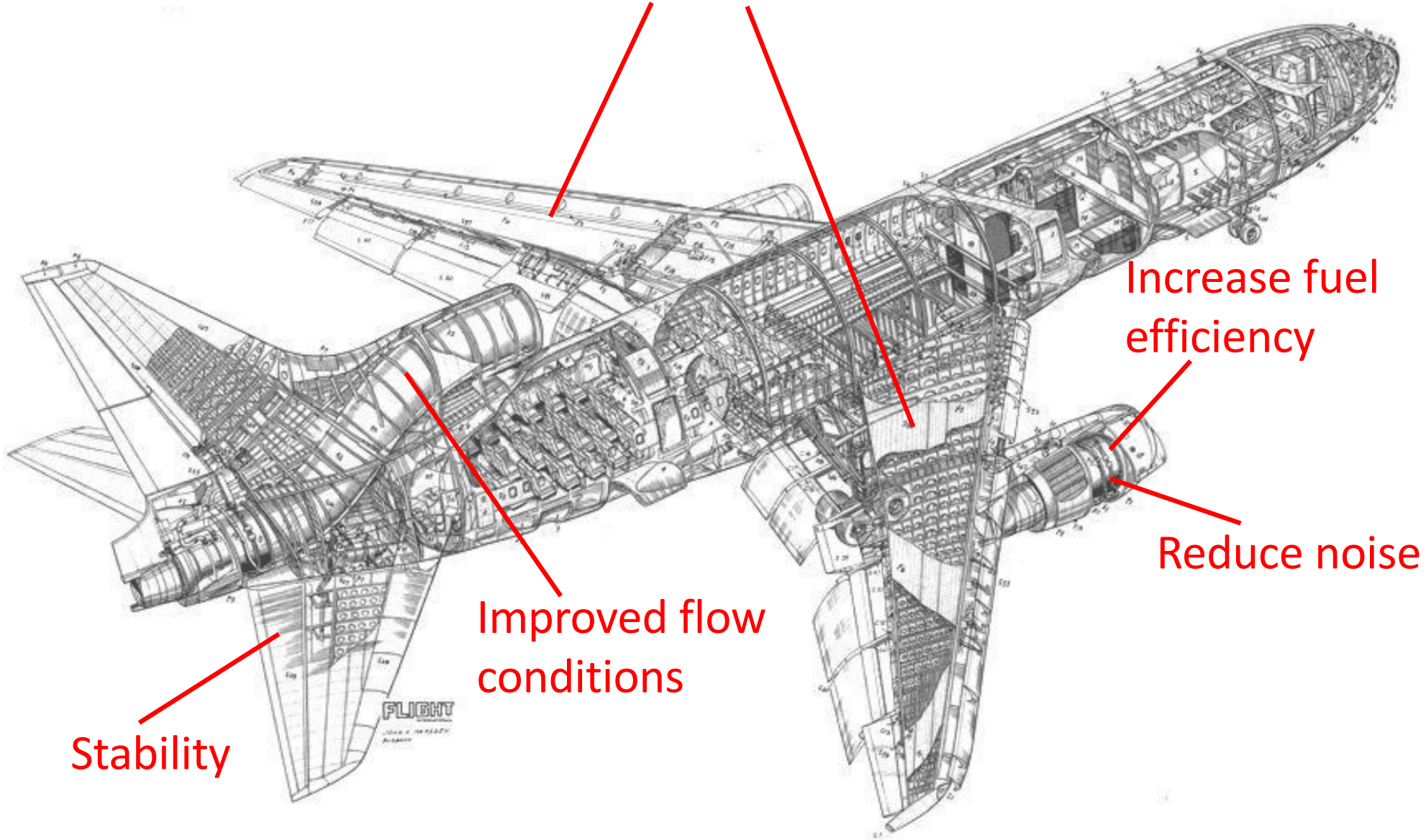
The basics

- Commercial aircraft - reduce cost, increase comfort
- Military aircraft - high-speed maneuvers, stealth
- Environmental factors - carbon emissions, noise

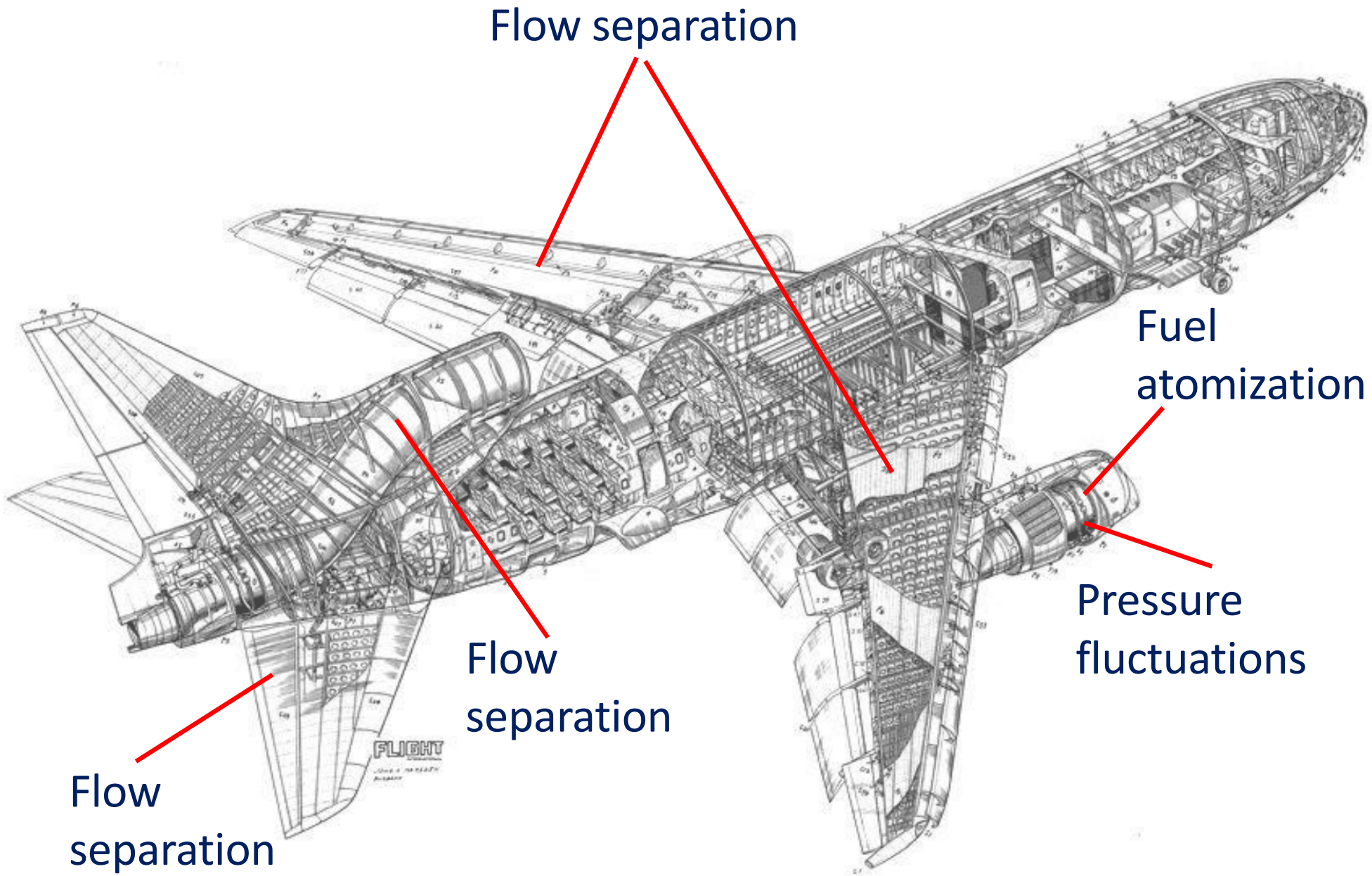


Lockheed L-1011 Tristar

The basics


Increase lift/reduce drag
Increase fuel efficiency
Reduce noise
Improved flow conditions
Stability
FLIGHT

The basics

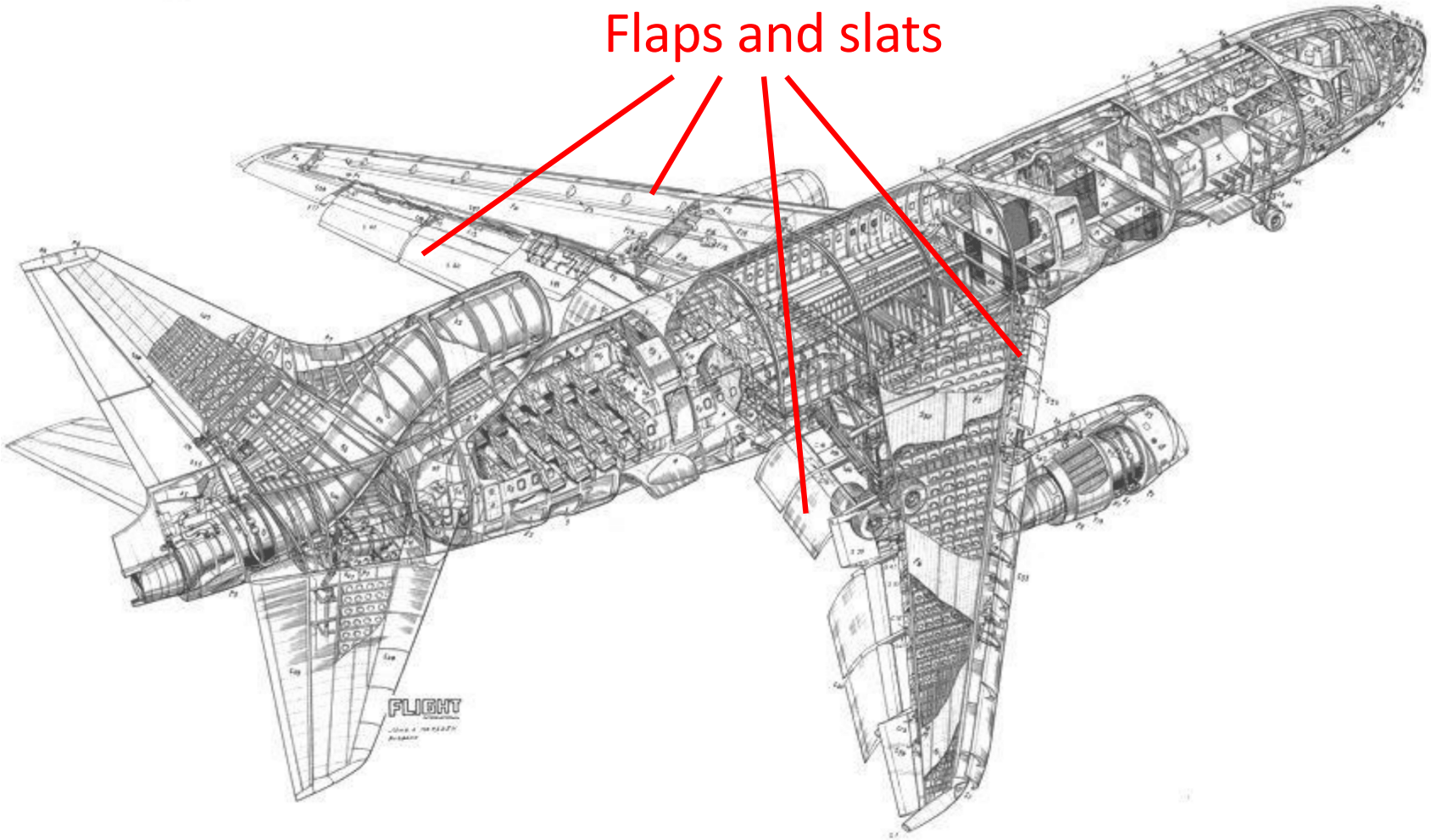

Flow separation
Fuel atomization
Pressure fluctuations
Flow separation
Flow separation
FLIGHT

Flow control

What is flow control?

Alter flows to achieve a desired effect

- Passive flow control – geometrical changes, no/little energy required

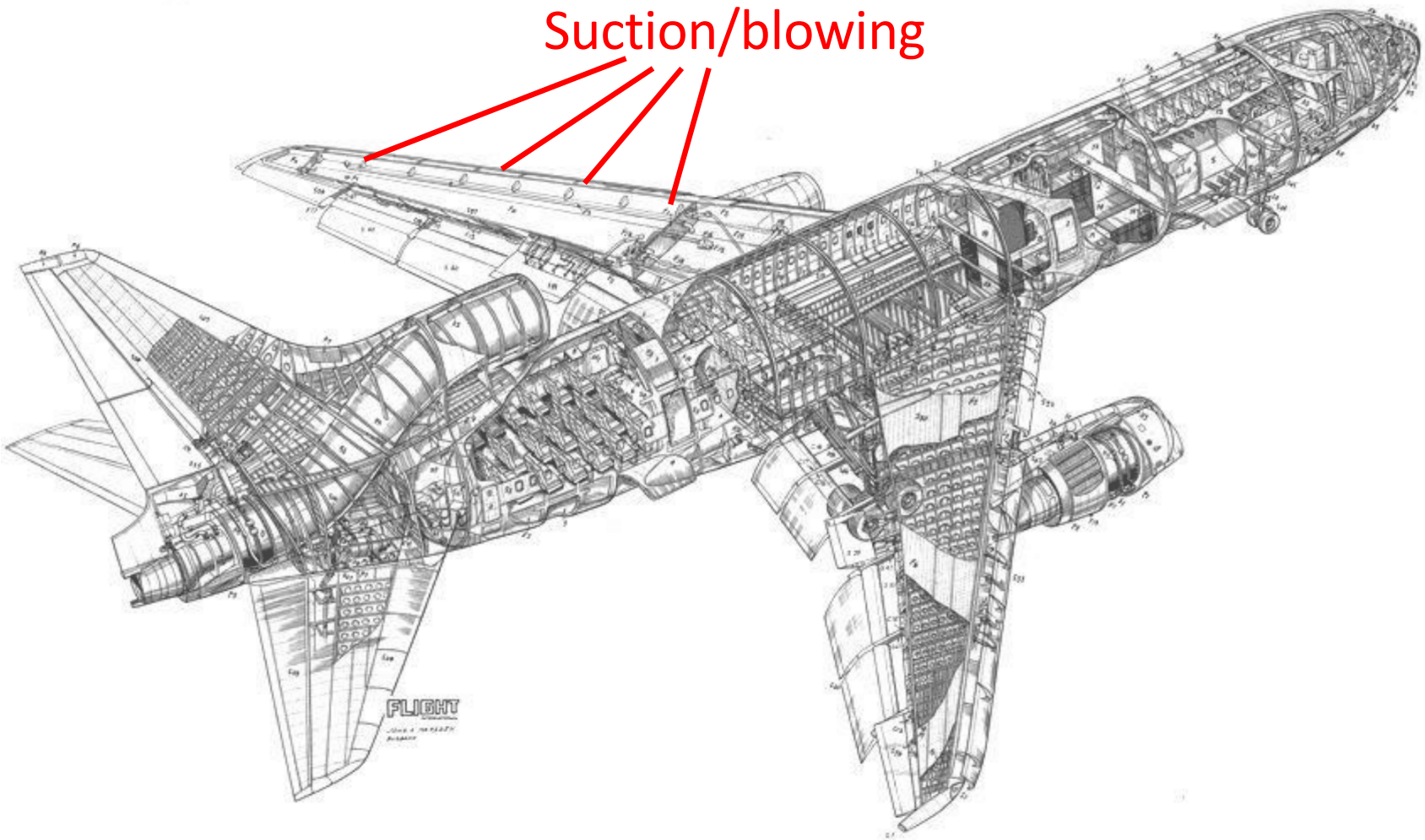


Flow control

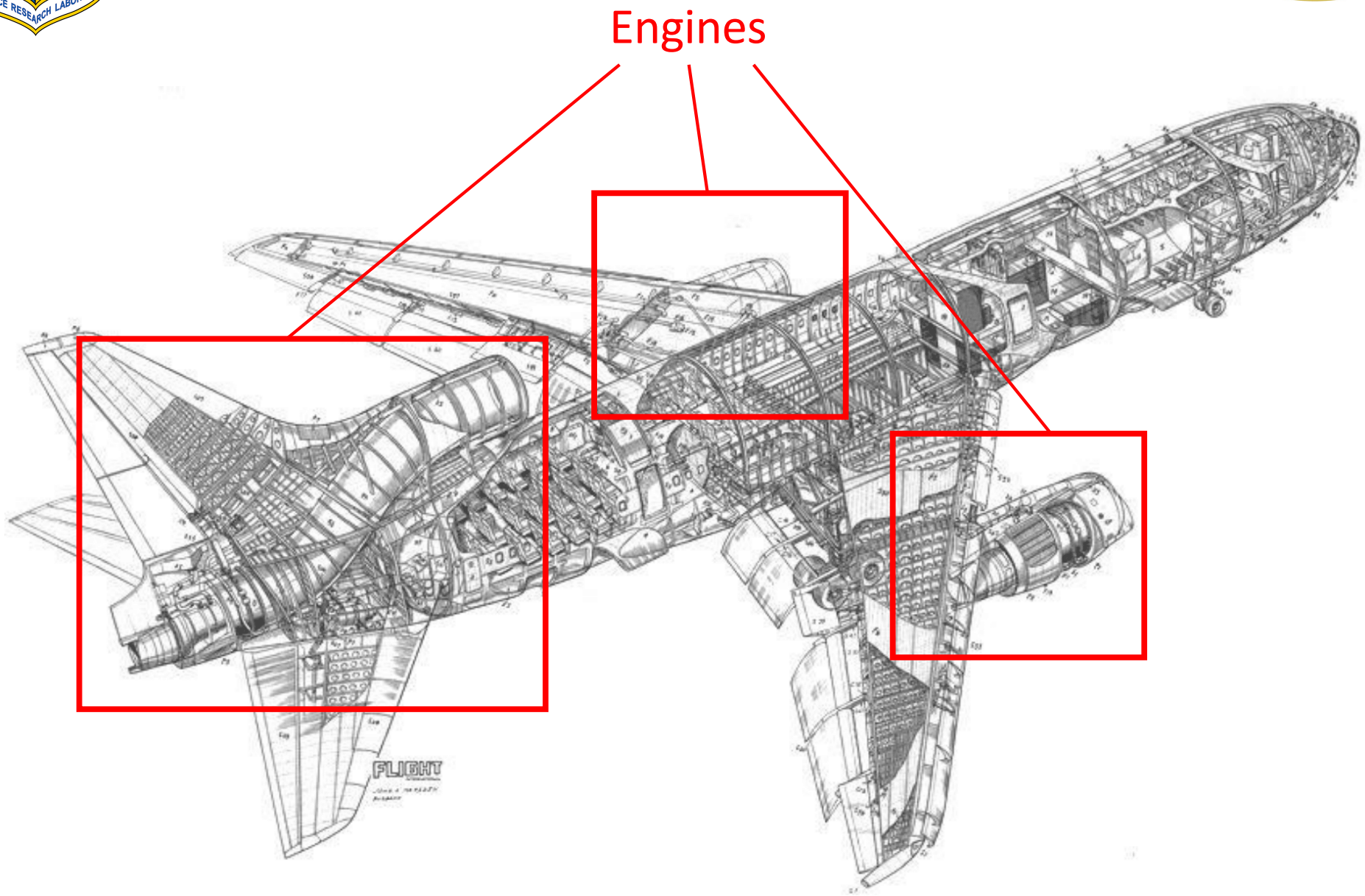
What is flow control?

Alter flows to achieve a desired effect

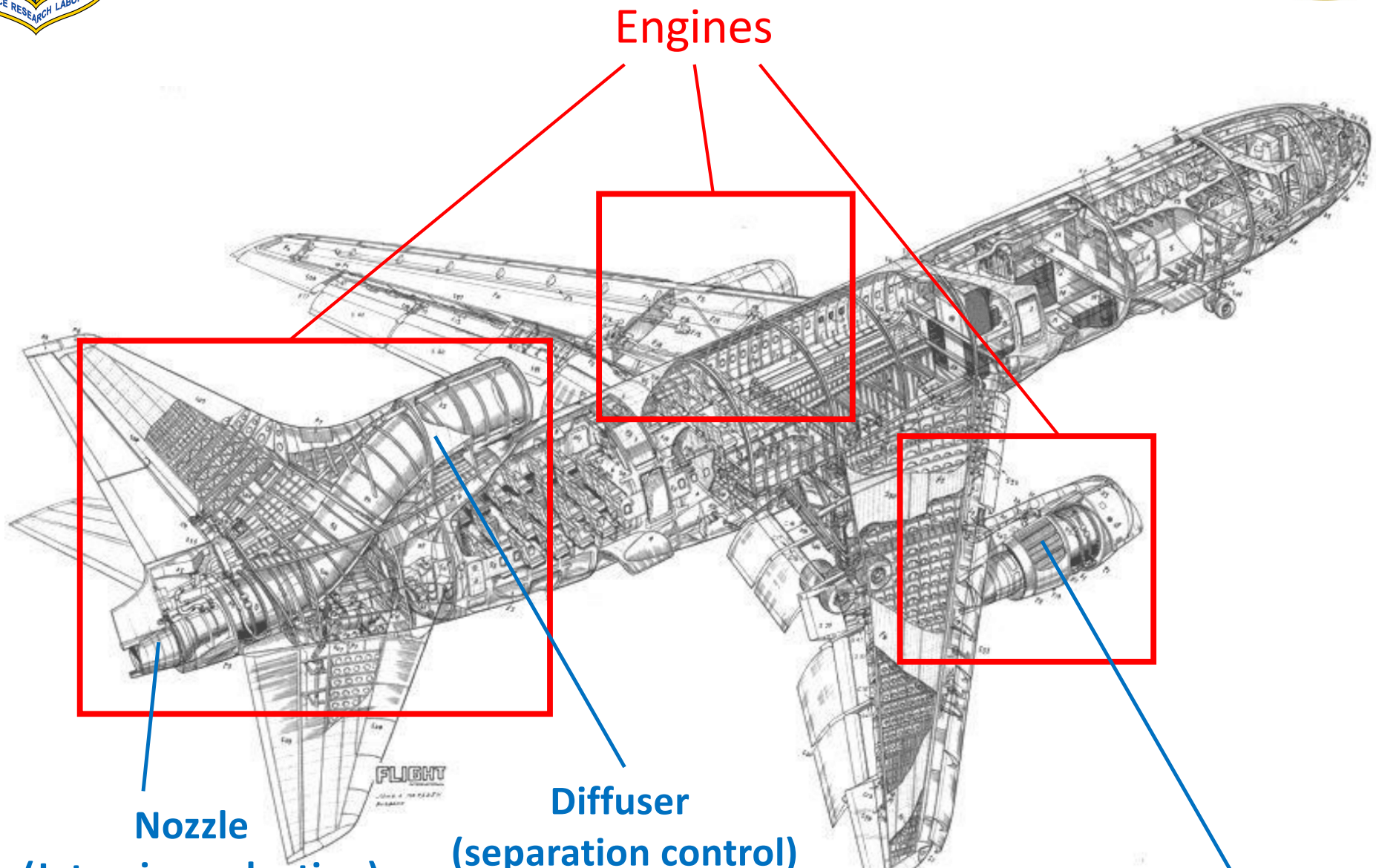
- Active flow control – dynamic actuators, requires energy input



The focus



The focus – Active flow control



Motivation

- Flow separation in diffusers deteriorate engine performance
  - S-duct – allows the engine to be installed inline with the aircraft axis
  - Conceals the engine fan – reduces radar cross-section

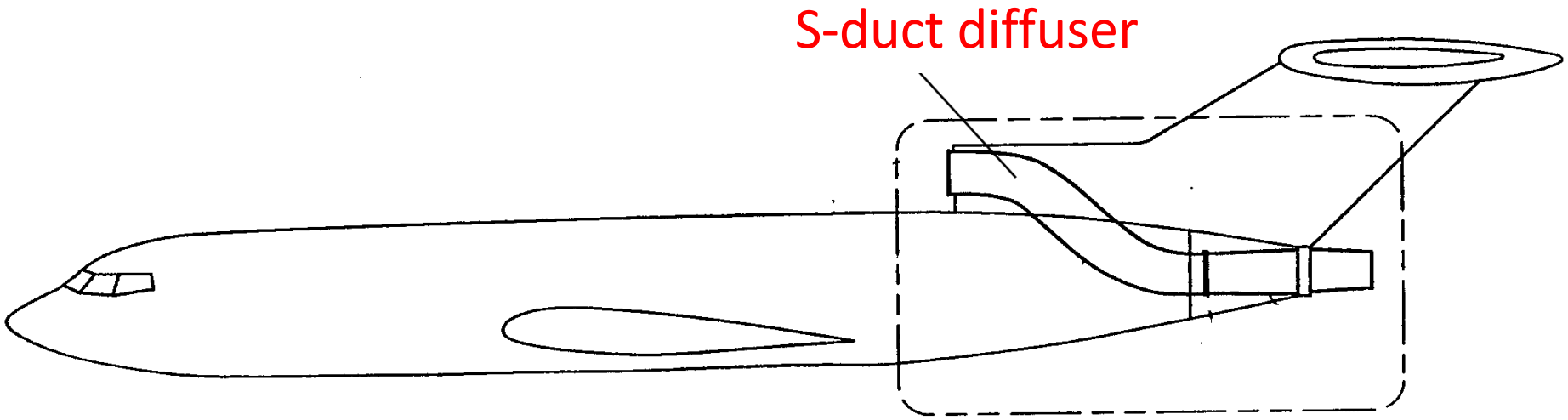


Image courtesy: www.patentbuddy.com

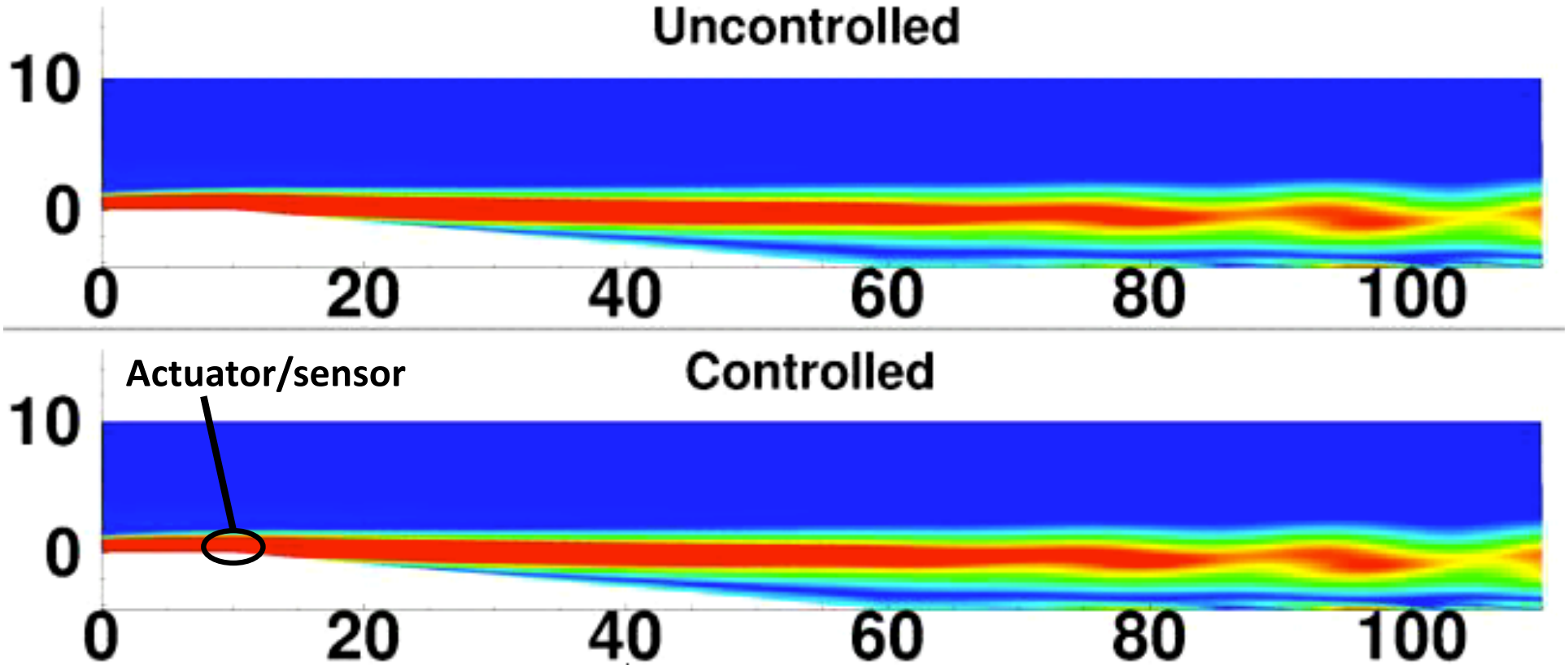
Motivation

- Flow separation in diffusers deteriorate engine performance

- Reduce flow unsteadiness leading to improved flow into the compressor/fan
- Reduce stagnation pressure loss at the diffuser exit

Control of vortex shedding

5^0 ramp diffuser with a Mach 0.65 inflow



Mahesh Natarajan, Jonathan B. Freund, and Daniel J. Bodony., *Actuator selection and placement for localized feedback flow control*, Journal of Fluid Mechanics 809 (2016) 775-792

Motivation

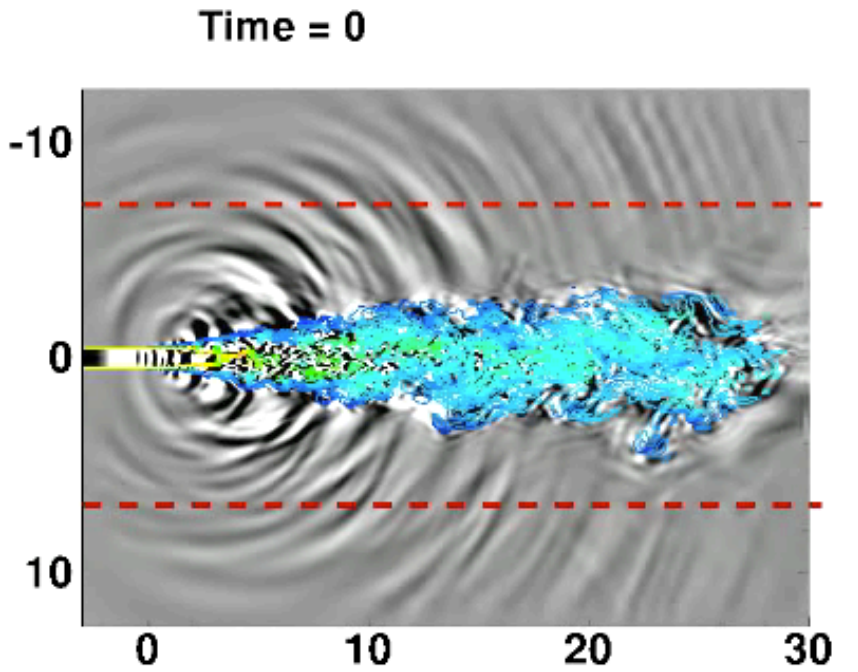
- Naval aircraft are extremely loud, people are close to the aircraft



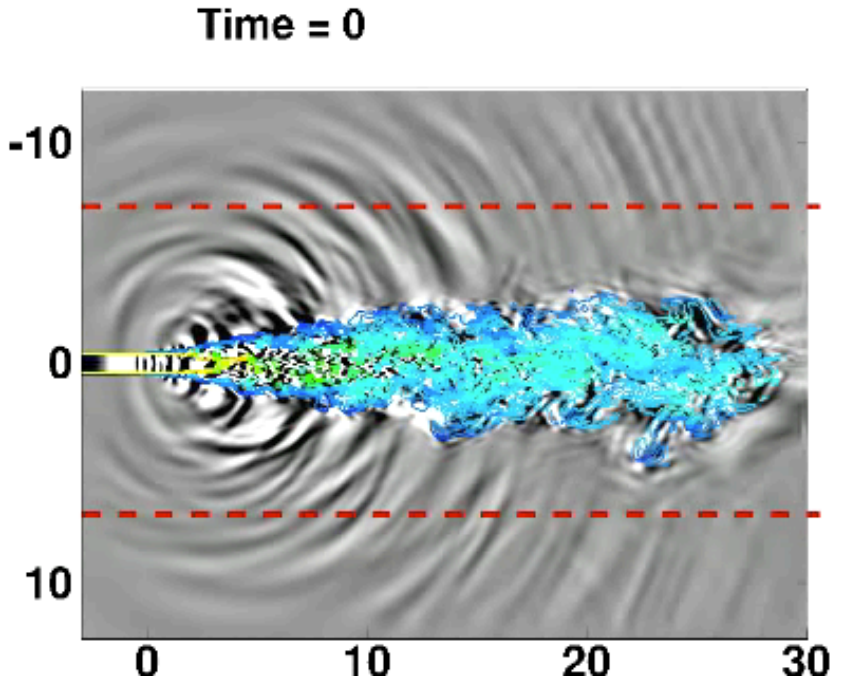
Image courtesy: Reuters

Noise reduction of a Mach 0.9 turbulent jet

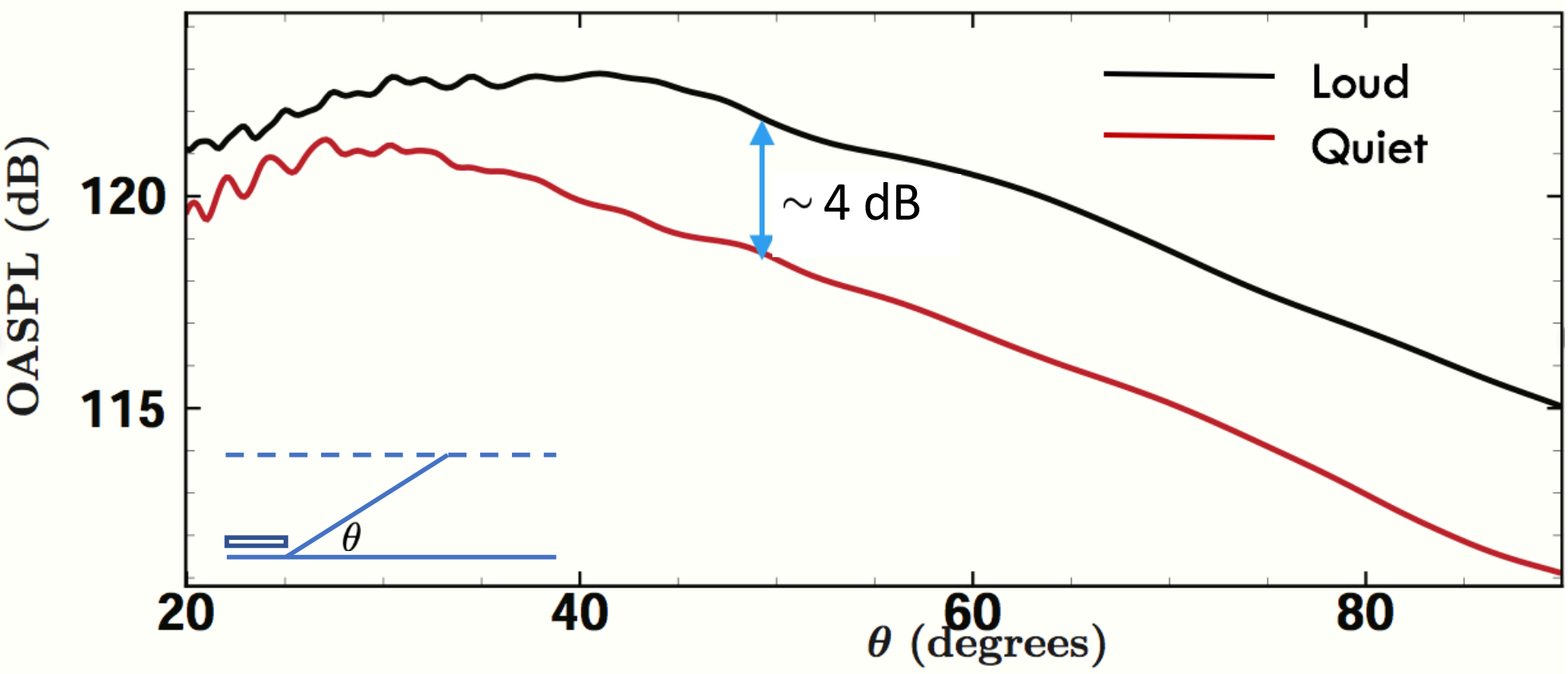
Loud



Quiet



Effect on radiated noise - OASPL



Controlling complex flows

Nearly every flow control effort starts with this statement:
We had *this* type of controller available and guessed that it should be placed *here*

- We argue that it is better to let the flow system tell you how it wants to be {changed, observed, controlled} for a given goal

Primary objective:
Develop an efficient method for rationally selecting co-located actuator/sensor type and location for controlling a compressible viscous flow

Outline of the strategy

Basic Idea - I

Place the controller at the location in the flow-field that is most responsive to perturbation

Basic Idea - II

Global modes contain receptivity information

- The linearized Navier-Stokes equations in discrete form is

$$\frac{\mathrm{d}\mathbf{Q}'}{\mathrm{d}t} = \mathcal{A}[\overline{Q}]\mathbf{Q}' + \underbrace{F(\vec{x},t)}_{\text{Control Forcing}}$$

- Using linear feedback $F \sim \delta\mathcal{A}\,\mathbf{Q}' \rightarrow \dfrac{\mathrm{d}\mathbf{Q}'}{\mathrm{d}t} = (\mathcal{A}[\overline{Q}] + \delta\mathcal{A})\mathbf{Q}'$

Question

What should be $\delta\mathcal{A}$ that changes the eigenstructure of $\mathcal{A}$ to optimize a given objective (eg. noise reduction)

Outline of the strategy

- We formulate the problem from a global mode perspective

$$\text{If } \mathbf{Q}' \equiv \widehat{\mathbf{Q}} e^{\omega t}, \text{ then } \omega \text{ and } \widehat{\mathbf{Q}} \text{ satisfy } (\omega M - \mathcal{A})\widehat{\mathbf{Q}} = 0$$

- The change in ω is related to $\delta\mathcal{A}$: $\delta\omega = \dfrac{\widehat{\mathbf{Q}^\dagger}^T \delta A \widehat{\mathbf{Q}}}{\widehat{\mathbf{Q}^\dagger}^T \widehat{\mathbf{Q}}}$

- The operator change $\delta\mathcal{A}$ is parametrized as (in 3-D)

$$\begin{bmatrix} c_{11} & c_{12} & c_{13} & c_{14} & c_{15} \\ c_{21} & c_{22} & c_{23} & c_{24} & c_{25} \\ c_{31} & c_{32} & c_{33} & c_{34} & c_{35} \\ c_{41} & c_{42} & c_{43} & c_{44} & c_{45} \\ c_{51} & c_{52} & c_{53} & c_{54} & c_{55} \end{bmatrix} \otimes e^{-(x-x_0)^2/\ell_x^2 - (y-y_0)^2/\ell_y^2 - (z-z_0)^2/\ell_z^2}$$

which localizes the control at point (x_0, y_0, z_0) and permits different actuator/sensor pairs $\{c_{ij}\}$

Outline of the strategy

- What we then seek are the $(x_0, y_0, z_0), (l_x, l_y, l_z), \{c_{ij}\}$ that alter the eigenstructure optimally w.r.t the objective function – reduce the growth rate of the target mode(s). This is a simple optimization problem:

Optimization statement

Find $(x_0^*, y_0^*, z_0^*), (l_x^*, l_y^*, l_z^*), \{c_{ij}^*\}$ to optimize $\mathcal{J}$

which tells us

(x_0^*, y_0^*, z_0^*) - Where to place the actuator

(l_x^*, l_y^*, l_z^*) - How big the actuator needs to be

i in $\{c_{ij}^*\}$ - What quantity to force

j in $\{c_{ij}^*\}$ - What quantity to sense

α - The gain

Linear feedback control

- The NS equations are (in discrete form)

$$\frac{\mathrm{d}\mathbf{Q}}{\mathrm{d}t} = \tilde{\mathbf{R}}(\mathbf{Q})$$

- Linear feedback control is a forcing term proportional to the flow perturbation $\mathbf{Q}' \equiv \mathbf{Q} - \overline{\mathbf{Q}}$

$$\frac{\mathrm{d}\mathbf{Q}}{\mathrm{d}t} = \tilde{\mathbf{R}}(\mathbf{Q}) + \underbrace{\alpha \mathbf{C}(\mathbf{Q} - \bar{\mathbf{Q}})}_{\textbf{Forcing } \mathbf{F}(\tilde{\mathrm{x}},\mathrm{t})}$$

- Linearization and using the global mode assumption $\mathbf{Q}' = \hat{\mathbf{Q}} e^{\omega t}$

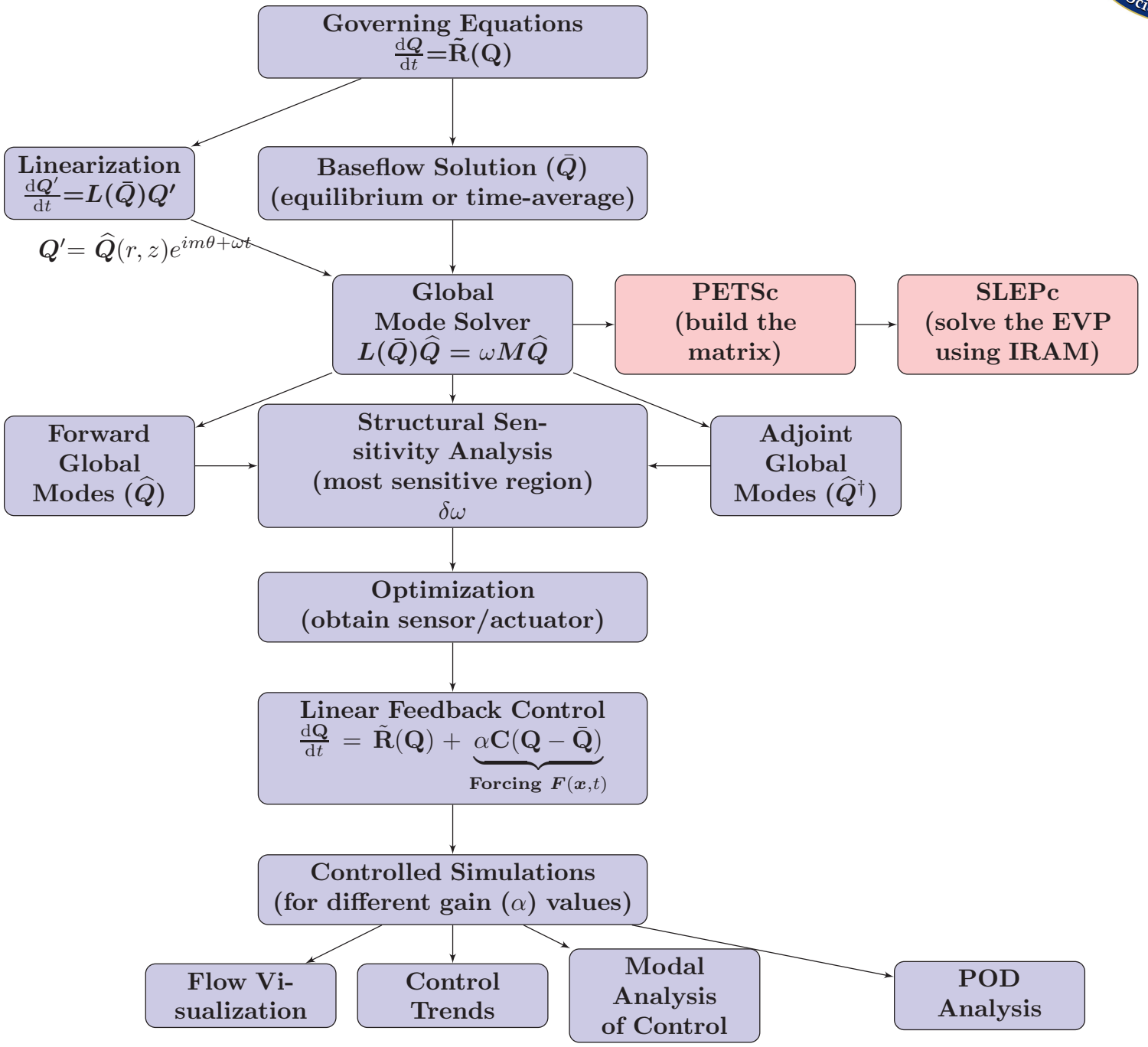
$$L\hat{\mathbf{Q}} = \omega M \hat{\mathbf{Q}} \qquad \text{(Forward)}$$

$$L^{\dagger}\widehat{\mathbf{Q}^{\dagger}} = \omega M \widehat{\mathbf{Q}^{\dagger}} \qquad \text{(Adjoint)}$$

- Eigenvalue sensitivity is $\delta\omega = \dfrac{\widehat{\mathbf{Q}^{\dagger}}^{T} C \hat{\mathbf{Q}}}{\widehat{\mathbf{Q}^{\dagger}}^{T} M \hat{\mathbf{Q}}}$

- Optimize $\delta\omega$ to affect a particular flow mechanism – gives the controller

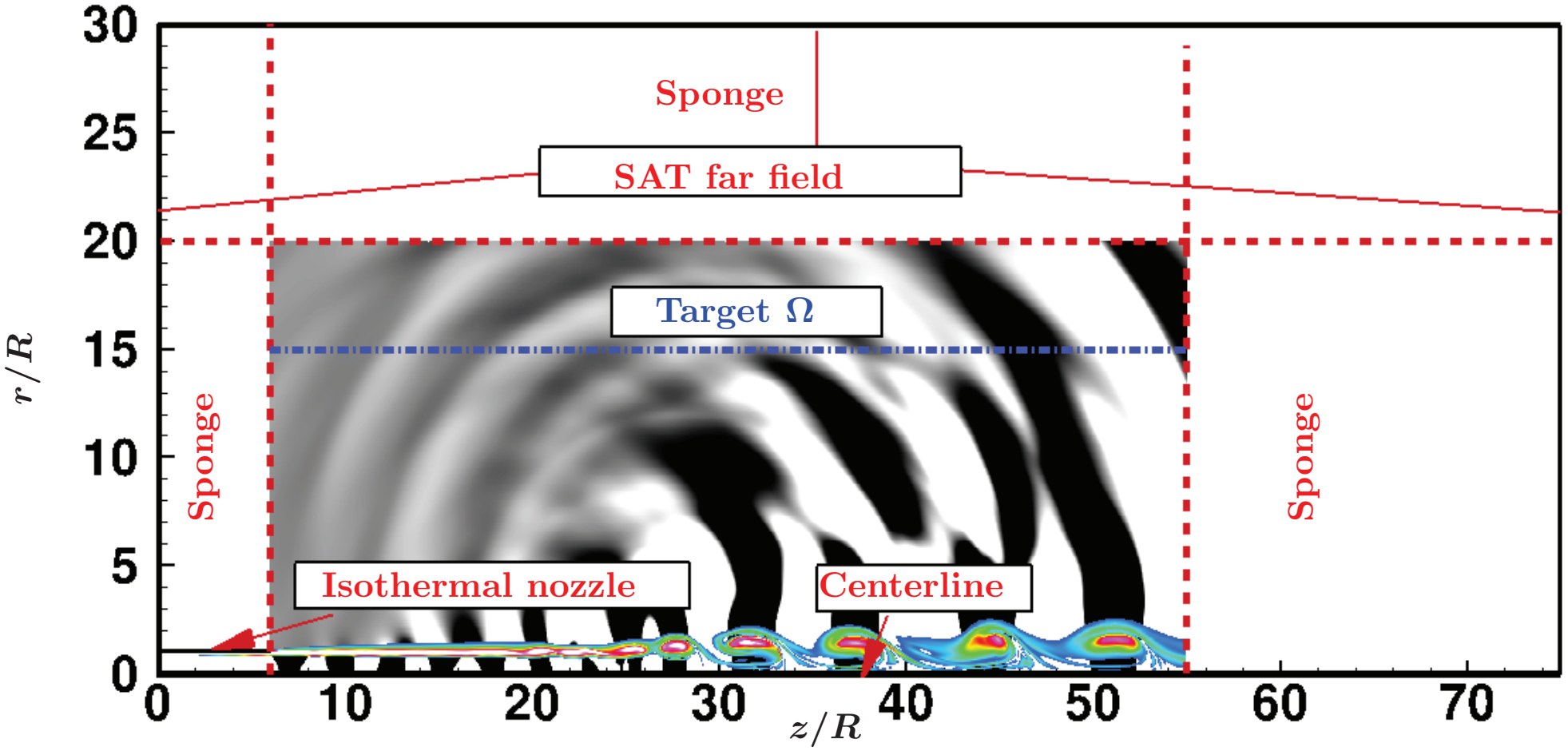
Control formulation



Axisymmetric jet – flow conditions and BCs

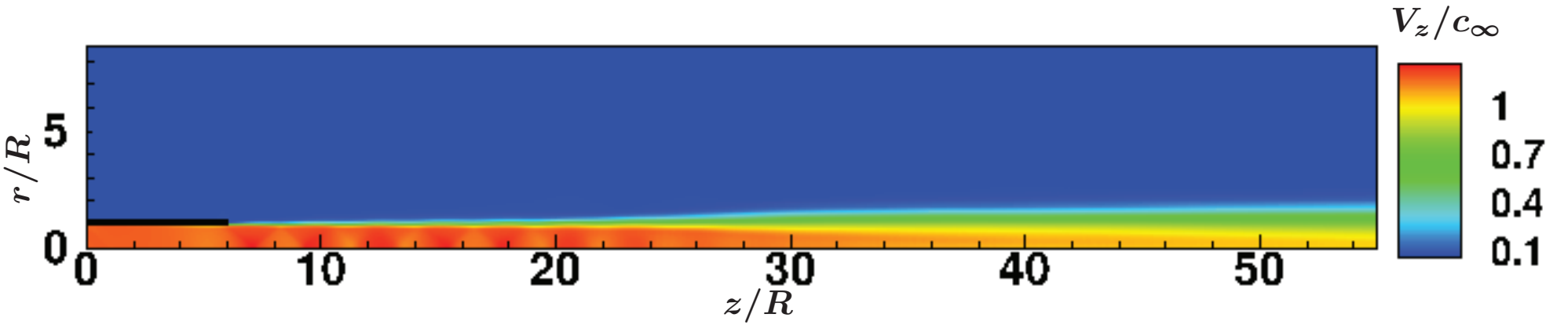
$$M_j = 1.5, T_j/T_\infty = 0.6, Re_D = 10000$$

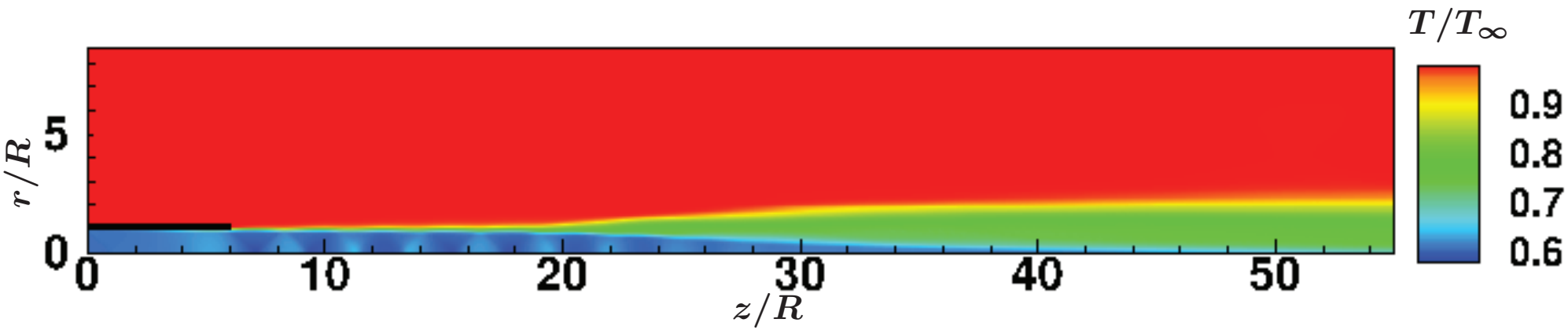
- Isothermal nozzle with $L/R = 6, t/R = 0.05, T_w/T_\infty = 1$



Axisymmetric jet – Time-average

- The time average baseflow was computed from the direct numerical simulation



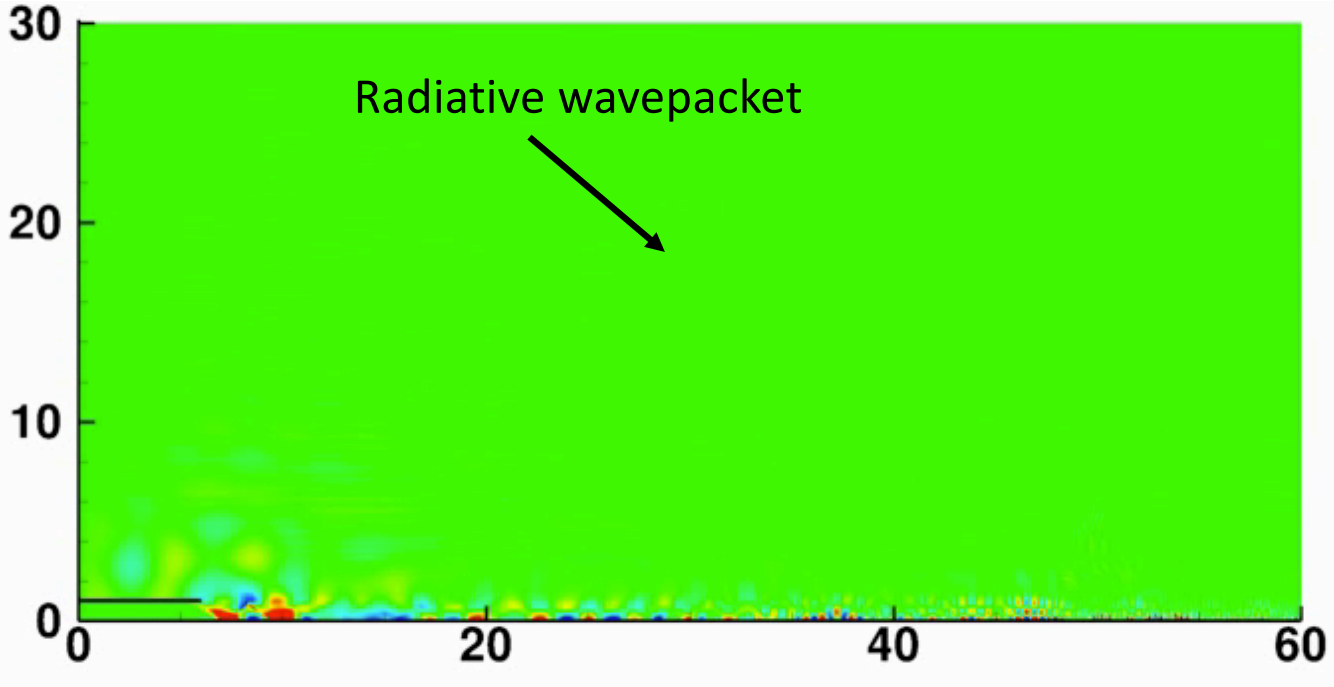


Optimal transient response

- Due to non-normality of the Navier-Stokes operator, growth of wavepackets is possible for finite time by optimal transient response (OTR) (Schmid & Henningson 2001)

- OTR is a suggested mechanism for sound propagation to the far-field (Nichols and Lele 2011)

- Define the norm: $E(t) = \frac{1}{2}\int_{\mathcal{V}} \widehat{p}(t)\widehat{p}(t)^* \, dV$, maximize $G(t) \equiv \max \frac{E(t)}{E(0)}$

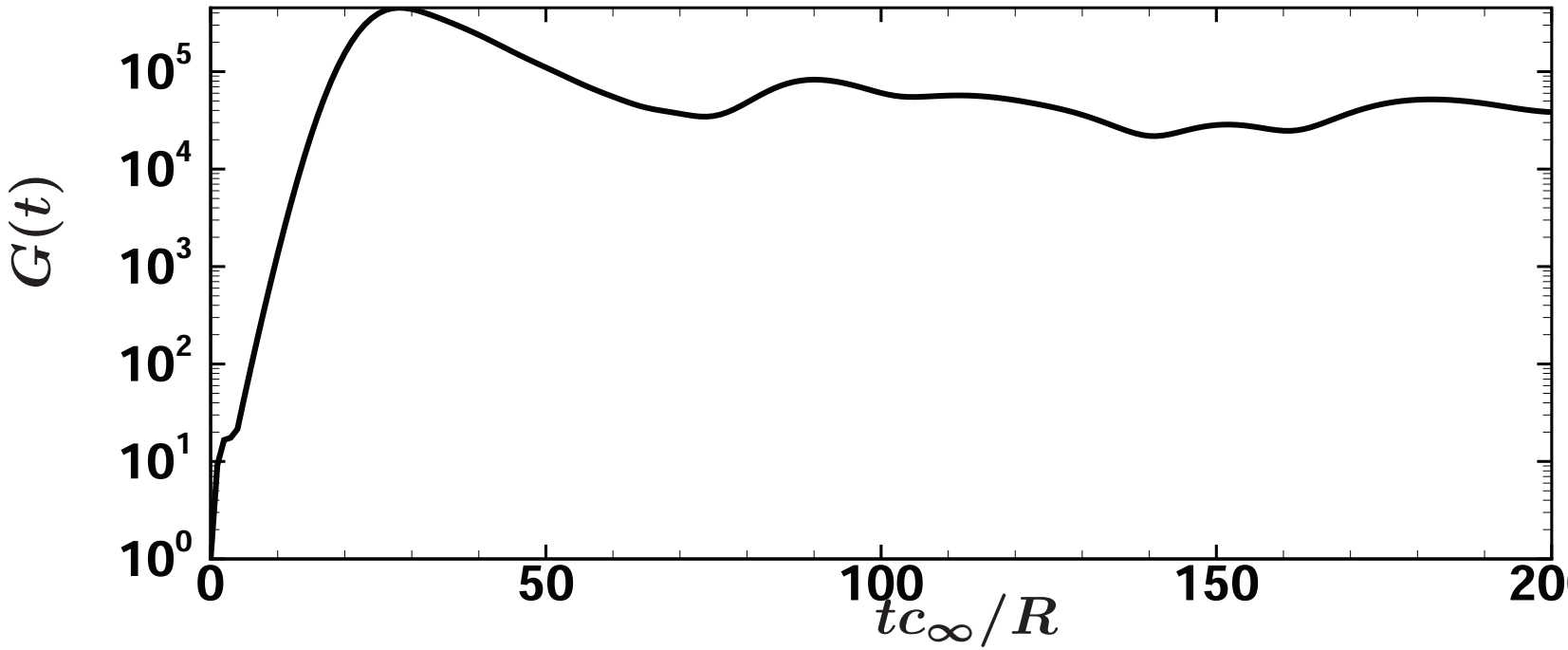


Optimal transient response

- Due to non-normality of the Navier-Stokes operator, growth of wavepackets is possible for finite time by optimal transient response (OTR) (Schmid & Henningson 2001)

- OTR is a suggested mechanism for sound propagation to the far-field (Nichols and Lele 2011)

- Define the norm: $E(t) = \frac{1}{2}\int_{\mathcal{V}} \widehat{p}(t)\widehat{p}(t)^* \, dV$, maximize $G(t) \equiv \max \frac{E(t)}{E(0)}$

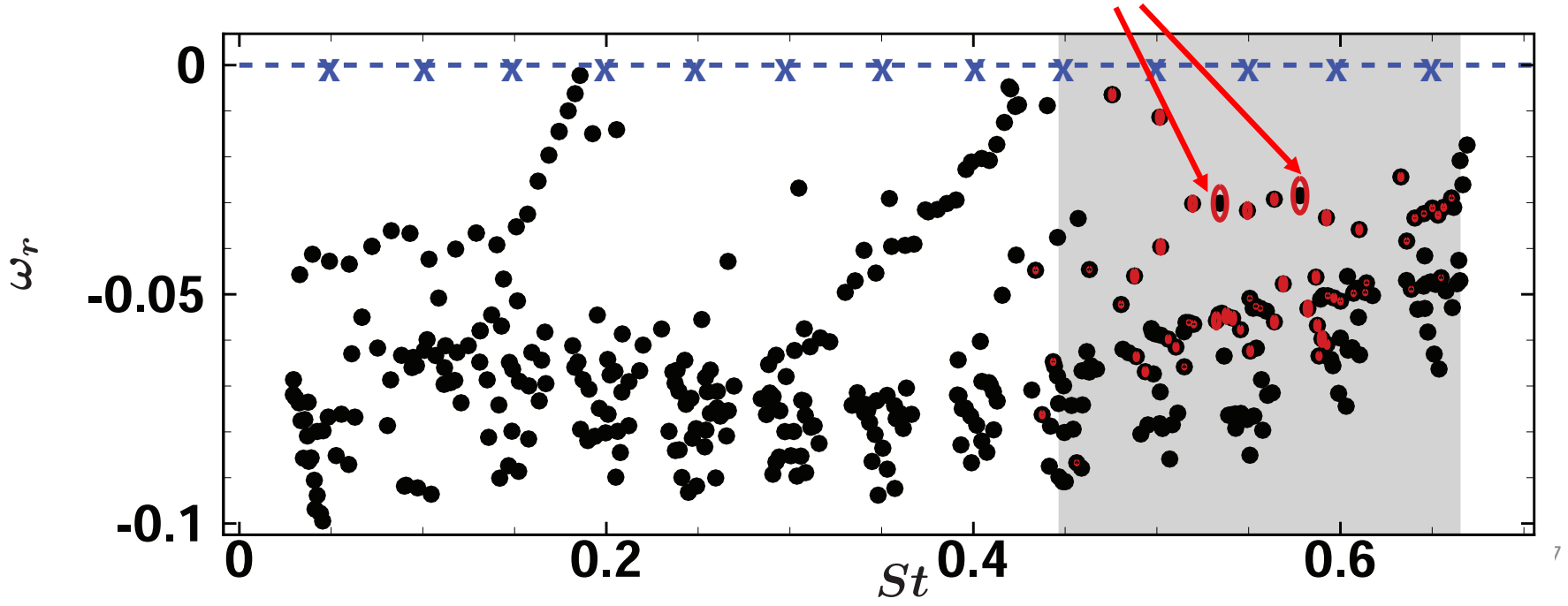


Optimal transient response

- Due to non-normality of the Navier-Stokes operator, growth of wavepackets is possible for finite time by optimal transient response (OTR) (Schmid & Henningson 2001)

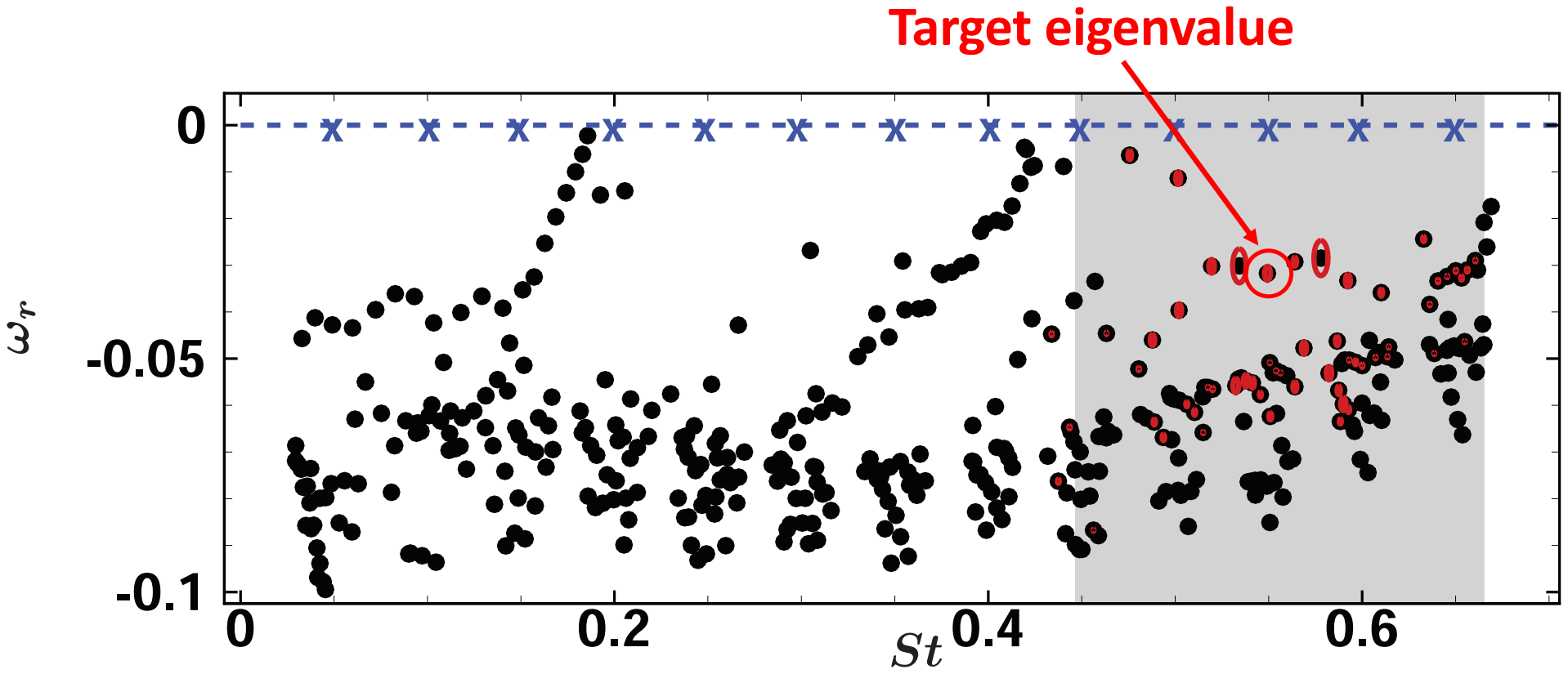
- OTR is a suggested mechanism for sound propagation to the far-field (Nichols and Lele 2011)

- Define the norm: $E(t) = \frac{1}{2}\int_{\mathcal{V}} \hat{p}(t)\hat{p}(t)^* \, dV$, maximize $G(t) \equiv \max \frac{E(t)}{E(0)}$



Target eigenvalue and global modes

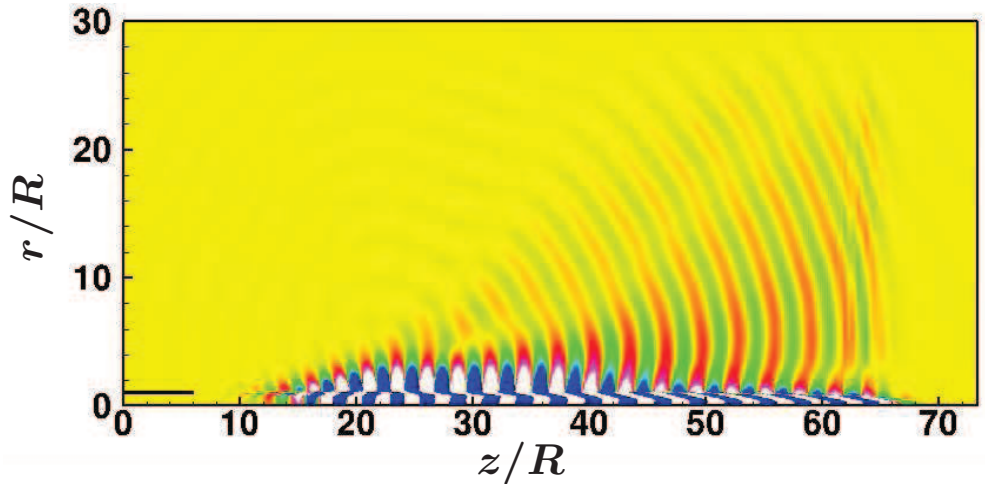
- The range of St -> 0.45 – 0.65 is found to have maximum contribution to the optimal transient response
- The target eigenvalue is chosen in the range at St -> 0.55



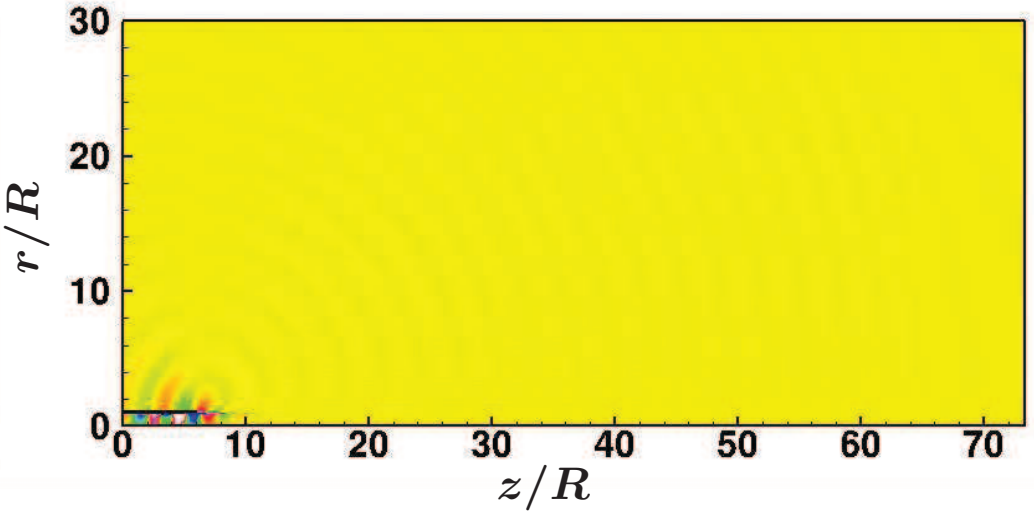
Target eigenvalue and global modes

- The range of St -> 0.45 – 0.65 is found to have maximum contribution to the optimal transient response
- The target eigenvalue is chosen in the range at St -> 0.55

Forward eigenmode $\mathrm{Re}(\widehat{V}_z)$

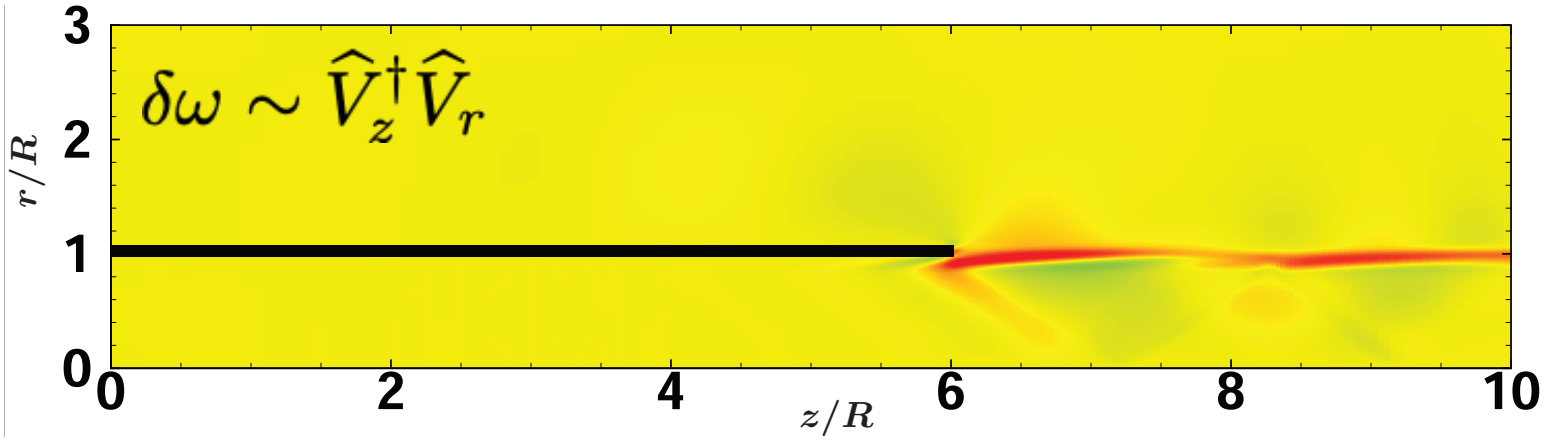


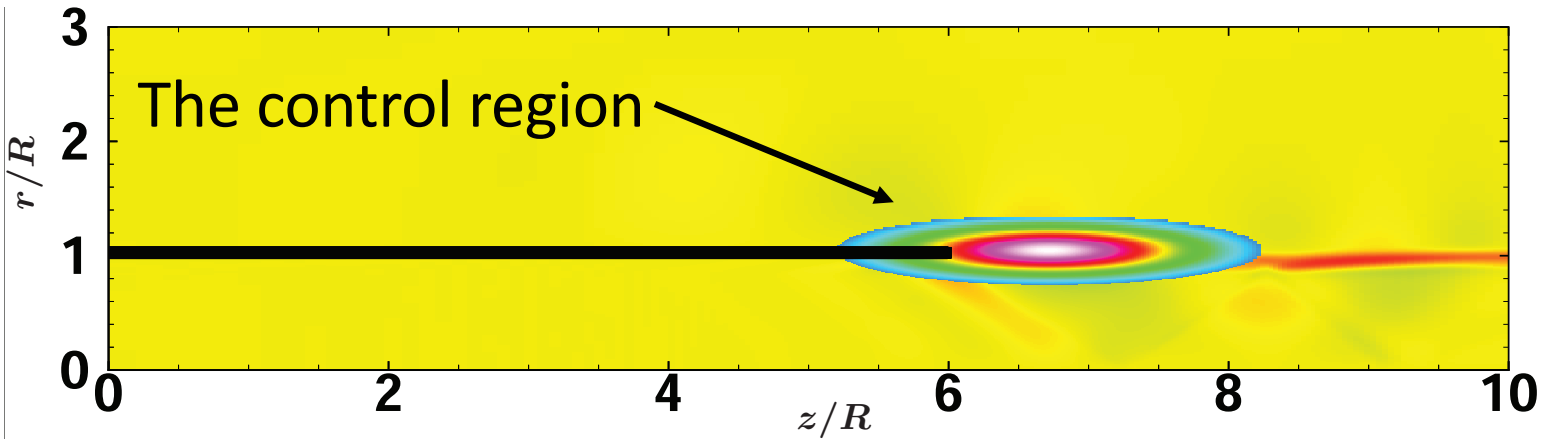
Adjoint eigenmode $\mathrm{Re}(\widehat{V}_z^{\dagger})$



Actuator/sensor development

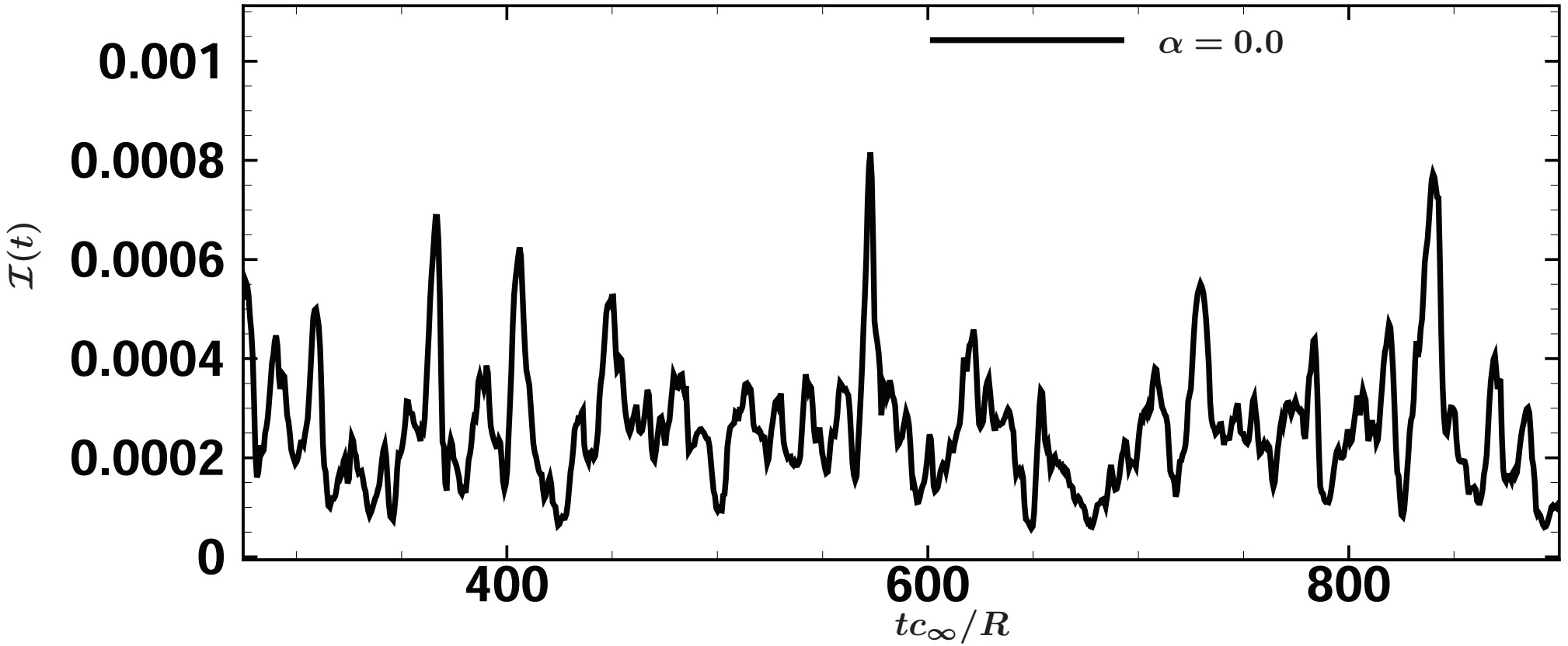
- Maximum sensitivity close to the nozzle
- The size and location of the control region is determined as part of the analysis, and changes with control-feedback pairs
- “Best” is found to be Vz control with Vr feedback





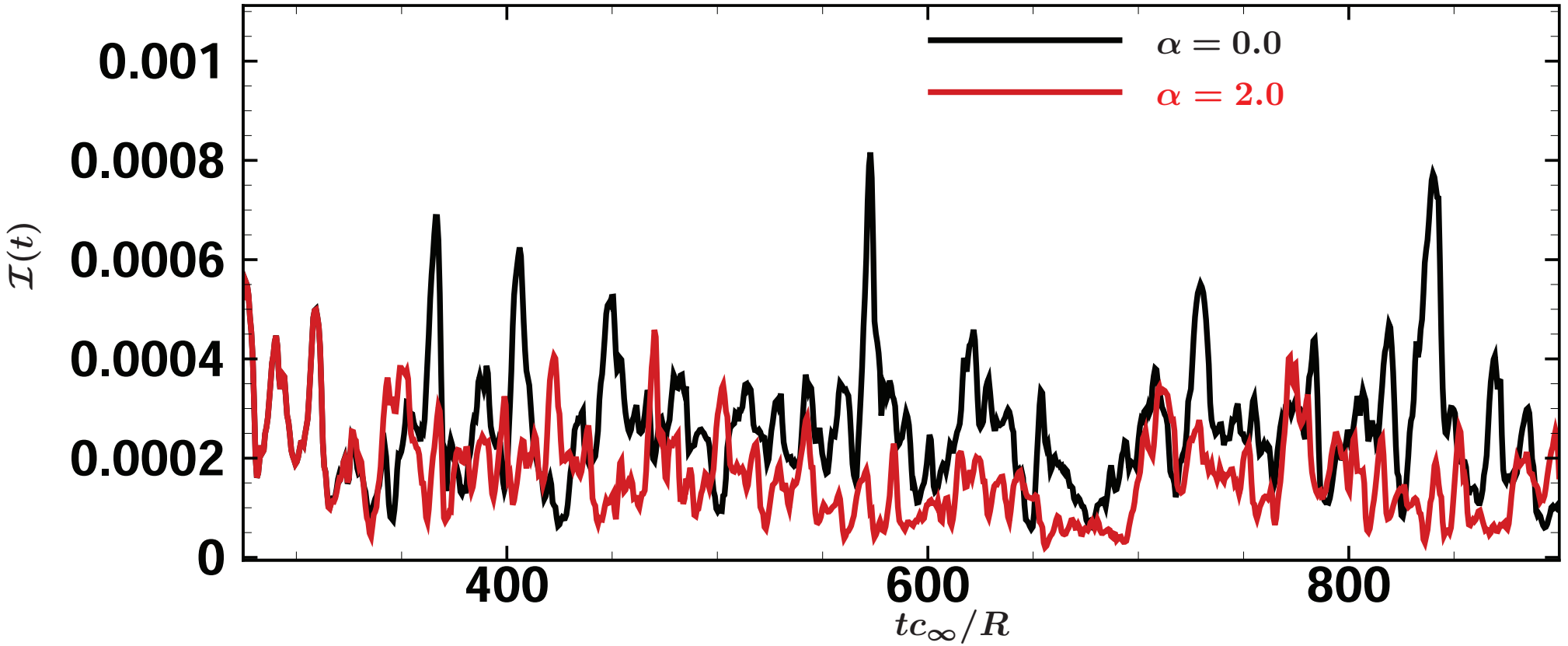
Objective function – Target surface r/R = 15

- The objective function is $\mathcal{I}(t) = \int_{\Omega} p'(\vec{x}, t)^2 \, d\Omega$



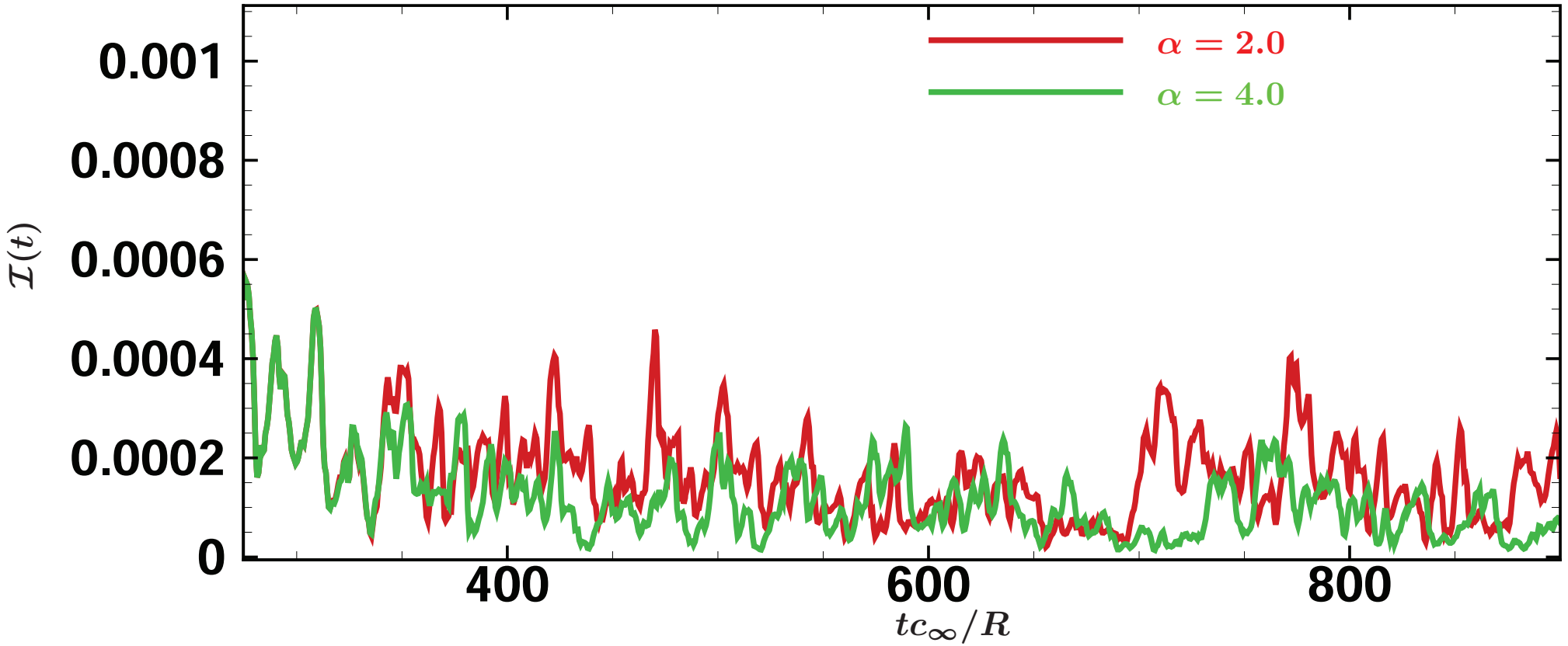
Objective function – Target surface r/R = 15

- The objective function is $\mathcal{I}(t) = \int_{\Omega} p'(\vec{x}, t)^2 \, d\Omega$



Objective function – Target surface r/R = 15

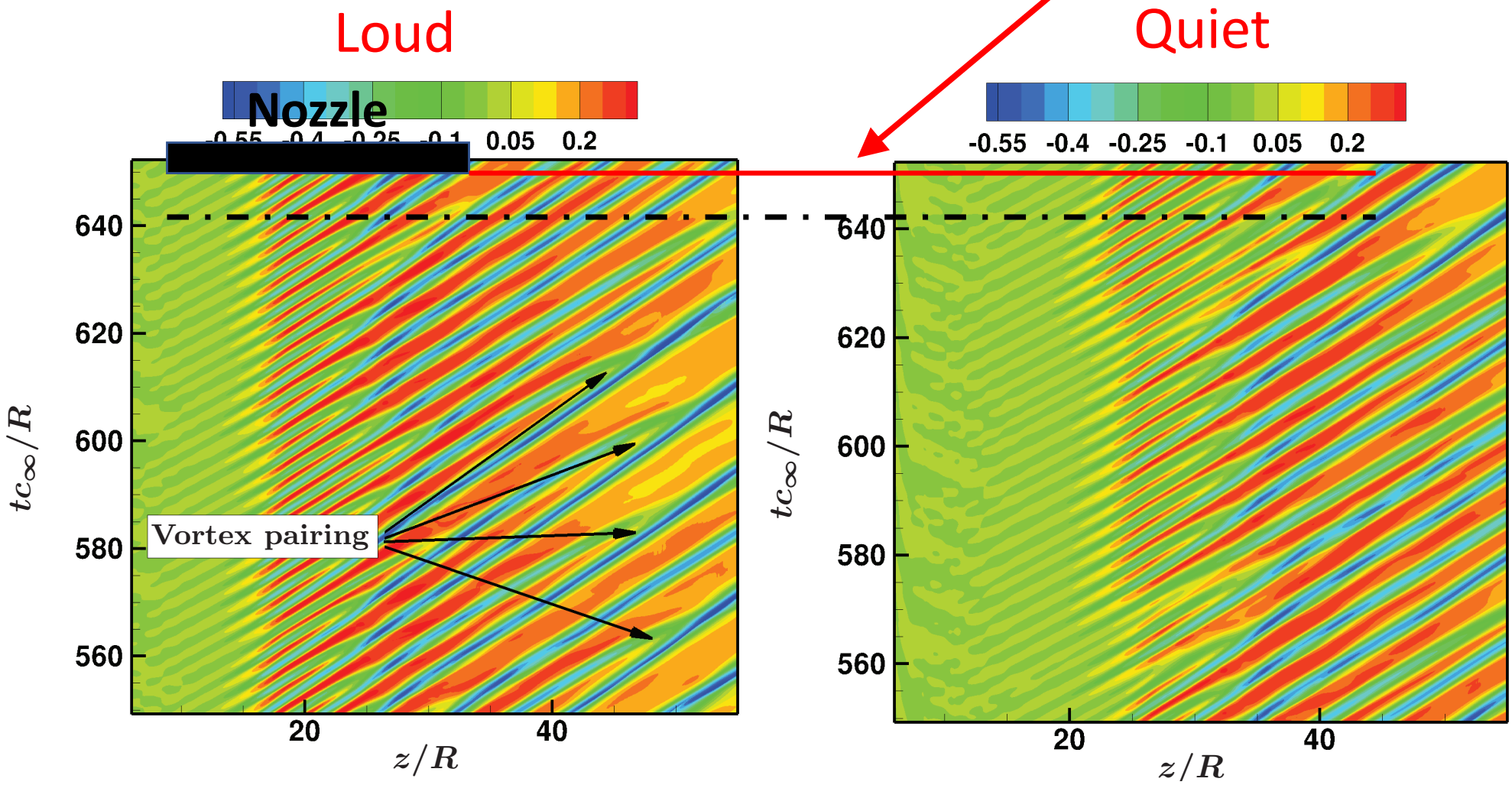
- The objective function is $\mathcal{I}(t) = \int_{\Omega} p'(\vec{x}, t)^2 \, d\Omega$



How does the control work – Vortex pairing

- Vortex pairing is one of the major noise producing mechanisms in jets

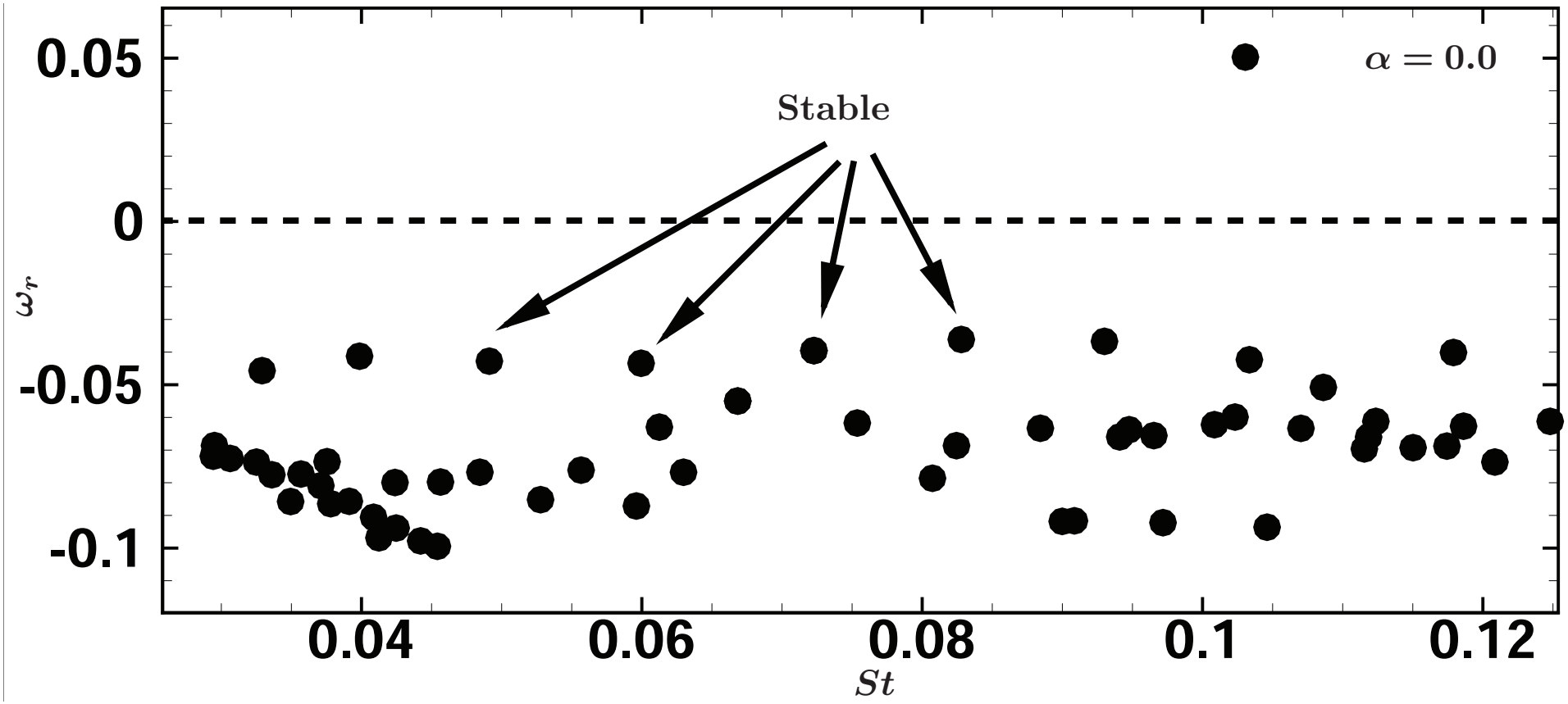
  $z-t$ diagram of $p'(z, r=1)$ along the lipline



How does the control work – Eigenspectrum at low St

- Global eigenanalysis was performed for the time-averaged flows for all cases

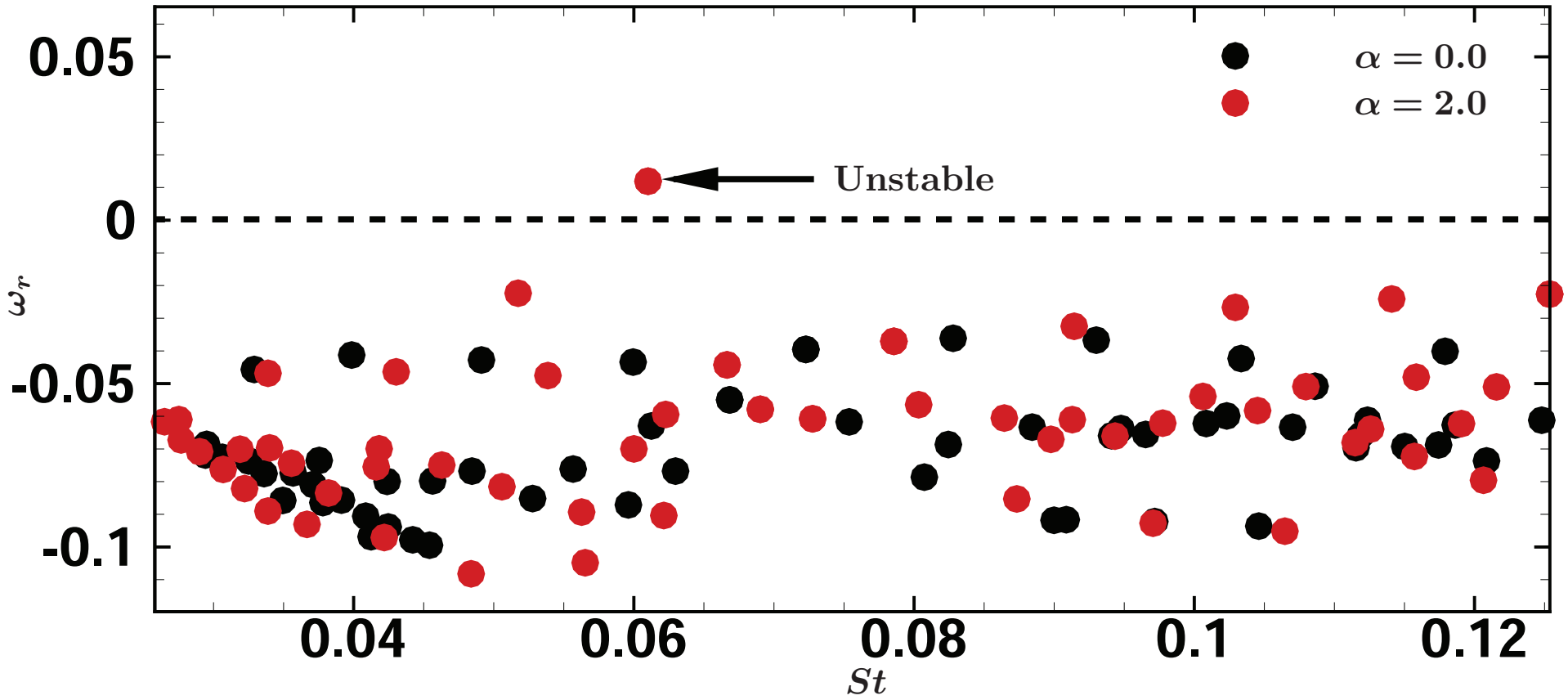
Loud flows - Stable eigenvalues at low Strouhal numbers



How does the control work – Eigenspectrum at low St

- Global eigenanalysis was performed for the time-averaged flows for all cases

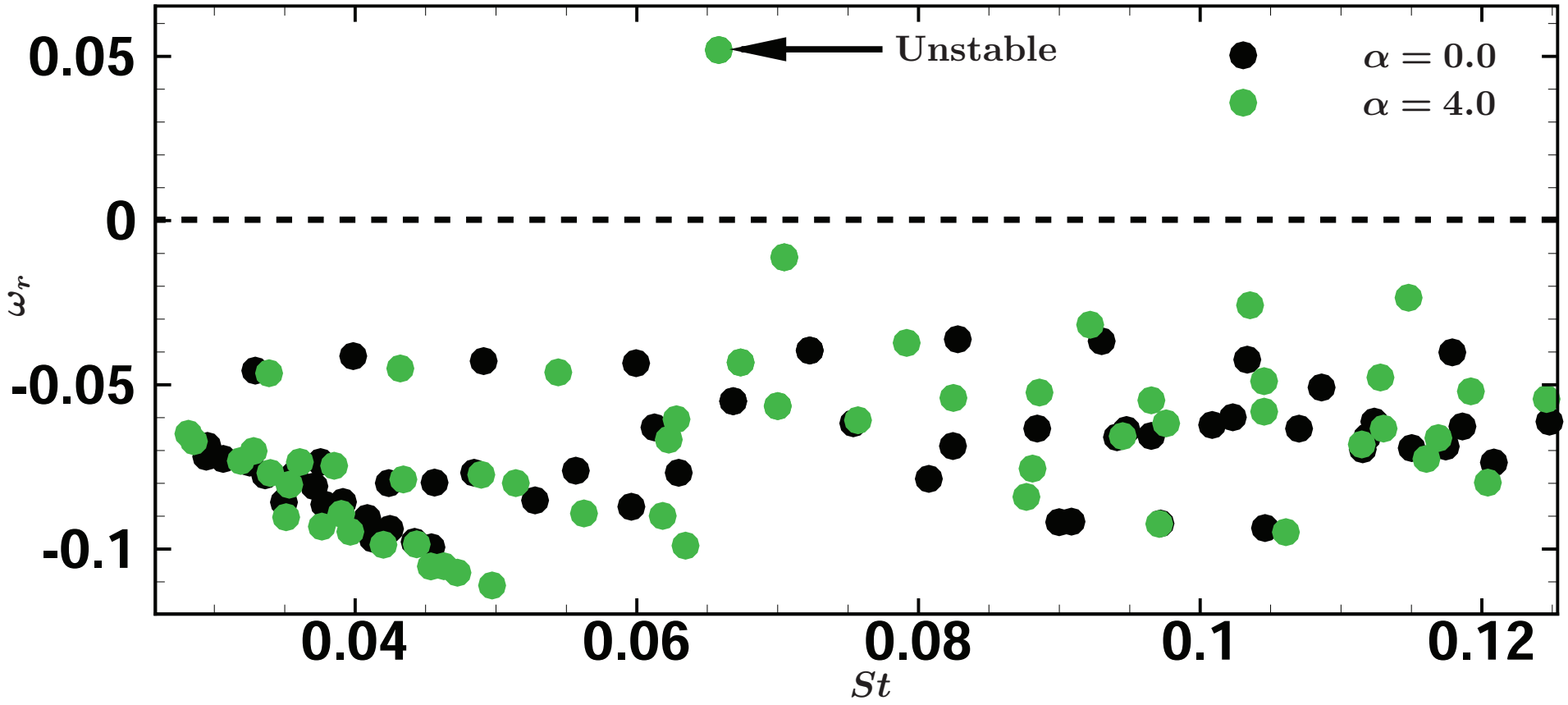
Quieter flows - Unstable eigenvalues at low Strouhal numbers



How does the control work – Eigenspectrum at low St

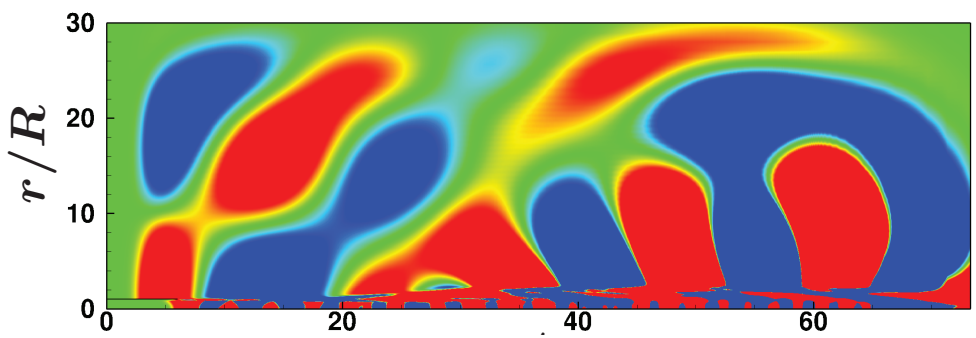
- Global eigenanalysis was performed for the time-averaged flows for all cases

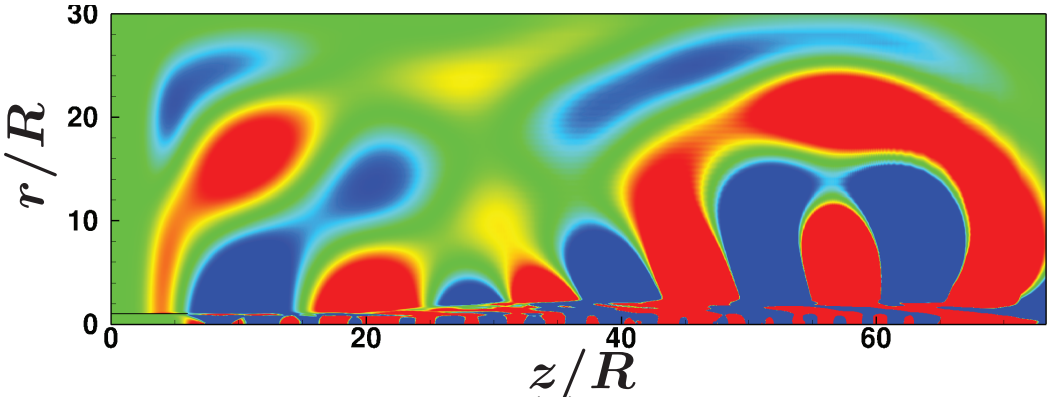
Quieter flows - Unstable eigenvalues at low Strouhal numbers



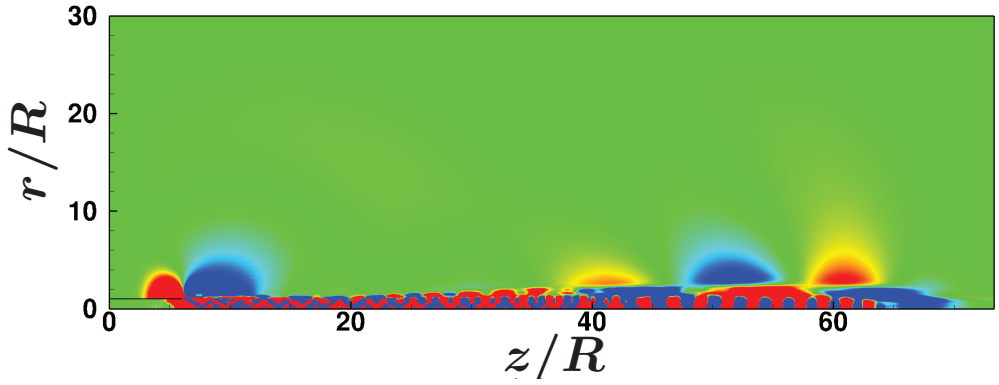
How does the control work – Eigenspectrum at low St

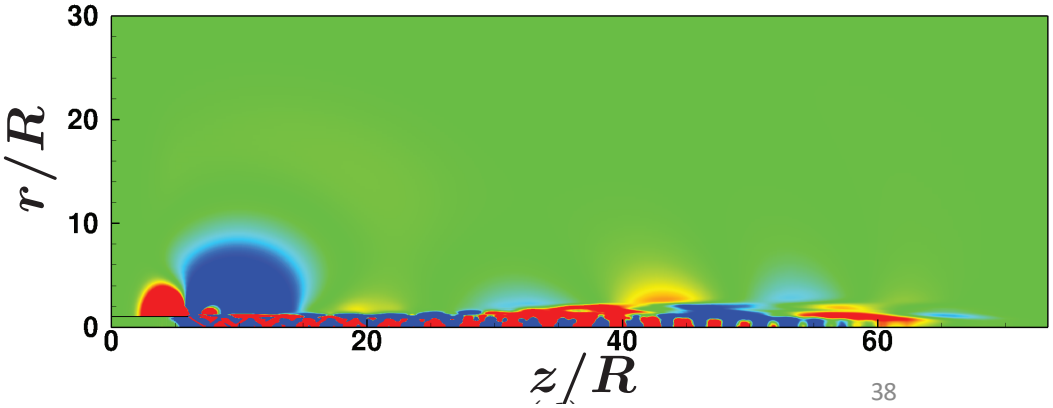
- Loud flows – Stable eigenmodes with acoustic footprint



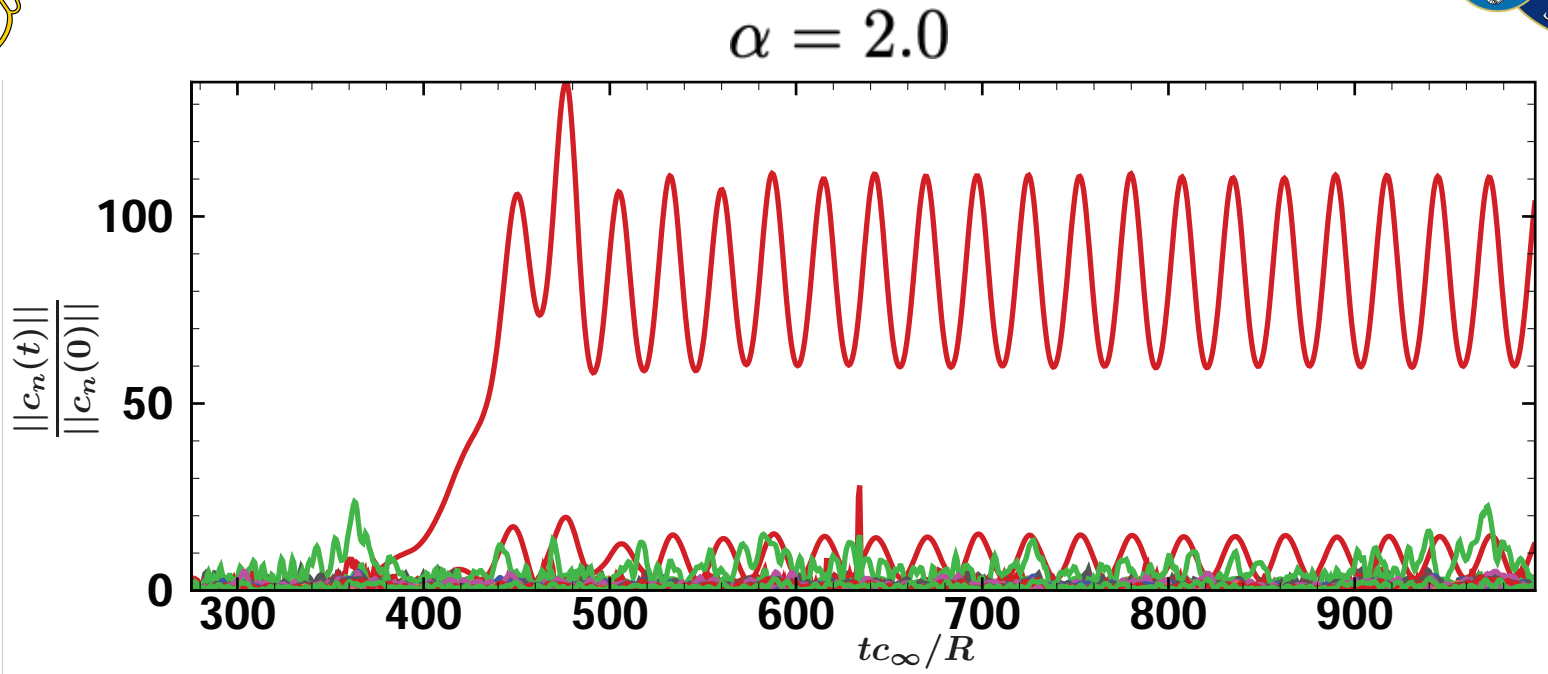


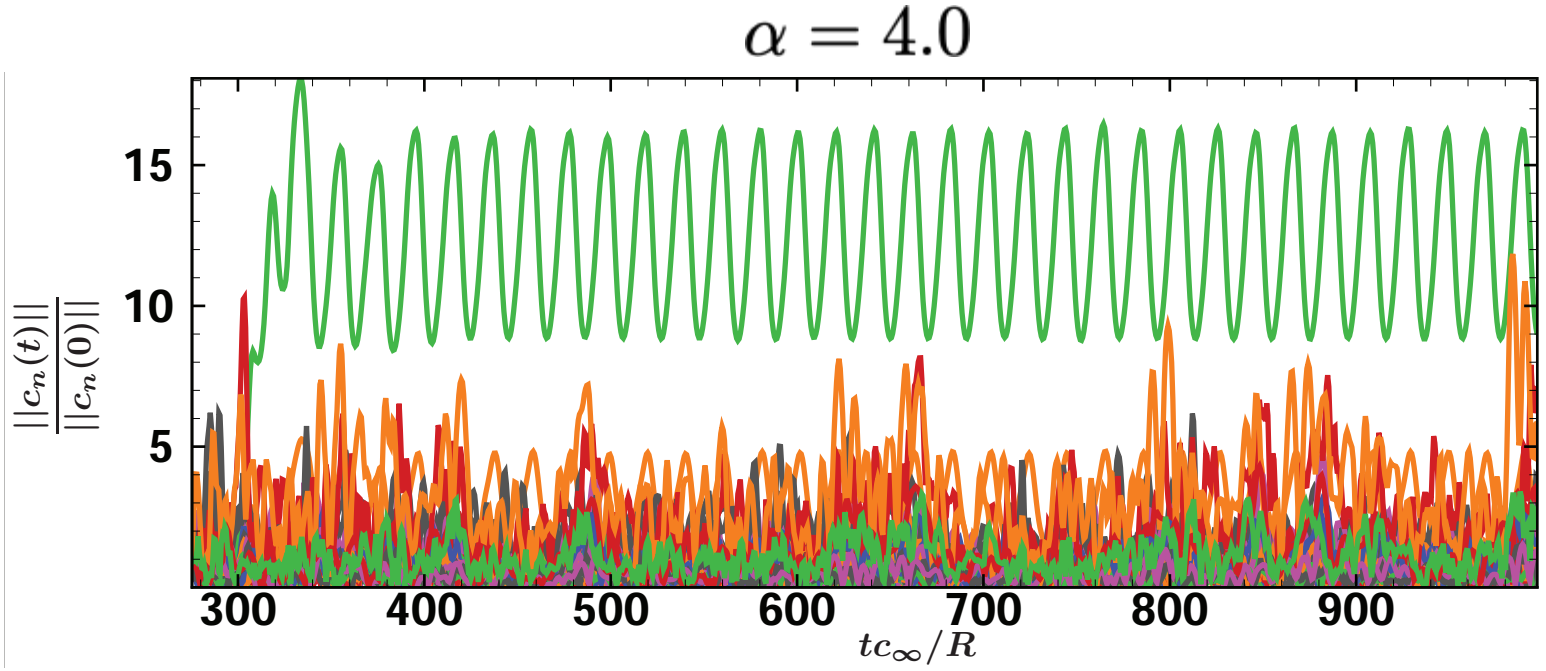
- Quieter flows – Unstable eigenmodes without acoustic footprint





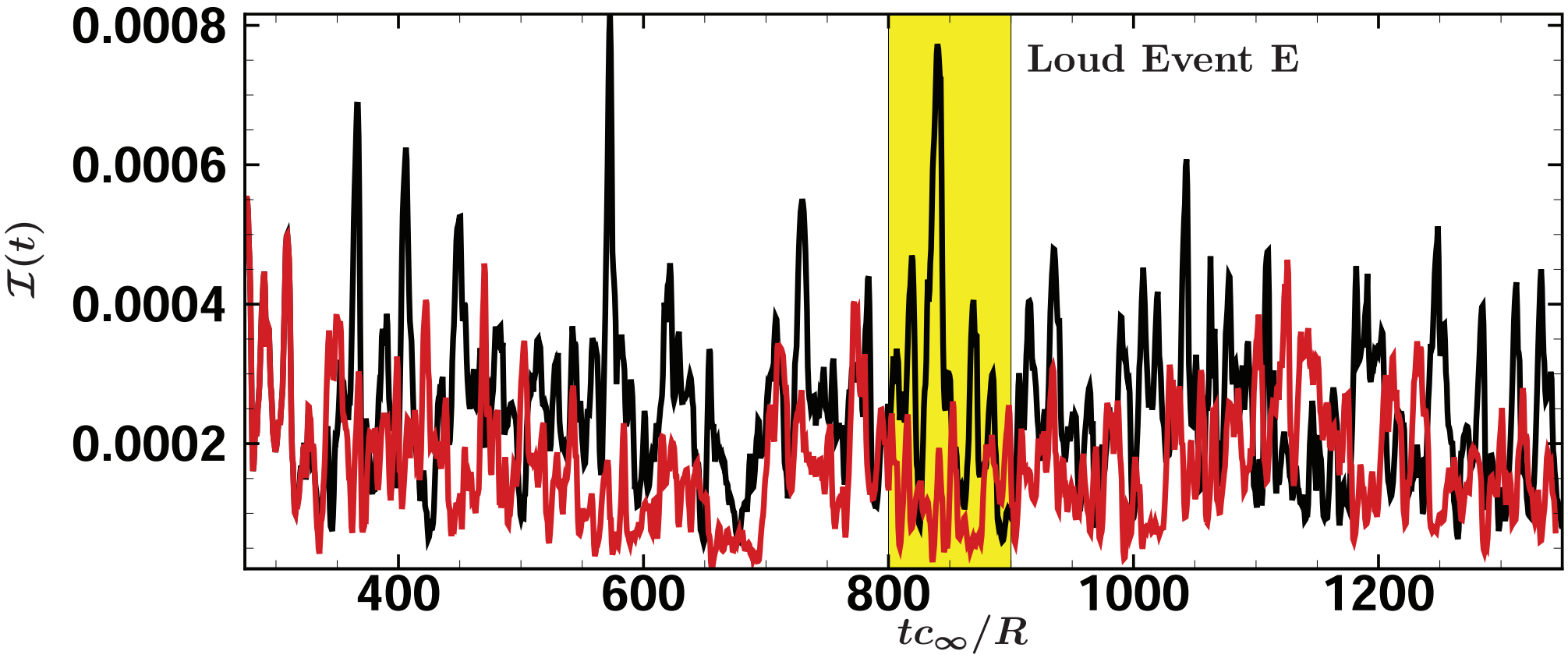
How does the control work – Mode amplification





How does the control work – POD Analysis

- Proper Orthogonal Decomposition (POD) analysis of a loud event gives valuable insights into the mechanism of control

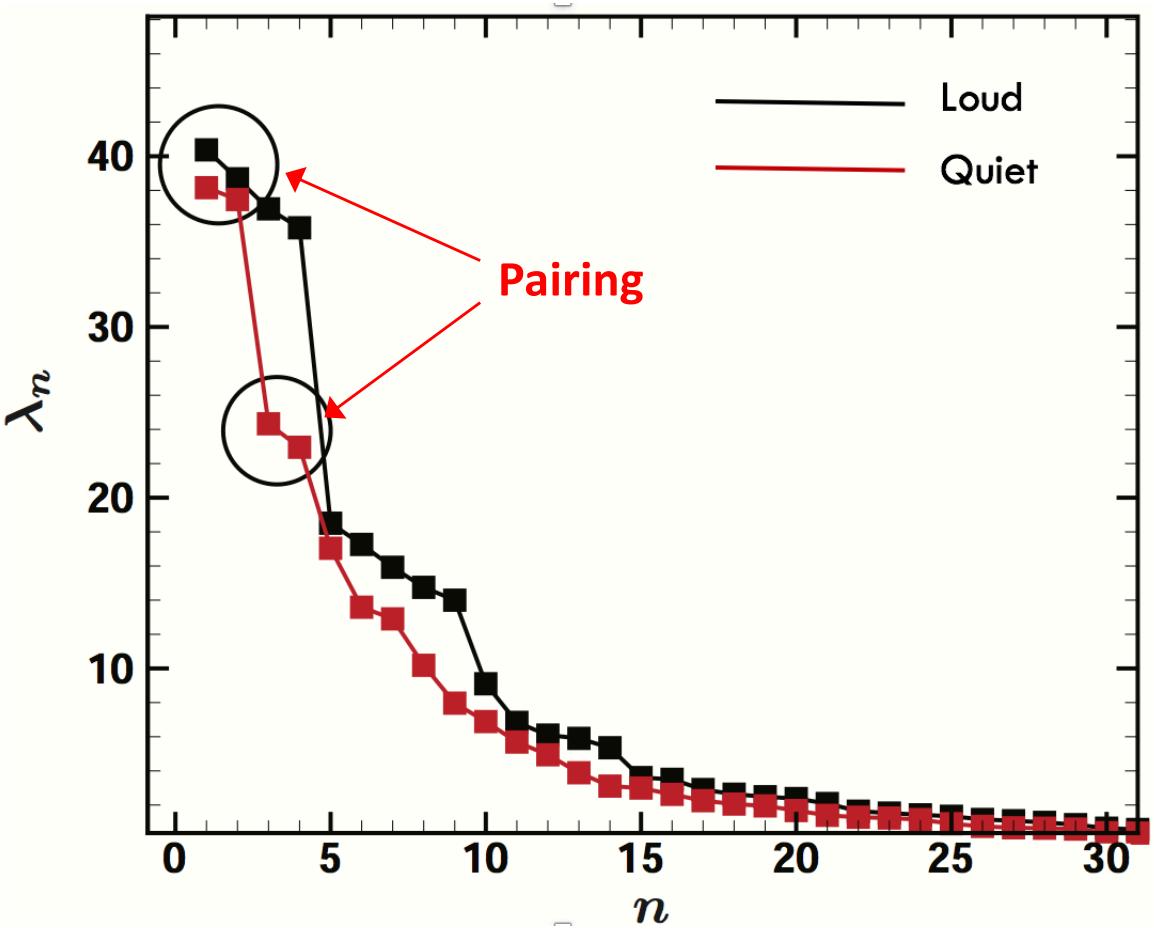


- A kinetic energy norm is used for the analysis $\int_{\mathcal{V}} V_r'^2 + V_z'^2 \, d\mathcal{V}$

How does the control work – POD Analysis

- POD analysis of loud and quiet flows

POD eigenspectrum

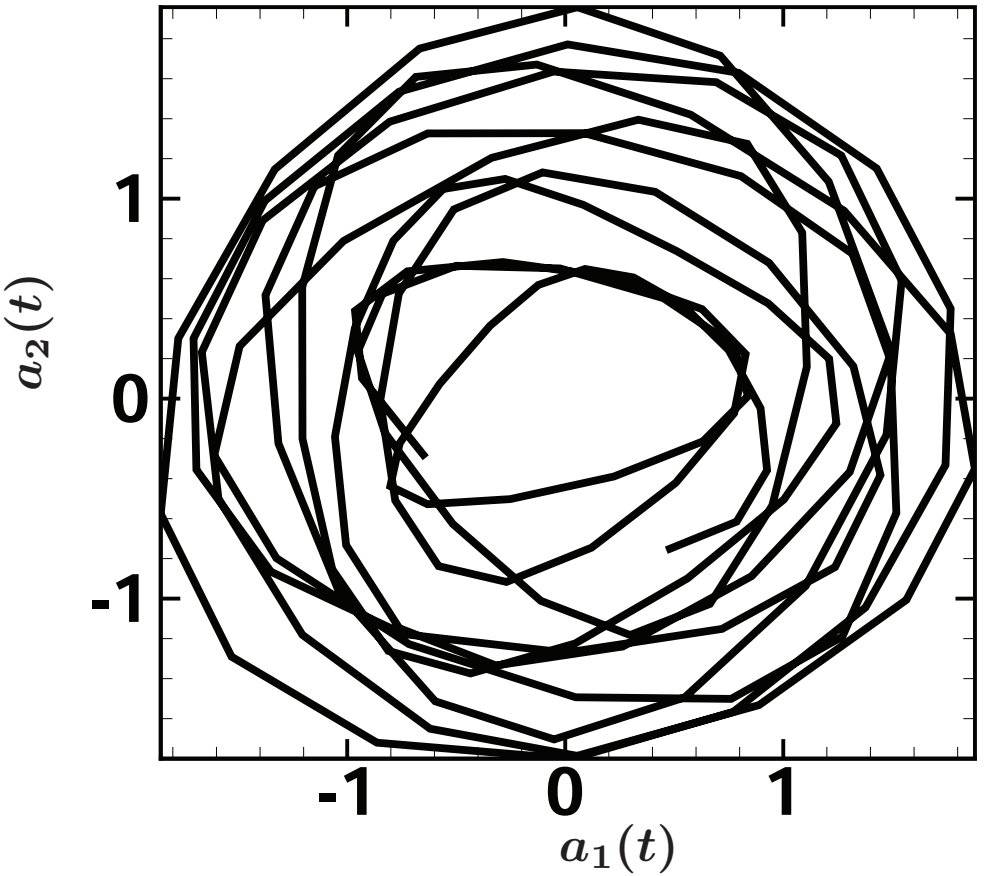


Pairing of energetic POD modes occur for quieter flows

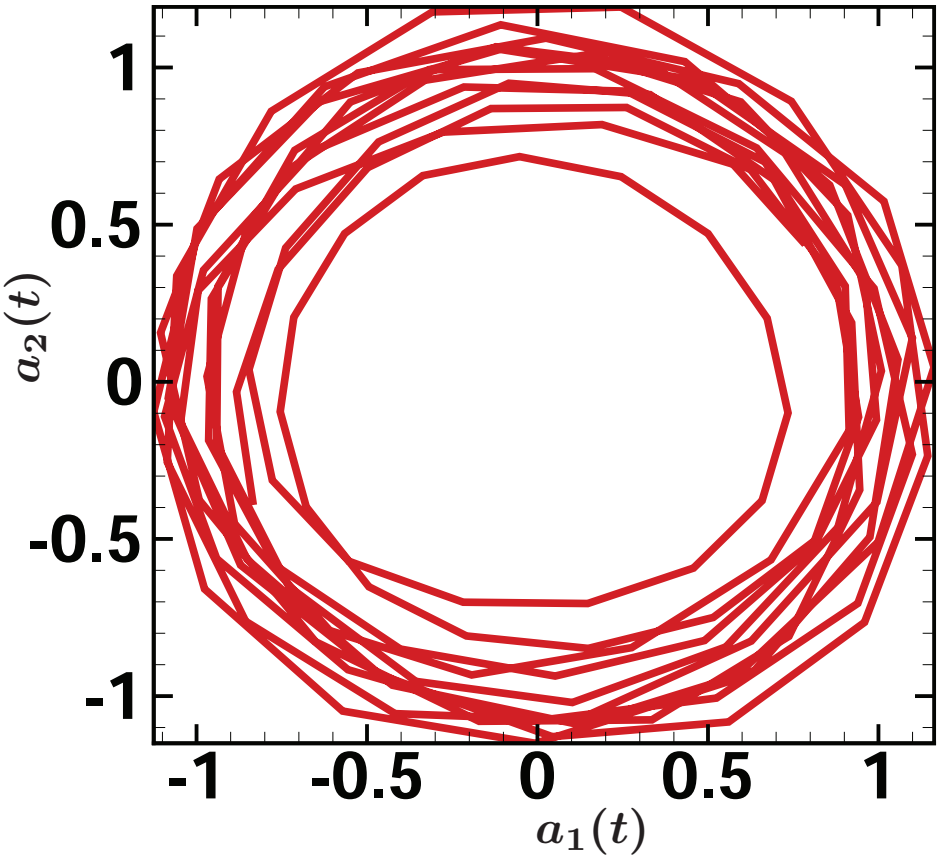
How does the control work – POD Analysis

- Phase plot of the POD coefficients of energetic modes provides insight on energetic flow structures

Loud



Quiet

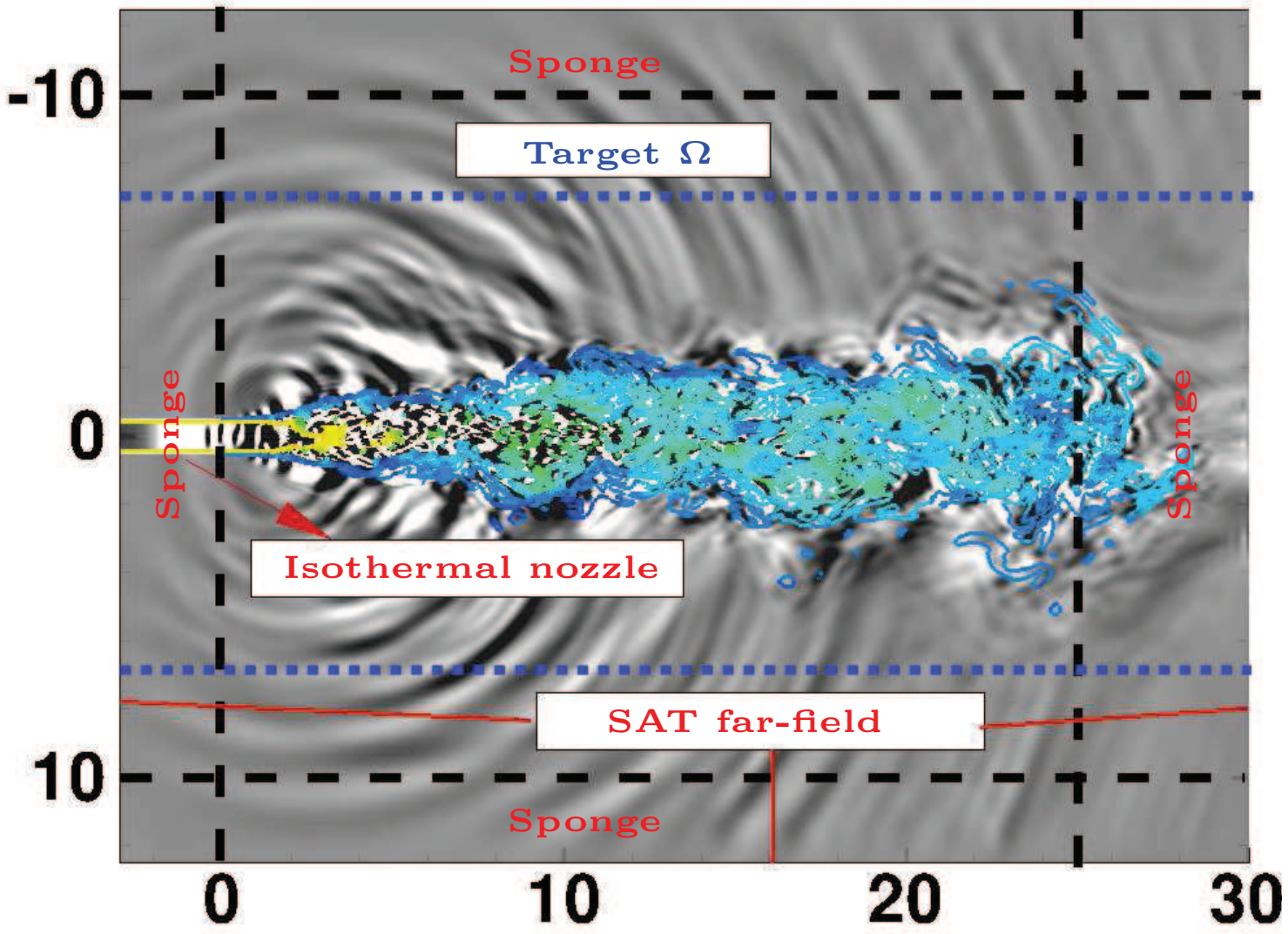


Quieter flows => Regularized energetic flow structures

Noise reduction in a Mach 0.9 turbulent jet

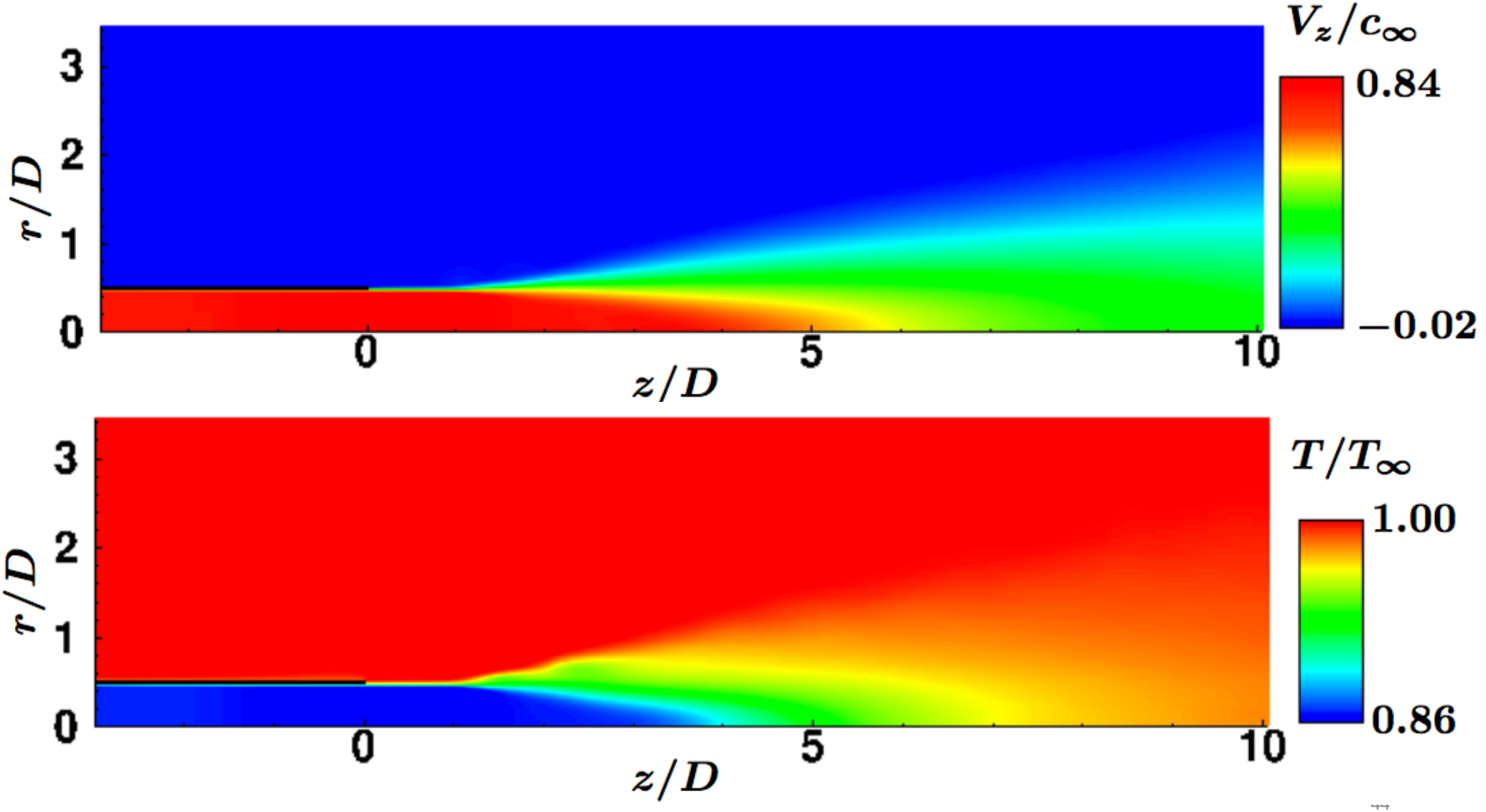
$$M_j = 0.9, Re = \frac{\rho_j U_j D}{\mu_j} = 88000, T_j/T_\infty = 0.86, \theta/D = 0.03$$

Isothermal nozzle with $T_w/T_\infty = 1, L/D = 3, t/D = 0.025$



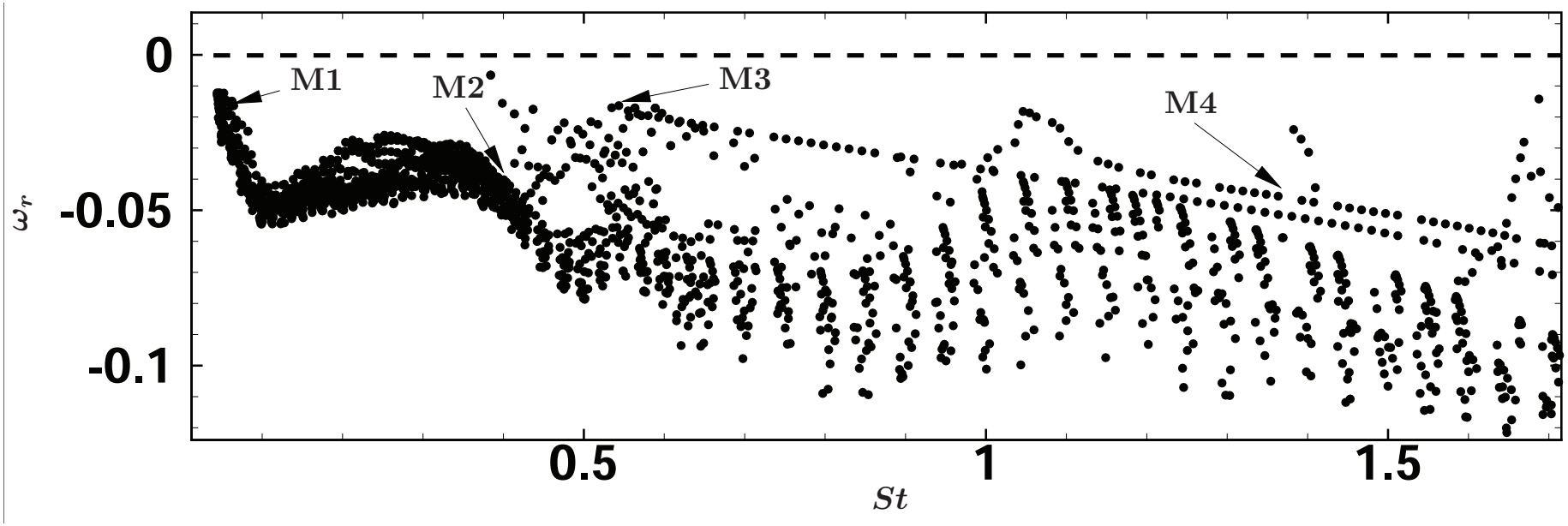
Time-and-azimuthal average

- The time average baseflow was computed from the large-eddy simulation

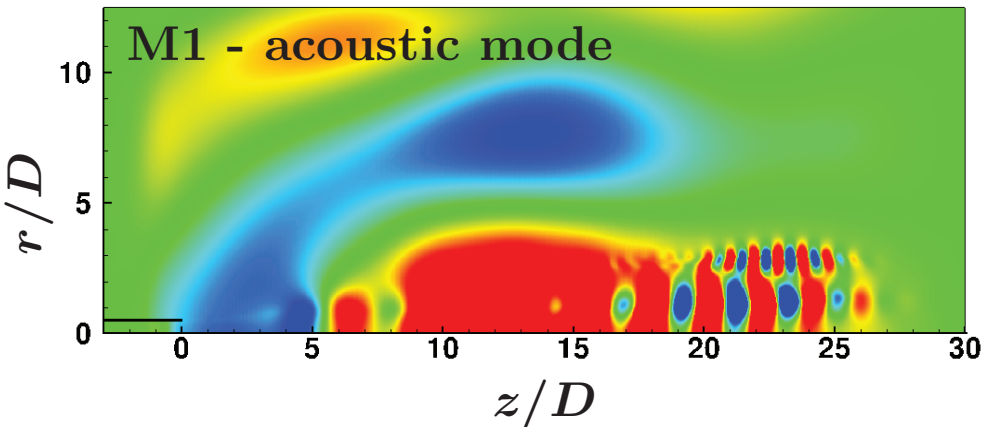


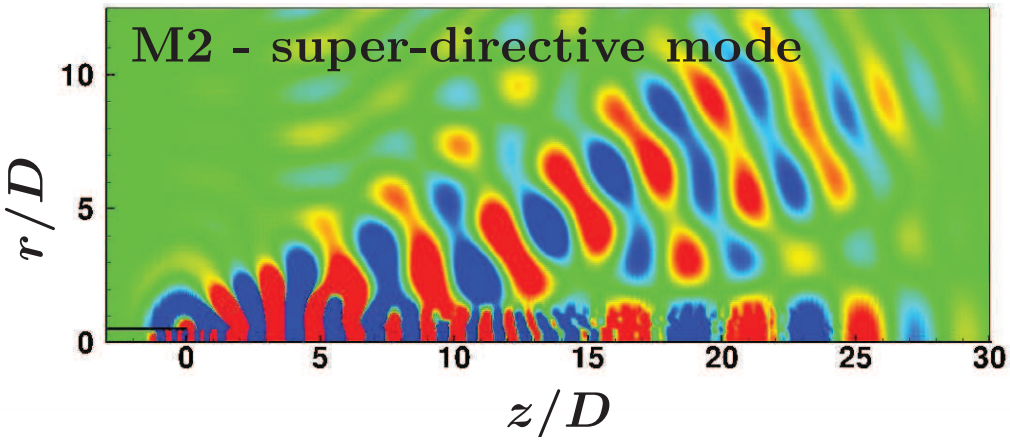
Eigenspectrum and global modes

- Global eigenanalysis is performed on the time-and-azimuthal averaged baseline flow



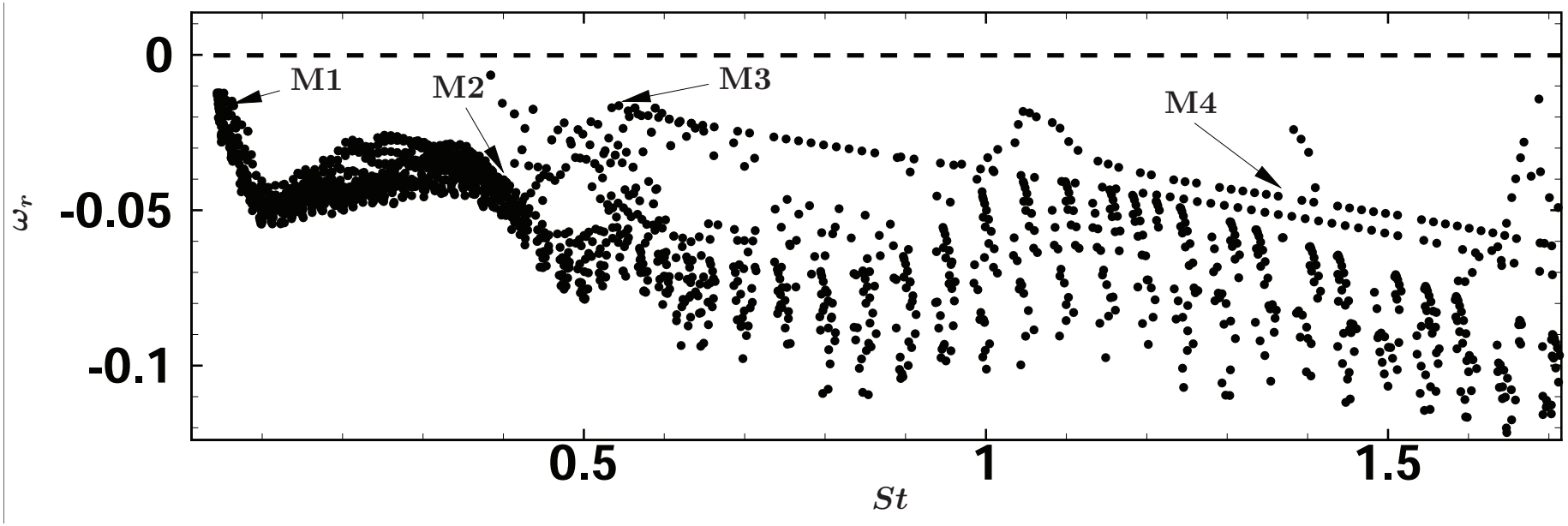
- Real part of pressure eigenmodes



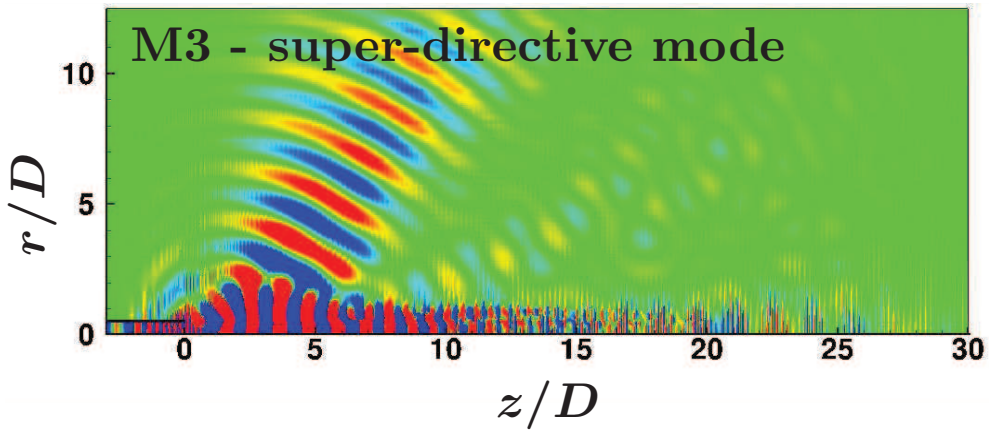


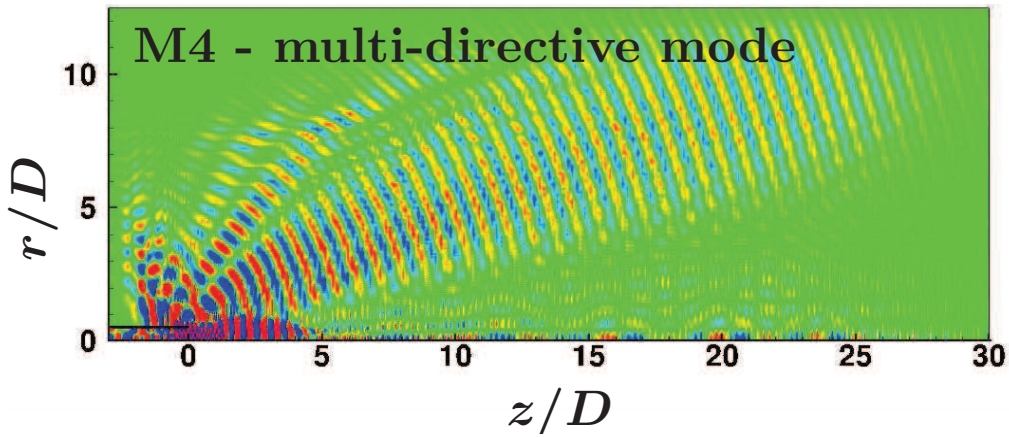
Eigenspectrum and global modes

- Global eigenanalysis is performed on the time-and-azimuthal averaged baseline flow



- Real part of pressure eigenmodes

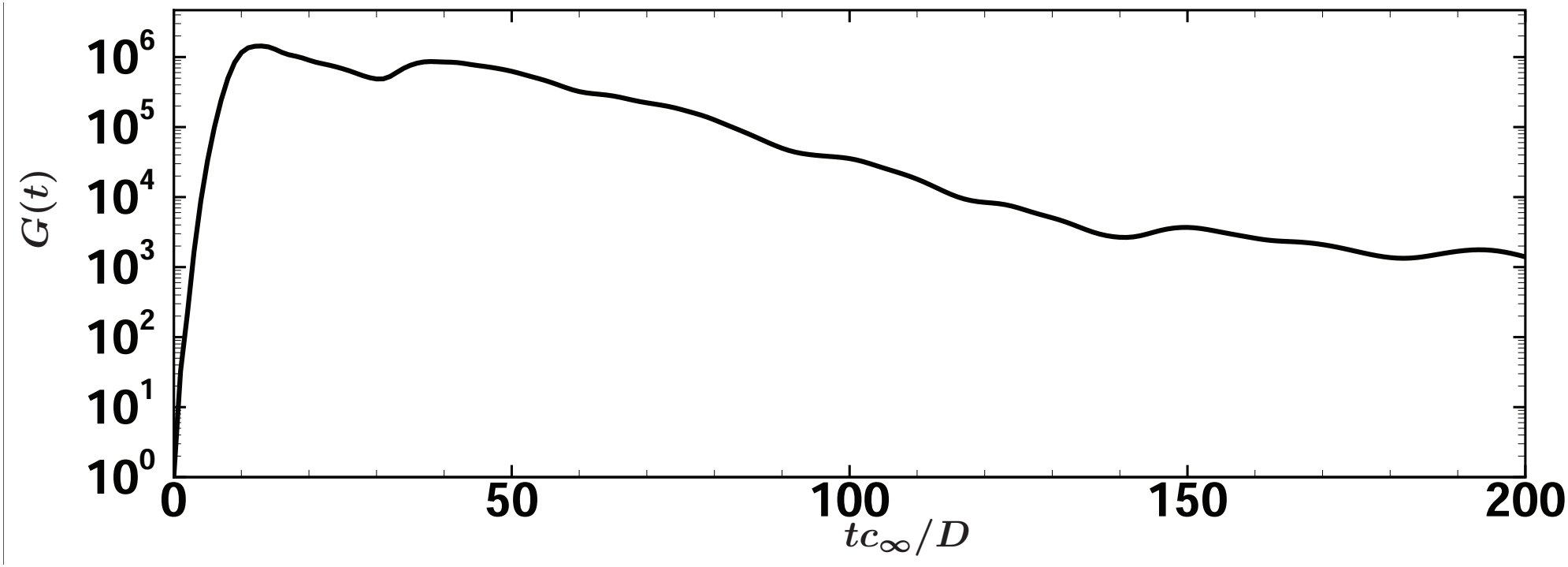




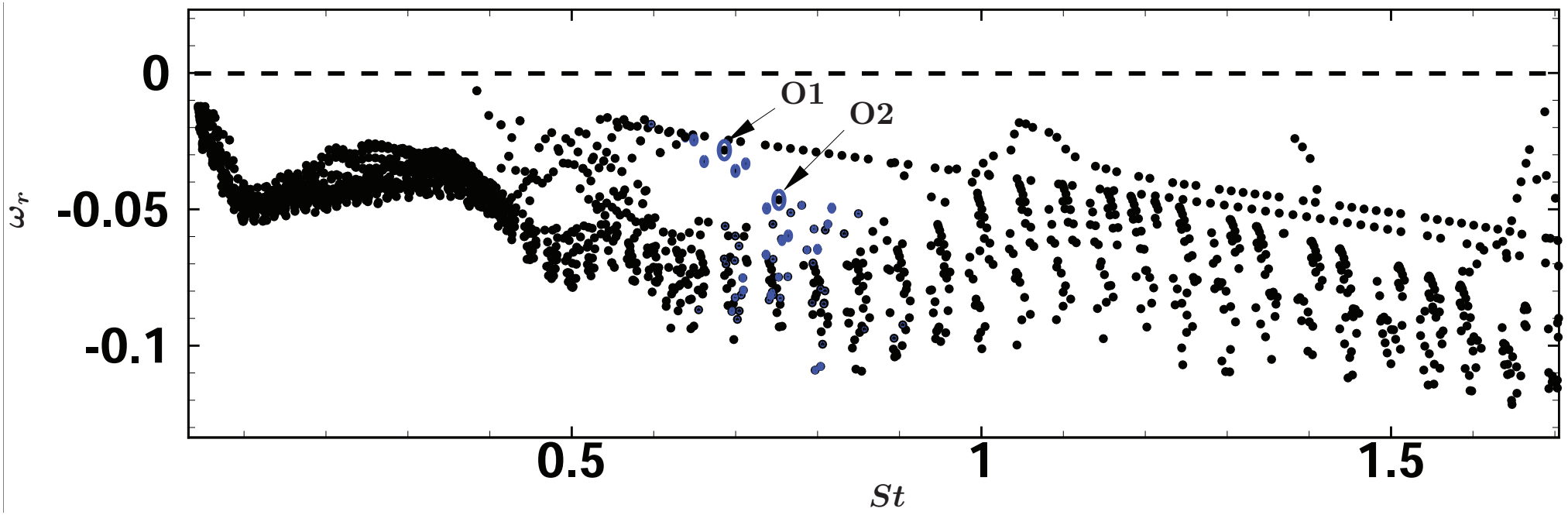
Optimal transient response – Mode contribution

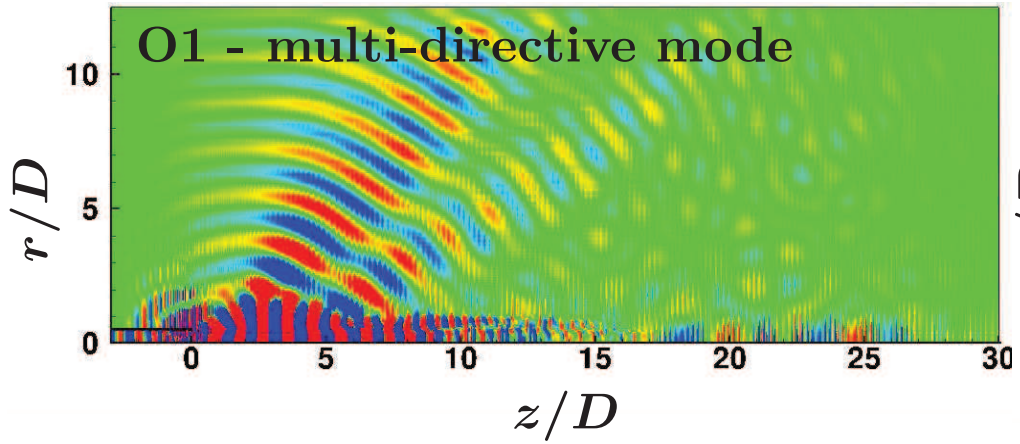
- Define the norm: $E(t) = \frac{1}{2}\int_{\mathcal{V}} \widehat{p}(t)\widehat{p}(t)^* \, dV$

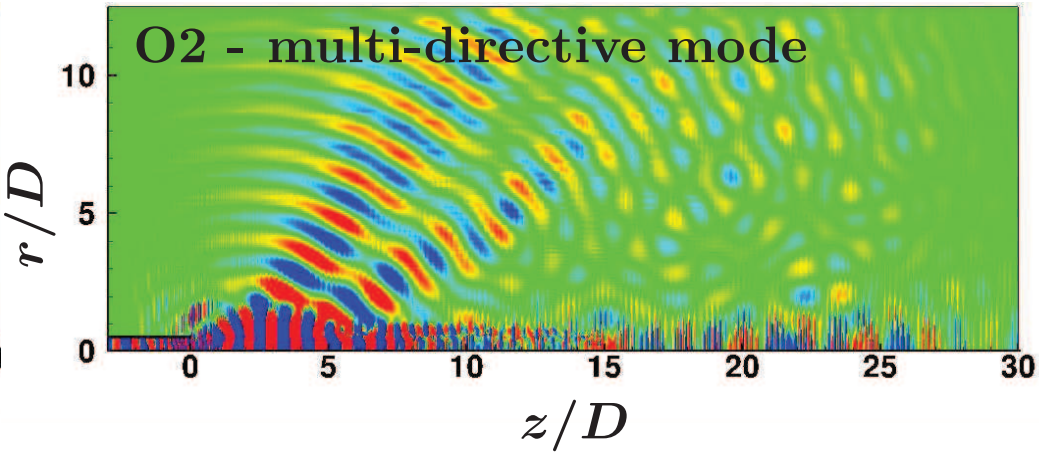
- Maximize $G(t) \equiv \max \frac{E(t)}{E(0)}$



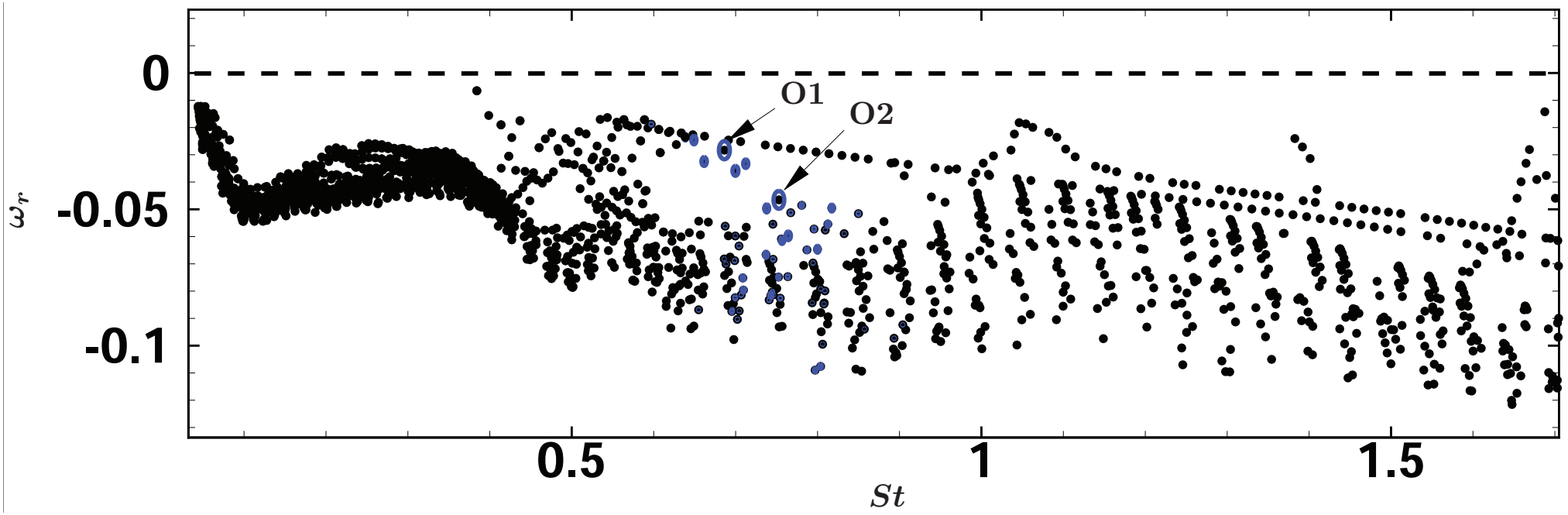
Optimal transient response – Mode contribution



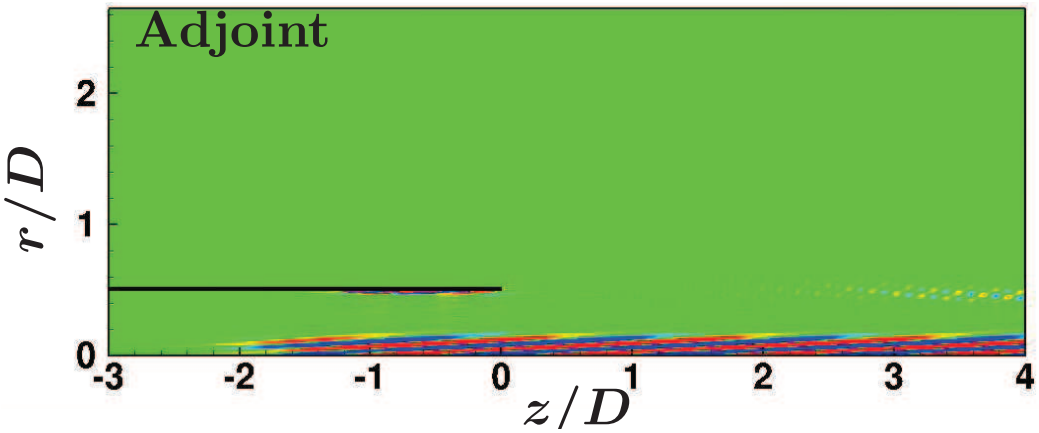


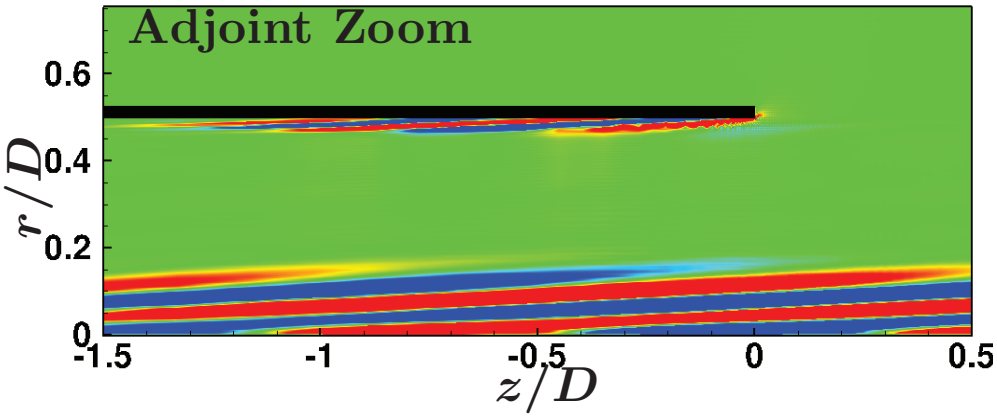


Optimal transient response – Mode contribution



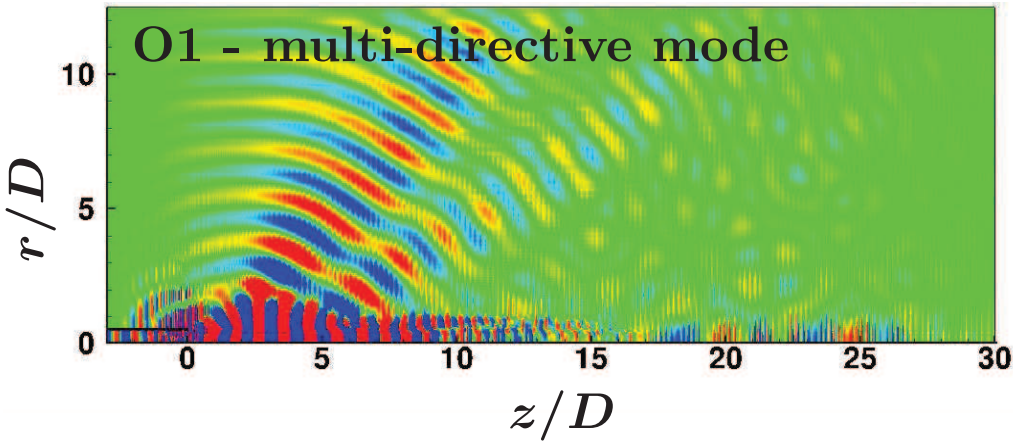
- $Re(V_z^\dagger)$ for O1 (maximal contribution to optimal transient response)

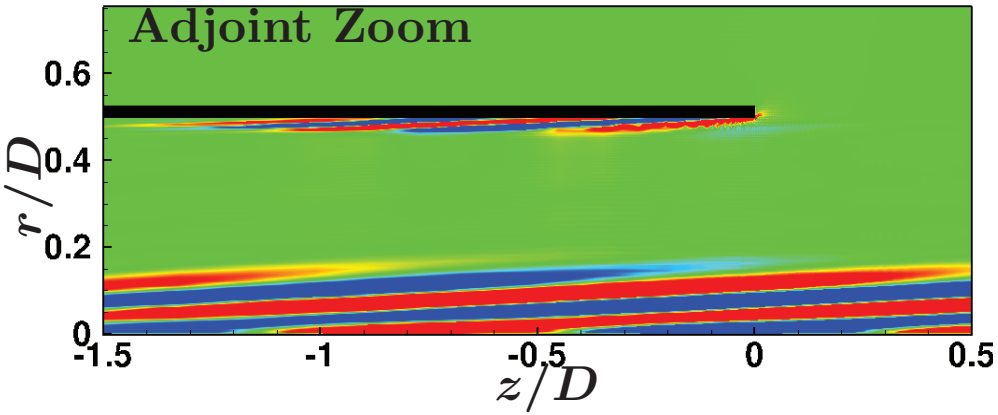




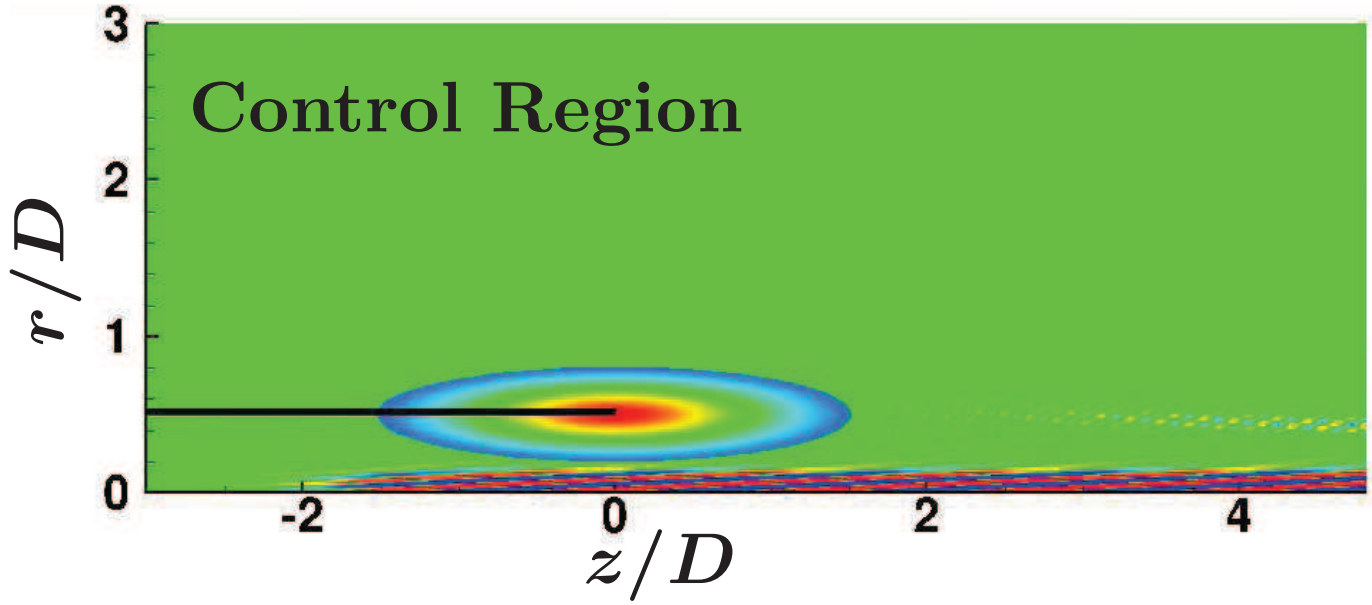
Actuator/sensor development

- Forward and adjoint of the eigenmode with maximum contribution to optimal transient response



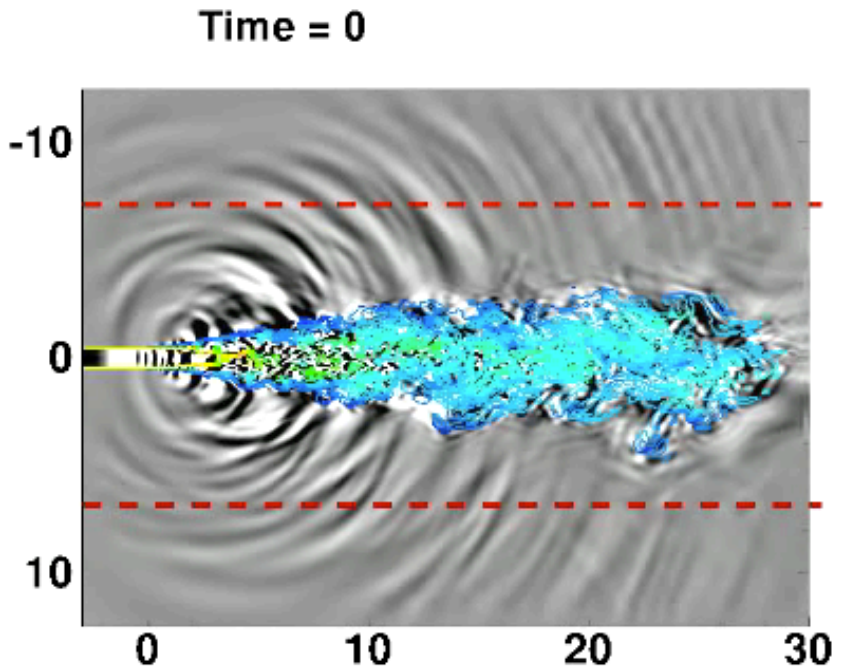


- Control region for V_z control - V_r feedback

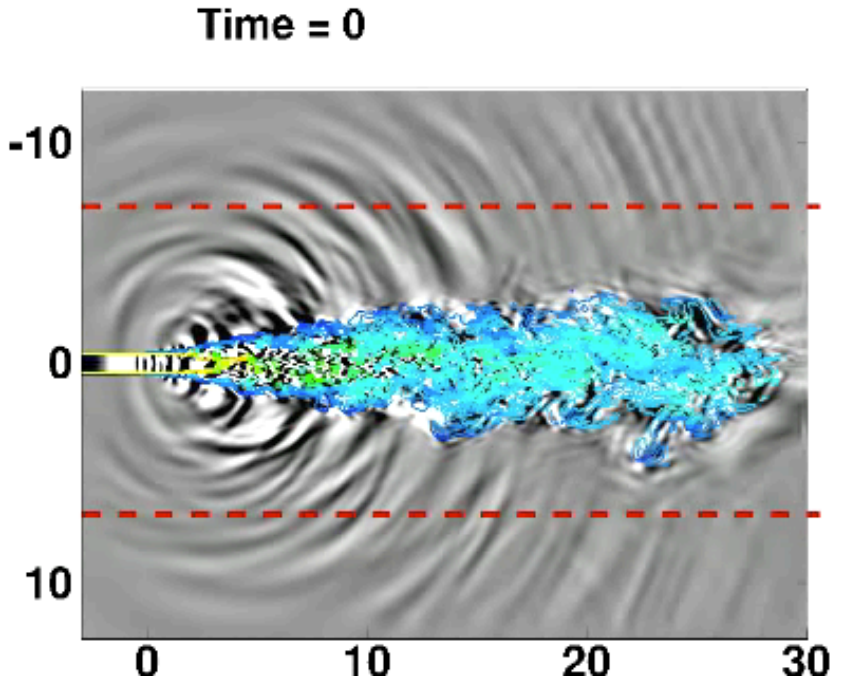


Noise reduction of a Mach 0.9 turbulent jet

Loud

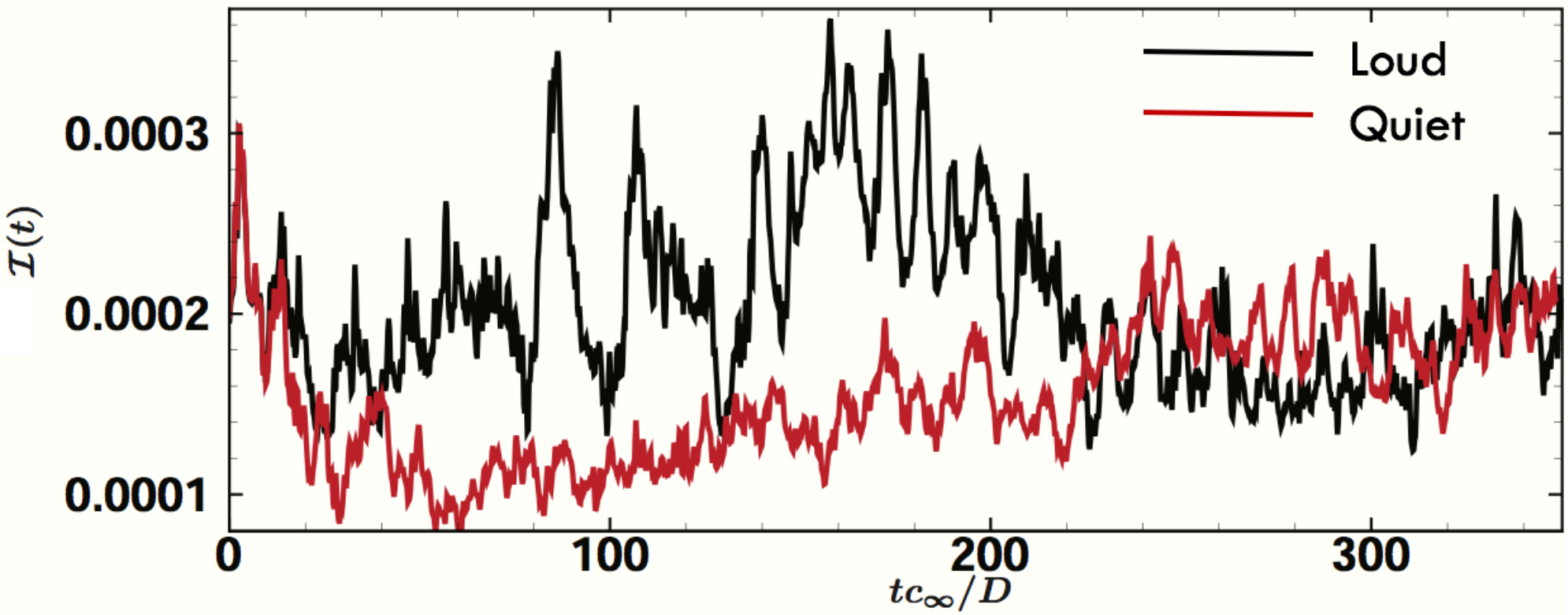


Quiet

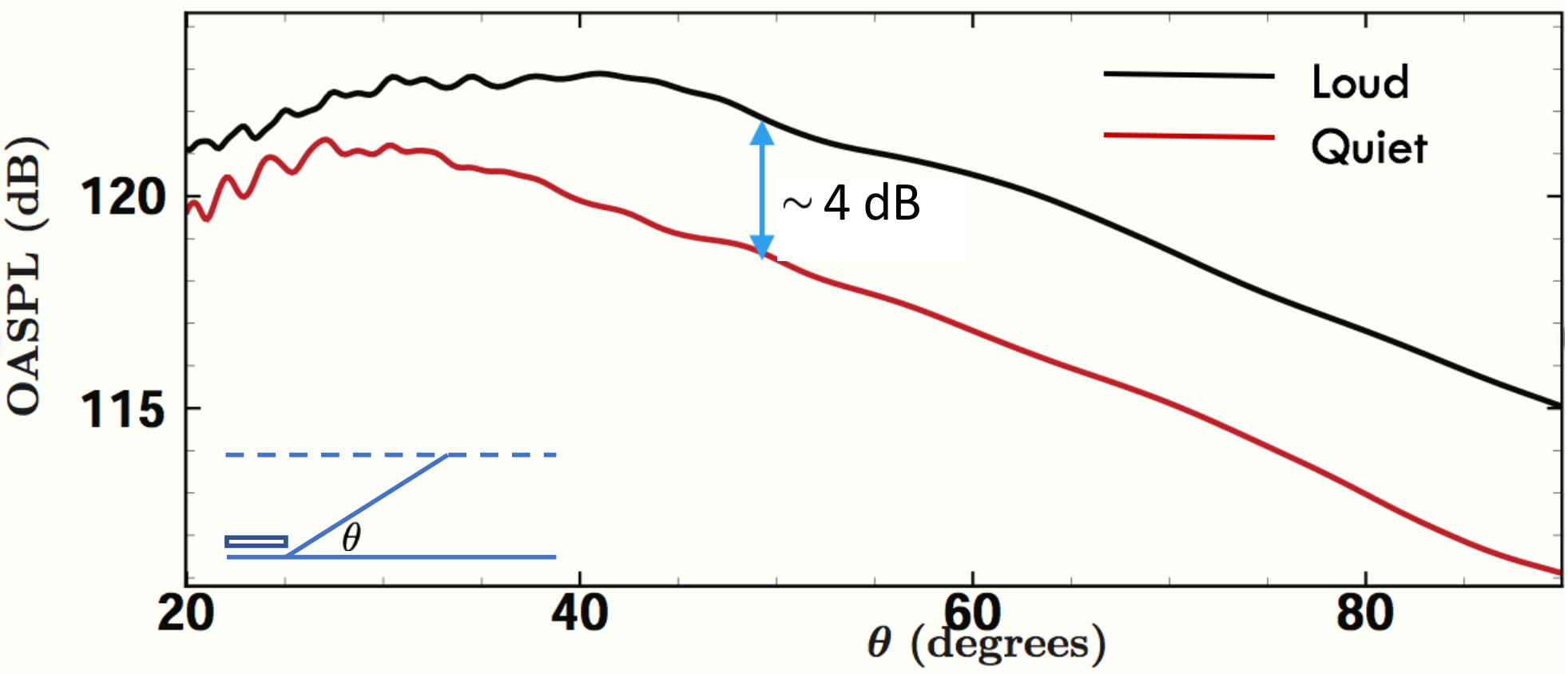


Objective function – target surface r/D=7

- The objective function is $\mathcal{I}(t) = \int_{\Omega} p'(\vec{x},t)^2 \, d\Omega$

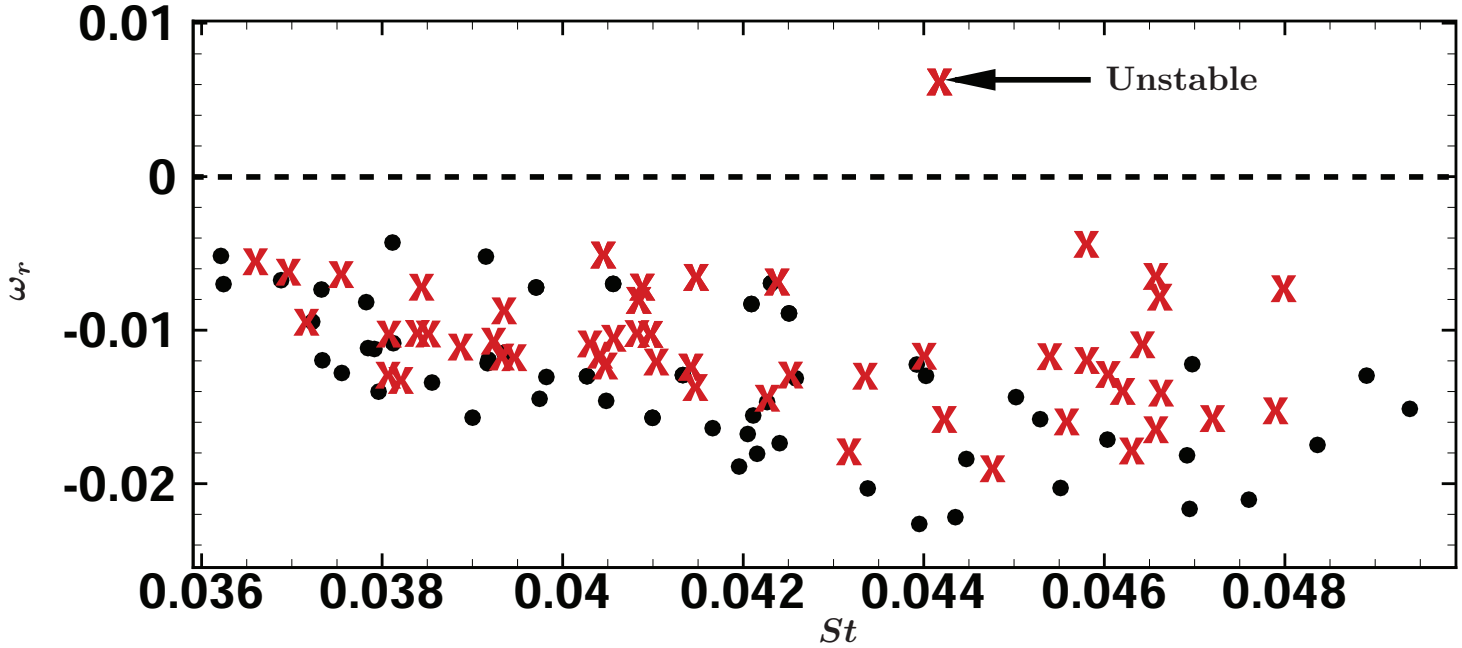


Effect on radiated noise - OASPL

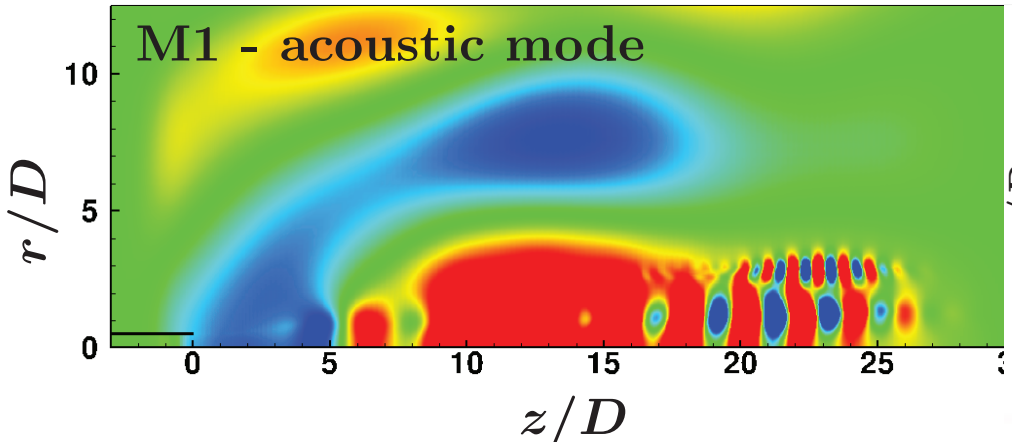


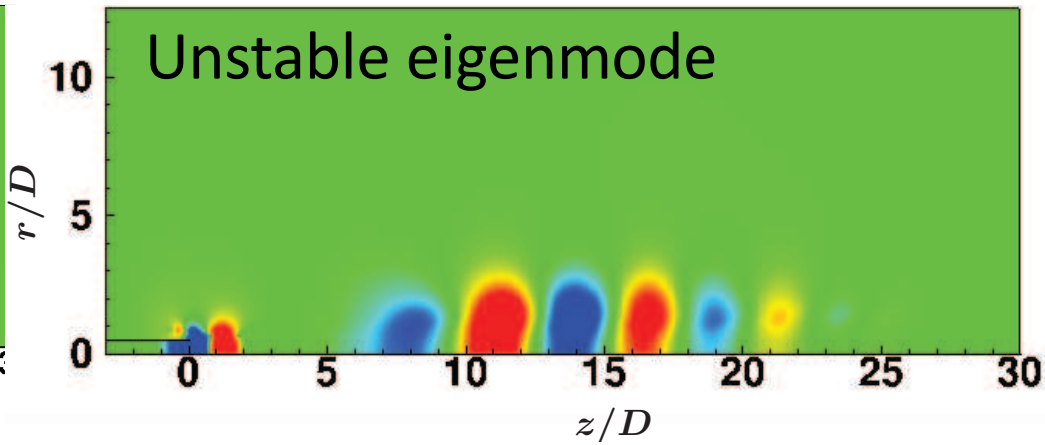
Quieter flow - eigenanalysis

- Eigenspectrum for time-and-azimuthal average of noise controlled flow



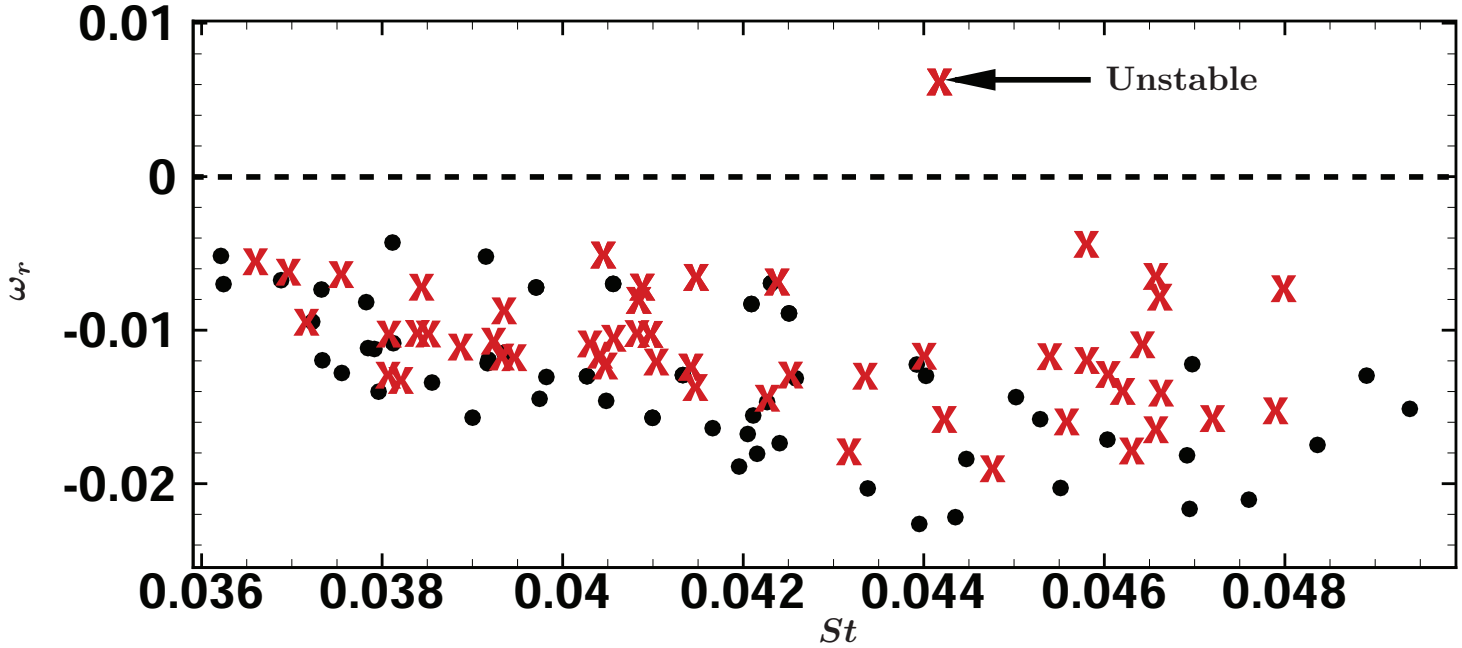
- Unstable eigenmode does not have an acoustic footprint



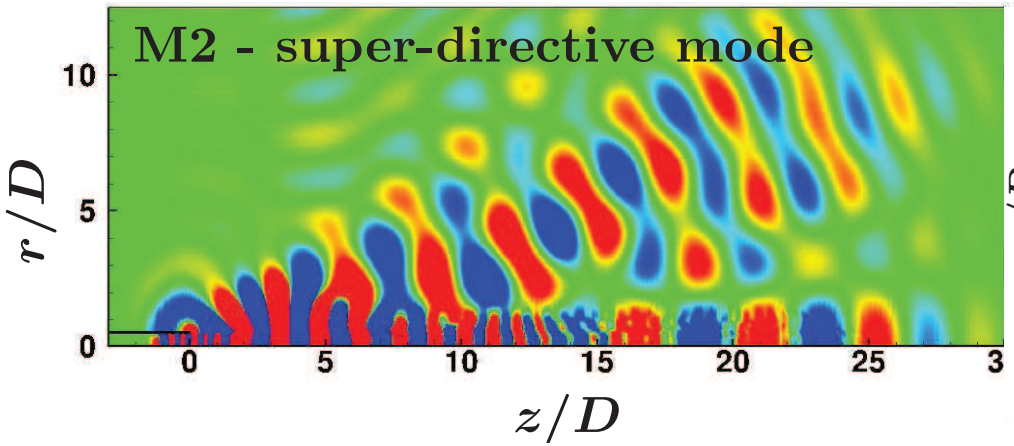


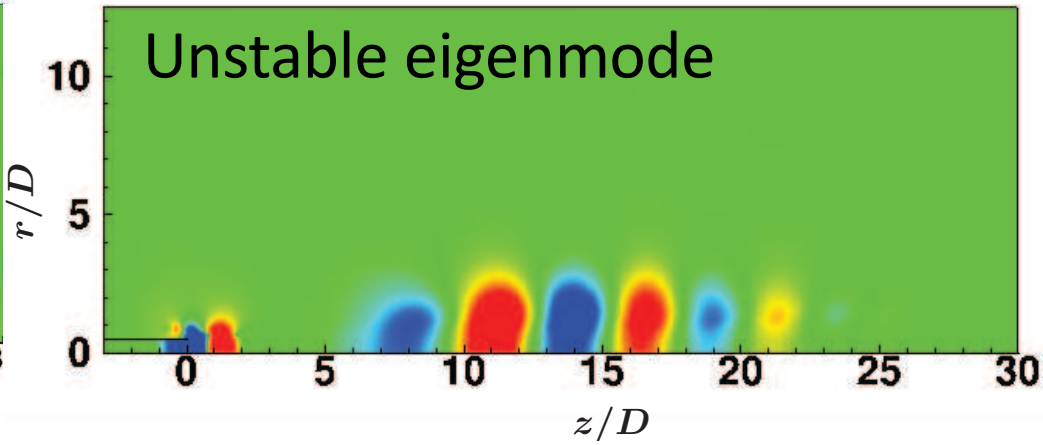
Quieter flow - eigenanalysis

- Eigenspectrum for time-and-azimuthal average of noise controlled flow



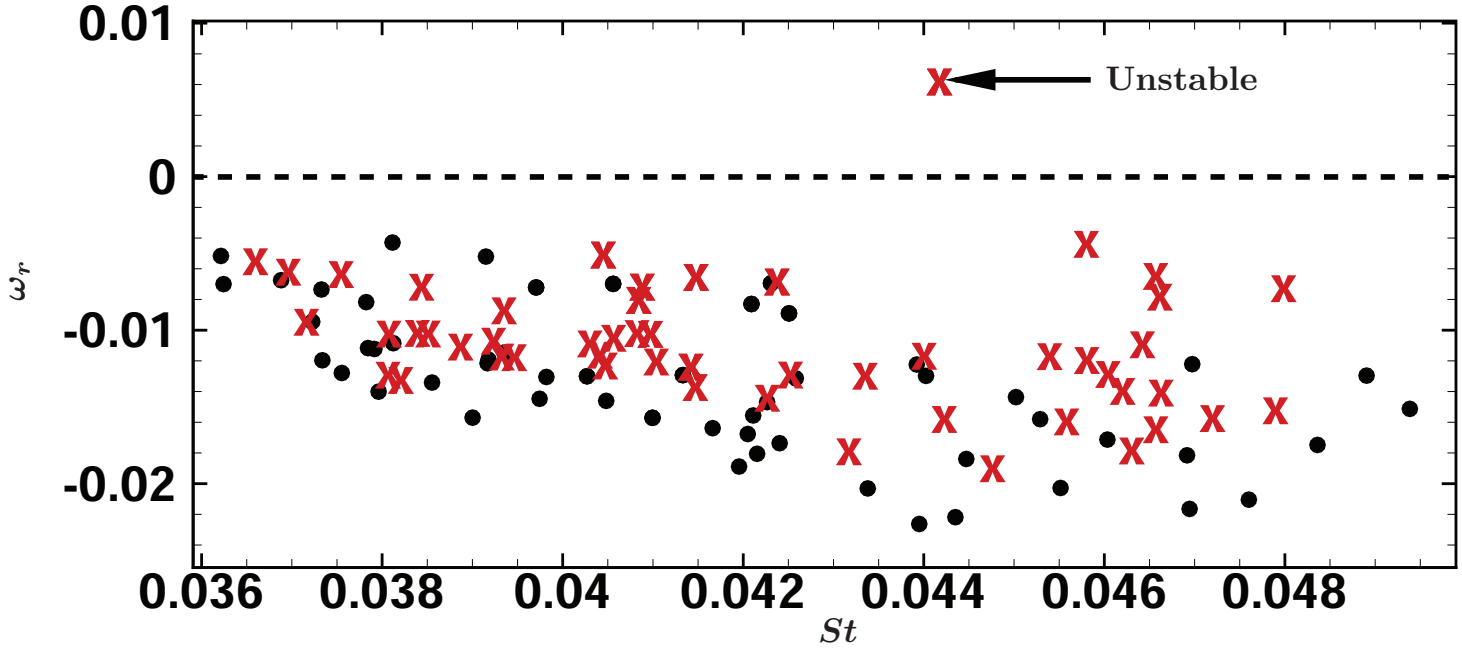
- Unstable eigenmode does not have an acoustic footprint



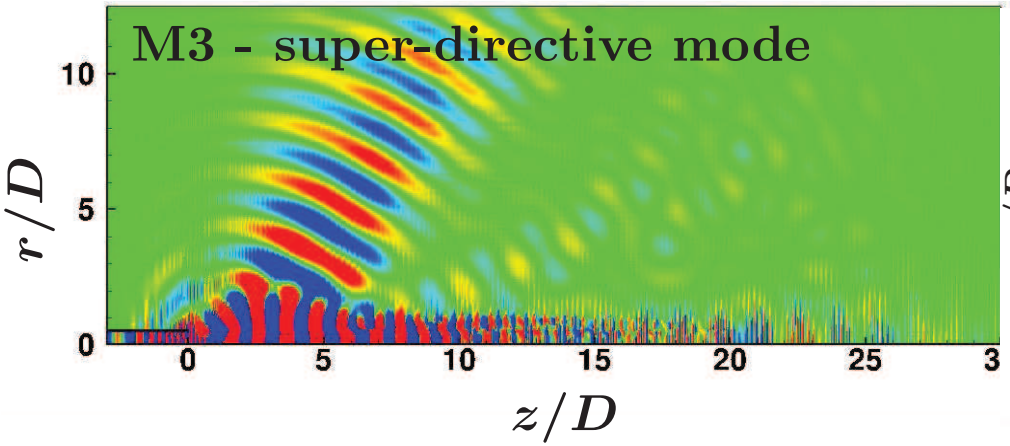


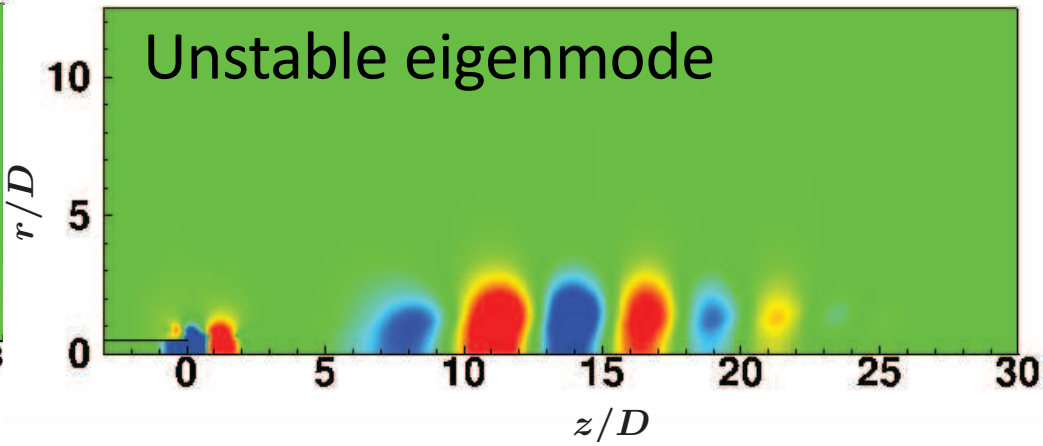
Quieter flow - eigenanalysis

- Eigenspectrum for time-and-azimuthal average of noise controlled flow



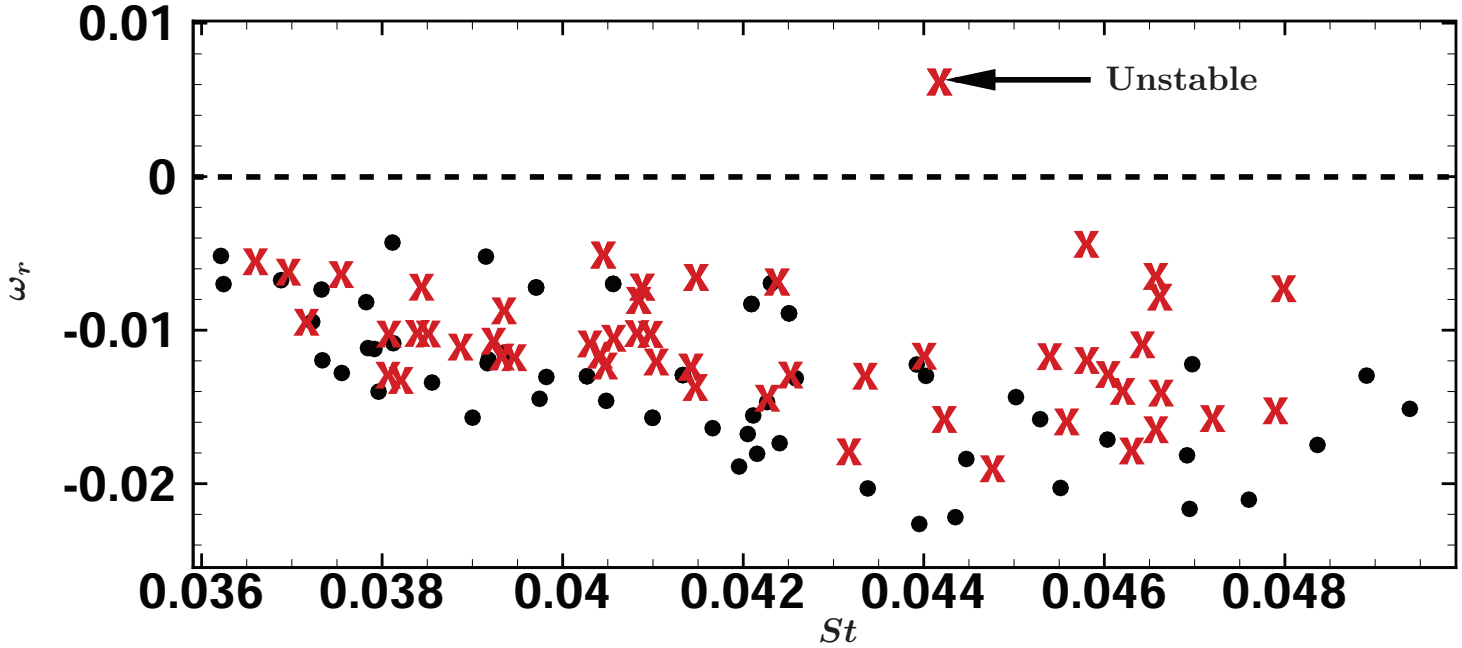
- Unstable eigenmode does not have an acoustic footprint



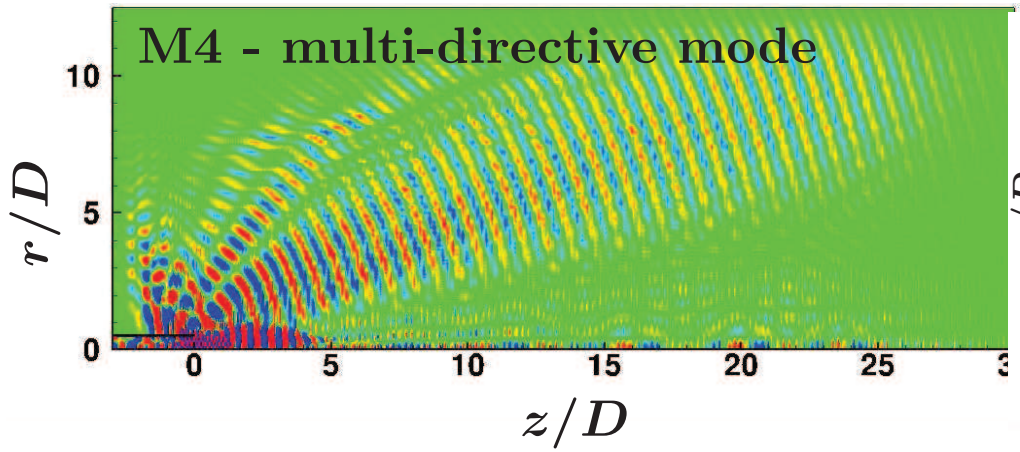


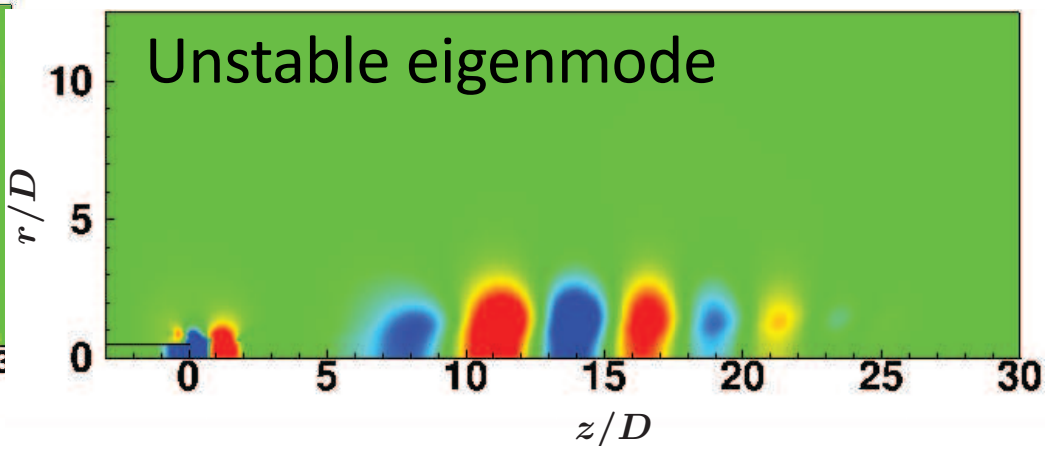
Quieter flow - eigenanalysis

- Eigenspectrum for time-and-azimuthal average of noise controlled flow



- Unstable eigenmode does not have an acoustic footprint

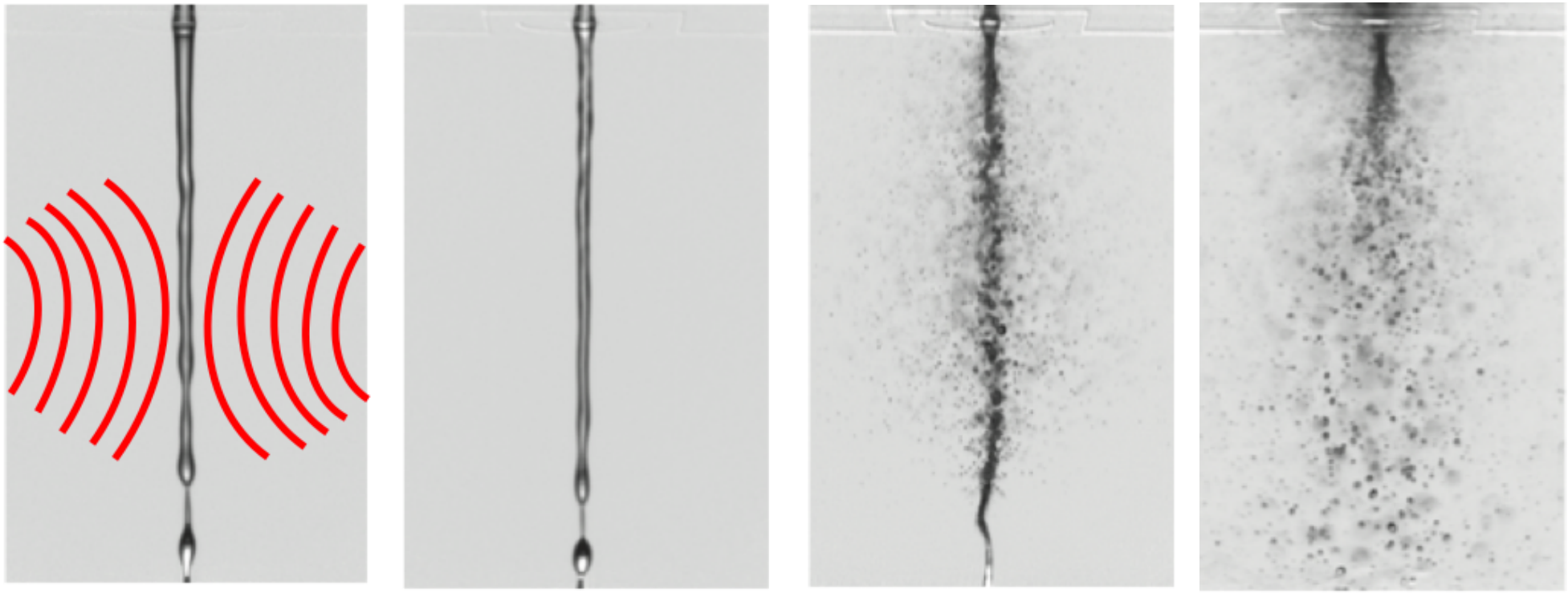




Spray control with acoustic excitation

- Control of primary atomization in fuel sprays in gas turbine combustors (Funded by the Office of Naval Research)
- High amplitude (12 kPa, 1 kHz) transverse acoustic waves are used
- Sound pressure level of 172 dB

Experiments (Ficuciello et. al. 2017)



Governing equations

Volume of fluid (VOF) method – unsplit, geometric transport (Owkes 2014)

- Fractional step time integrator with implicit handling of the pressure term (Kwatra 2009)

$$\frac{\partial \alpha_i}{\partial t} + \nabla \cdot (\alpha_i \vec{u}) = \alpha_i \nabla \cdot \vec{u}$$ Volume of fluid transport

$$\frac{\partial \rho_i \alpha_i}{\partial t} + \nabla \cdot (\rho_i \alpha_i \vec{u}) = 0$$ Density for each phase

$$\frac{\partial \vec{m}_i}{\partial t} + \nabla \cdot (\vec{m}_i \otimes \vec{u}) = -\nabla \cdot (p\mathbb{I}) + \nabla \cdot \overline{\overline{\tau}}$$ Momentum for each phase

$$\frac{\rho_i E_i \alpha_i}{\partial t} + \nabla \cdot (\rho_i \alpha_i E_i \vec{u}) = -\nabla \cdot (p \alpha_i \vec{u}) + \nabla \cdot (\vec{u} \cdot \overline{\overline{\tau}} + k \nabla T)$$ Total energy for each phase

- Stiffened gas equation of state

- Interface reconstruction using Piecewise Linear Interface Calculation (PLIC) – the liquid-gas interface is reconstructed as a plane in each cell

M. Owkes and O. Desjardins, *A computational framework for conservative, three-dimensional, unsplit, geometric transport with application to the volume-of-fluid (VOF) method*, J. Comp. Phys. (2014) 270, 587-612
N. Kwatra et al., *A method for avoiding the acoustic time step restriction in compressible flow*, J. Comp. Phys. (2009) 228 (11), 4146-4161

The all-Mach algorithm

- Advection step – Semi Lagrangian scheme

$$\frac{\partial \alpha_i}{\partial t} + \nabla \cdot (\alpha_i \vec{u}) = \alpha_i \nabla \cdot \vec{u}$$

$$\frac{\partial \rho_i \alpha_i}{\partial t} + \nabla \cdot (\rho_i \alpha_i \vec{u}) = 0$$

$$\frac{\partial \vec{m}_i}{\partial t} + \nabla \cdot (\vec{m}_i \otimes \vec{u}) = 0$$

$$\frac{\rho_i E_i \alpha_i}{\partial t} + \nabla \cdot (\rho_i \alpha_i E_i \vec{u}) = 0$$

No pressure

- Intermediate variables are computed - $\vec{u}^*$ and p^*
- Helmholtz equation for pressure

$$p^{n+1} - \rho^n (c^2)^n \Delta t^2 \nabla \cdot \left(\frac{\nabla p^{n+1}}{\rho^{n+1}} \right) = p^* - \rho^n (c^2)^n \Delta t \nabla \cdot \vec{u}^*$$

- Correction step

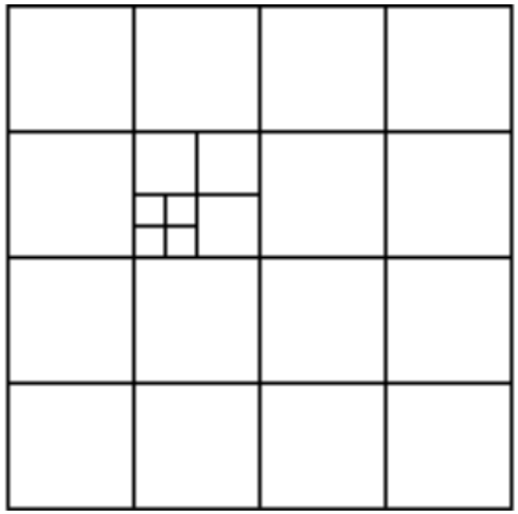
$$\rho \vec{u} = \rho \vec{u}^* - \Delta t \nabla p$$

$$u_{\text{face}} = u^*_{\text{face}} - \Delta t \frac{1}{\rho} \nabla p$$

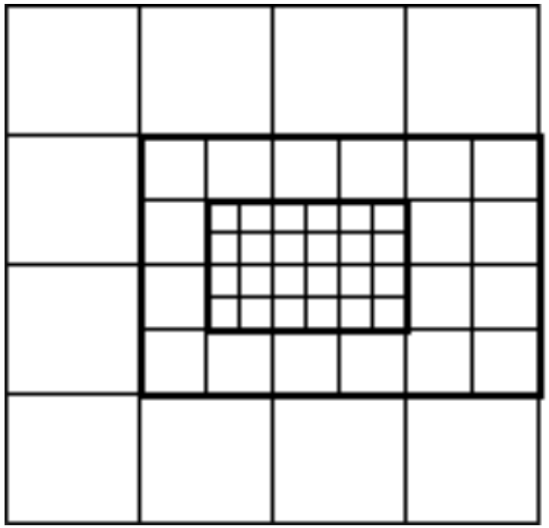
$$\rho_i E_i = \rho_i E_i^* - \Delta t \nabla \cdot (\alpha_i p \vec{u})$$

Adaptive mesh refinement

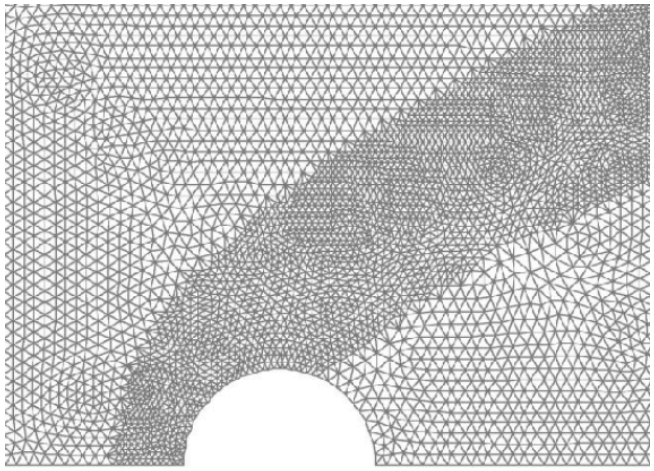
Oct-tree based



Block-structured



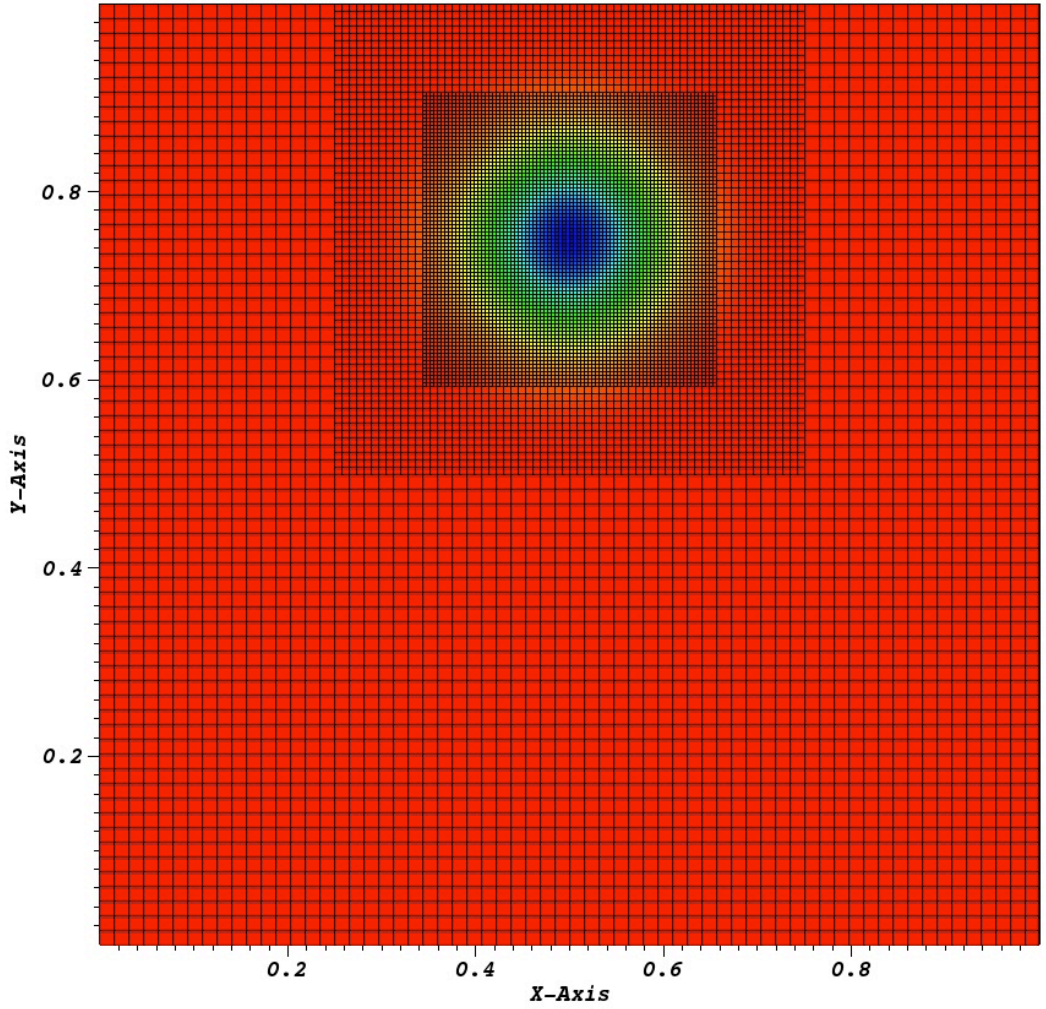
Unstructured



- Loop and cache optimizations can be performed over the arrays of cells when using adaptive blocks.
- Ghost cell to computational cell ratio is superior to other data structures.
- Since the blocks permit refinement of larger multi-cell regions at a time, mesh adaptation is required less frequently

The framework of AMReX (LBNL)

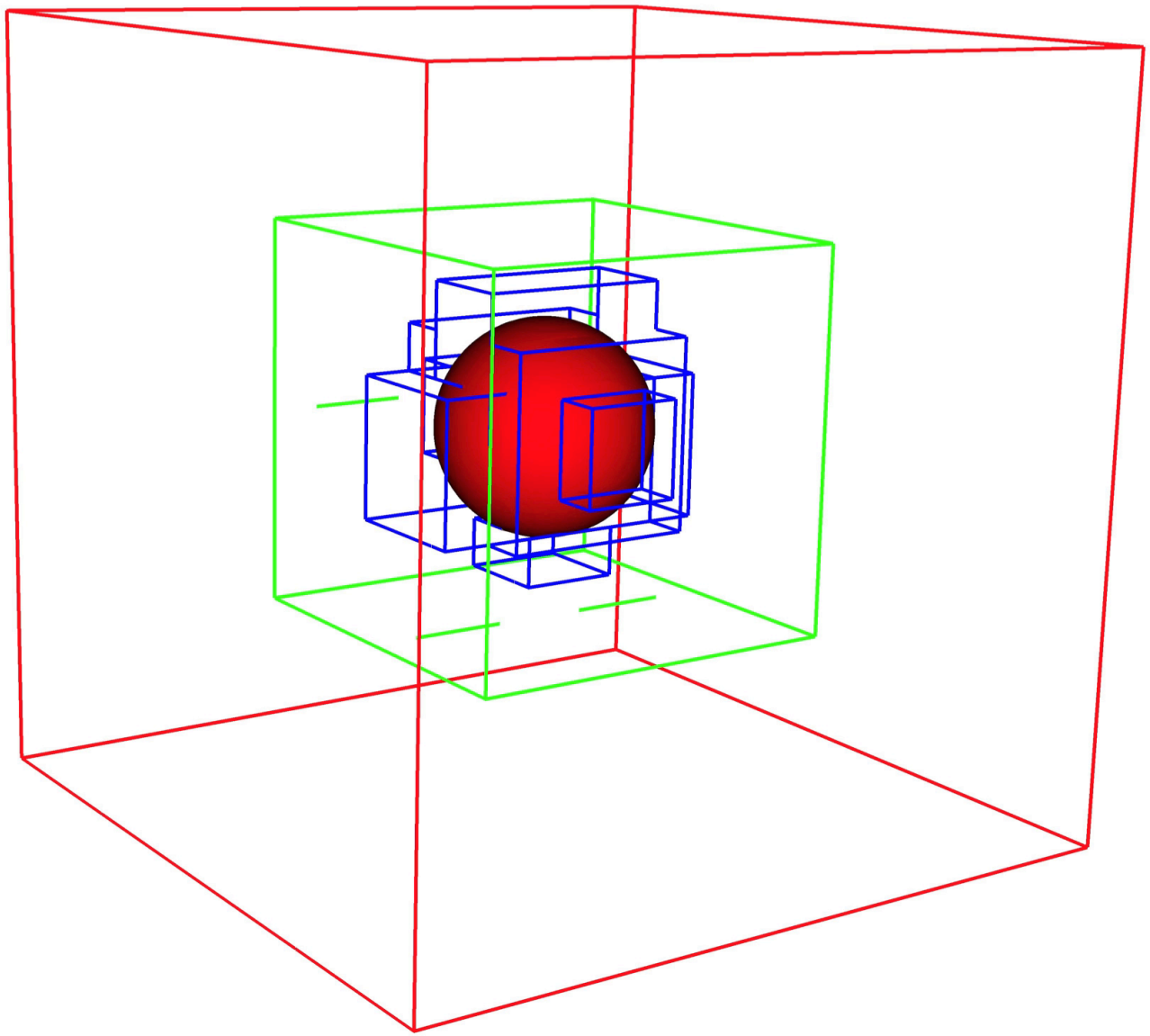
$$\frac{\partial \phi}{\partial t} + \nabla \cdot (\vec{u}\phi) = 0$$



What does AMReX do?

- Domain decomposition with distribution of grids to MPI processes
- Logical tiling of grids – reduce cache misses
- Support for multilevel mesh operations (coarsening/interpolation between different levels, ghost cell filling)
- Multigrid solvers for Poisson and Helmholtz equations
- Sub-cycling time-stepping algorithm
- Support for particles and particle-mesh operations

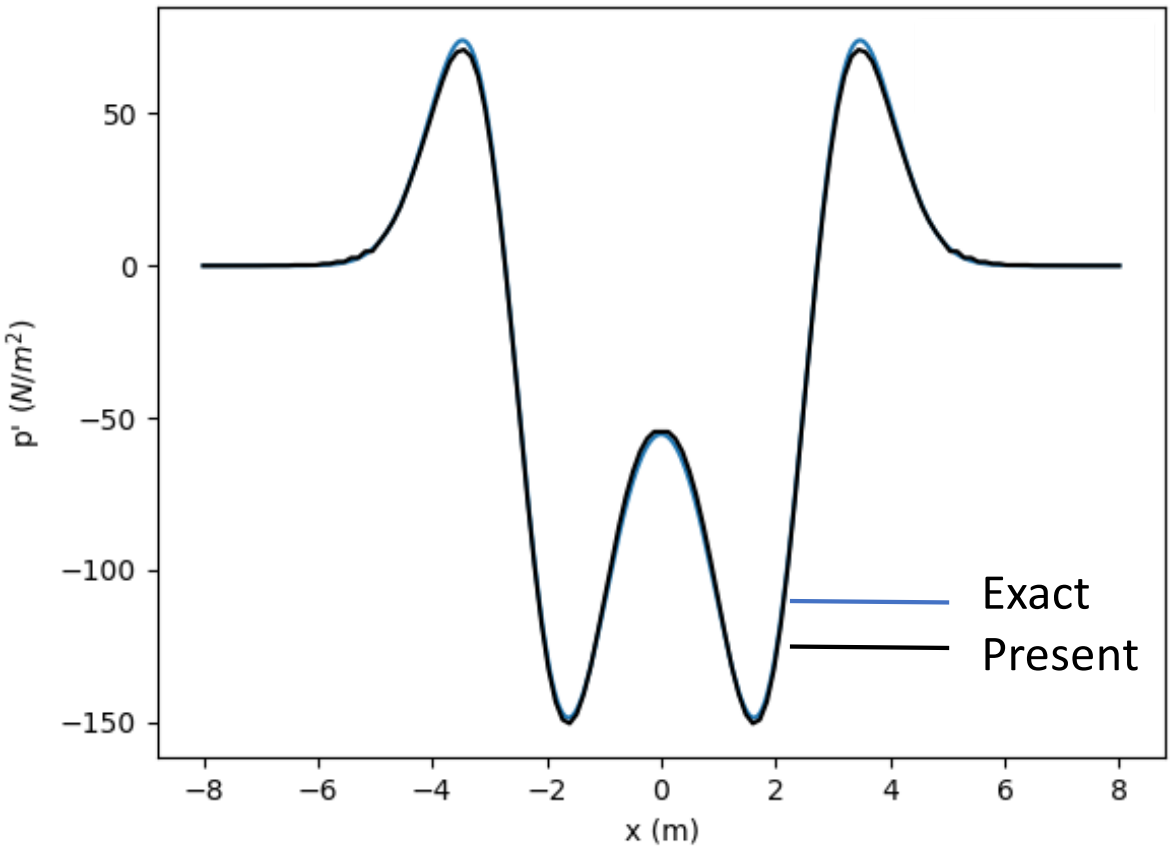
Acoustic Gaussian pulse



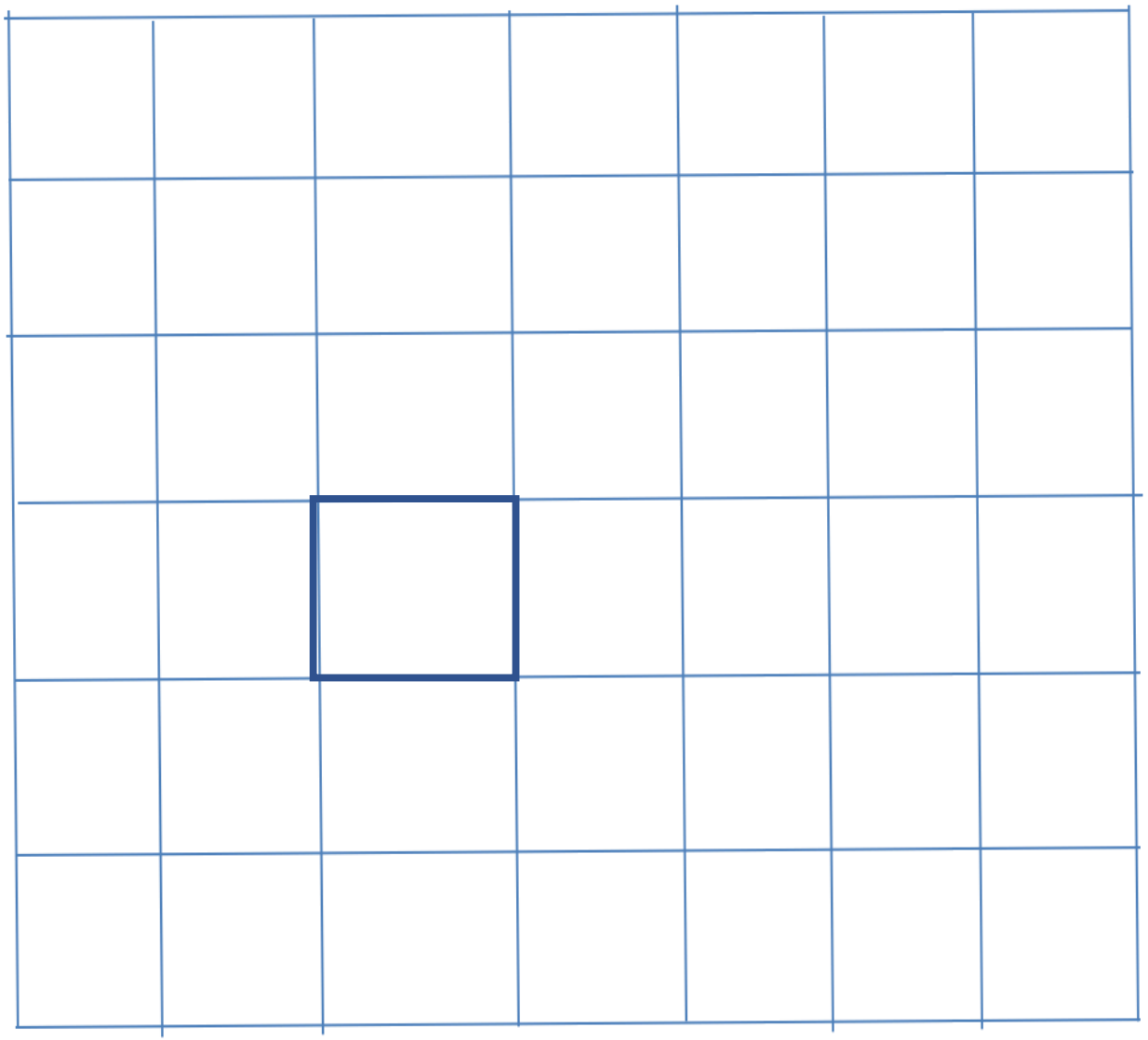
Acoustic Gaussian pulse

- Exact solution can be obtained from the Green's function method applied to the 3D wave equation for pressure

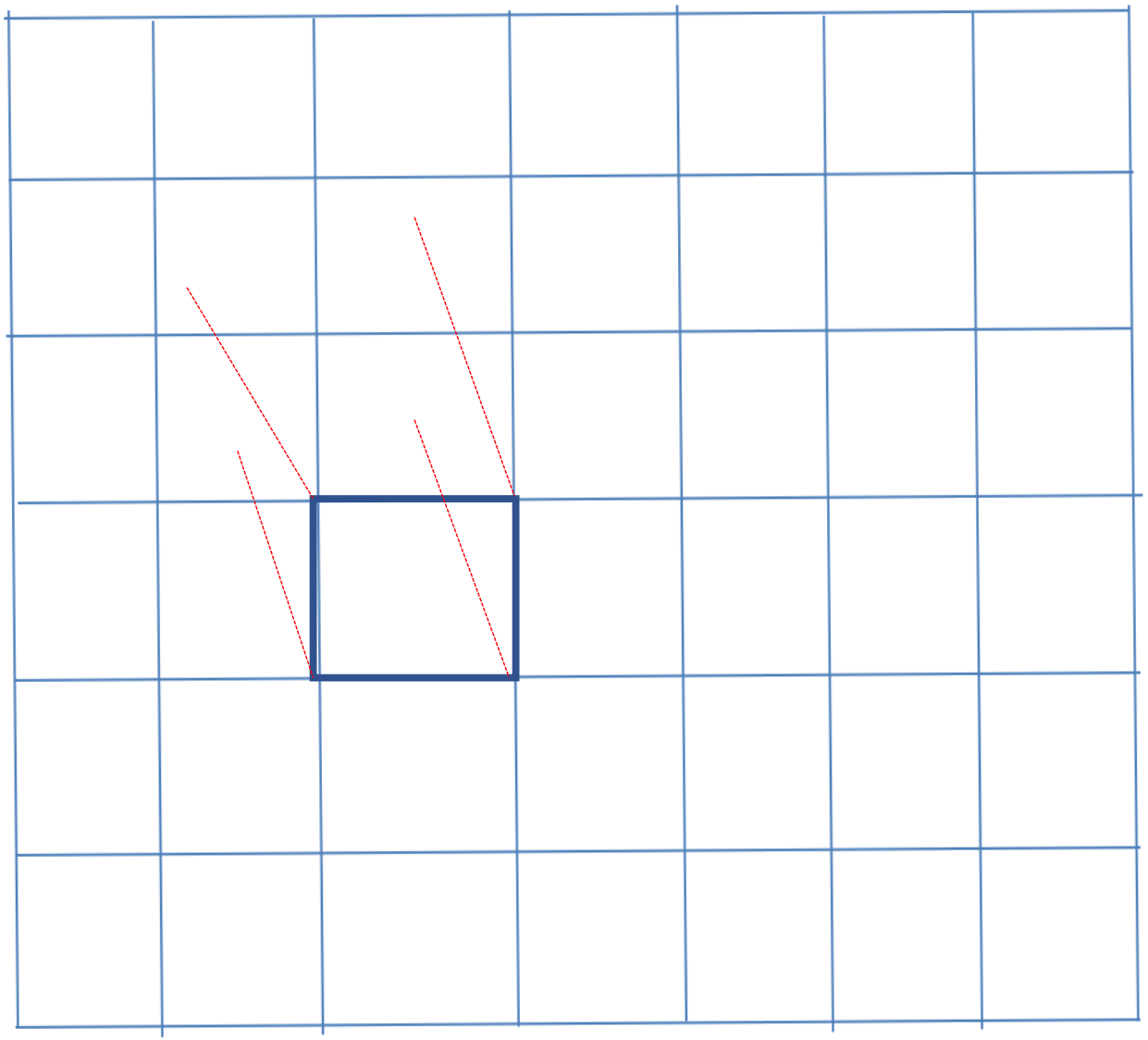
$$p'(r,t) = \frac{1}{2\alpha\sqrt{\pi\alpha}} \int_0^\infty \xi^2 e^{-\frac{\xi^2}{4\alpha}} \cos(c_0 t\xi) J_0(\xi r)\, d\xi$$



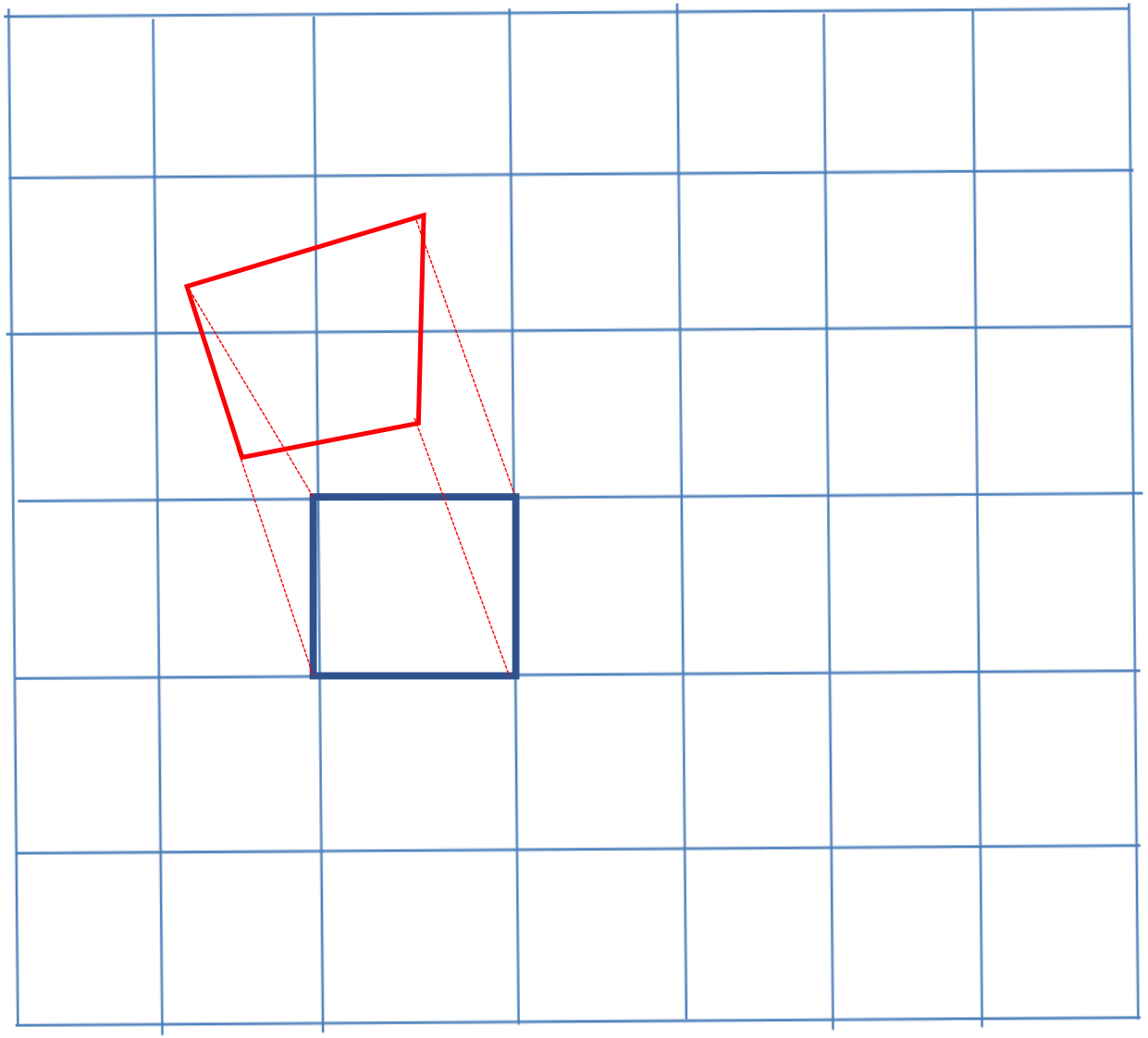
Semi Lagrangian advection



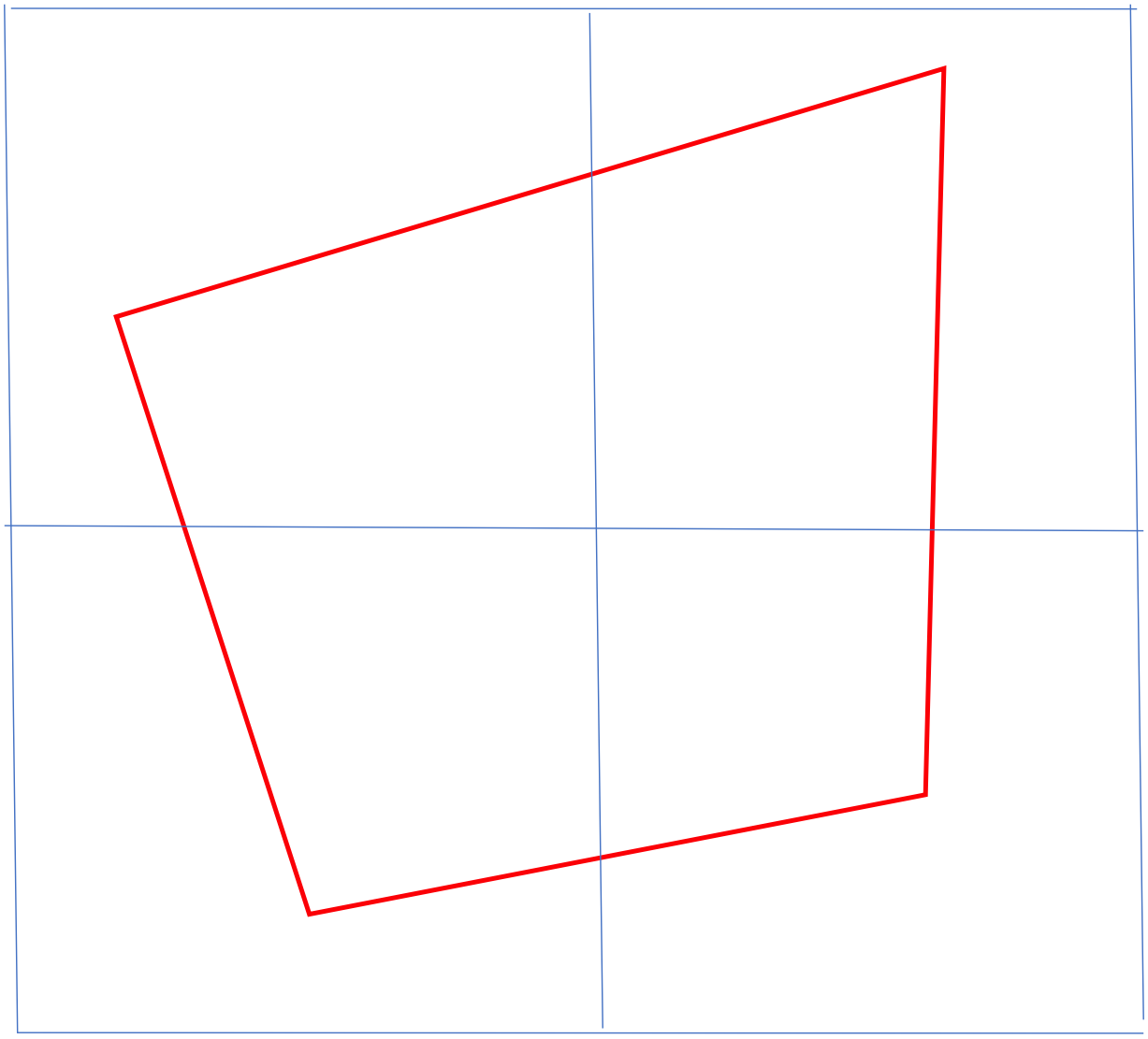
Semi Lagrangian advection



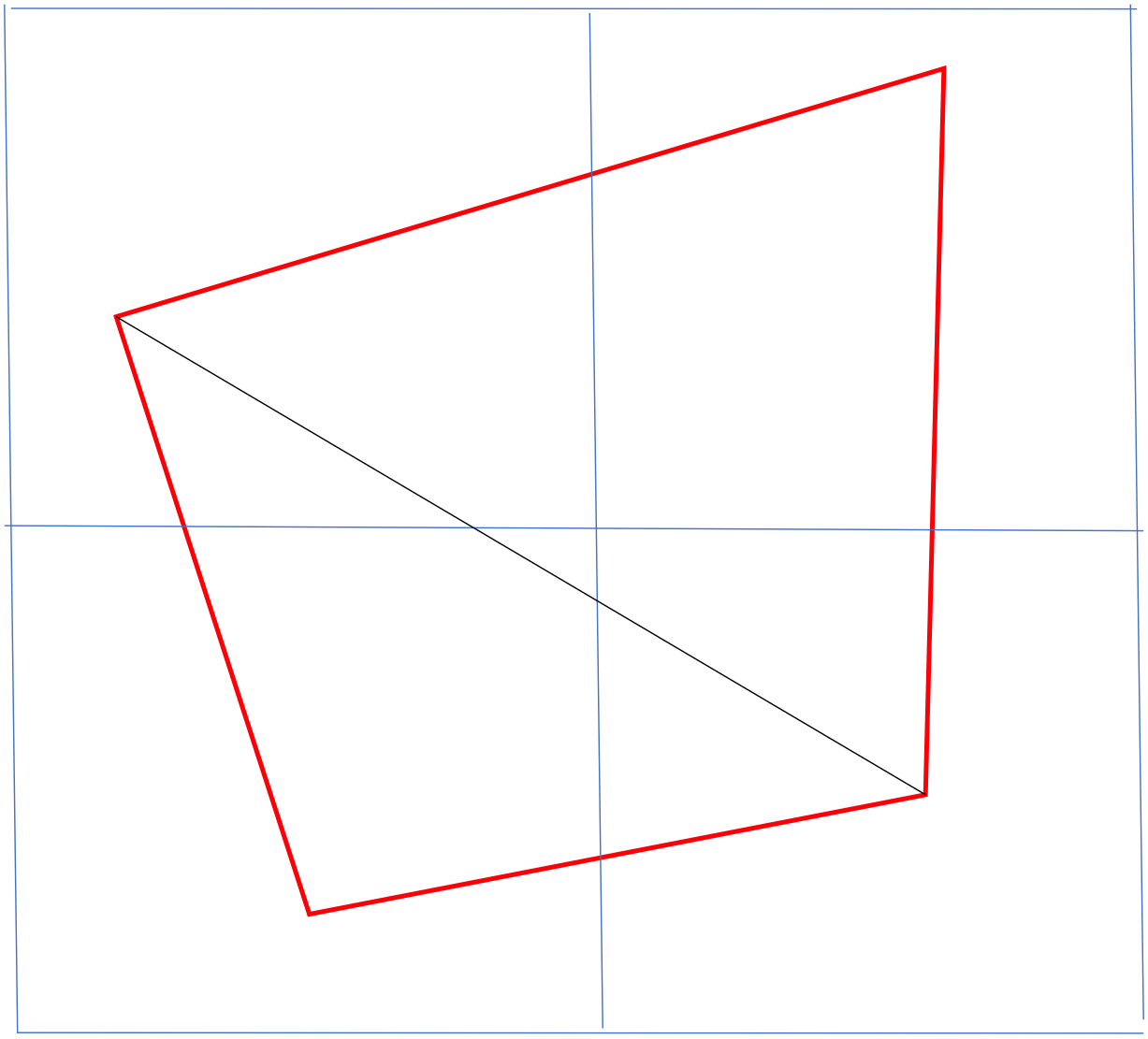
Semi Lagrangian advection



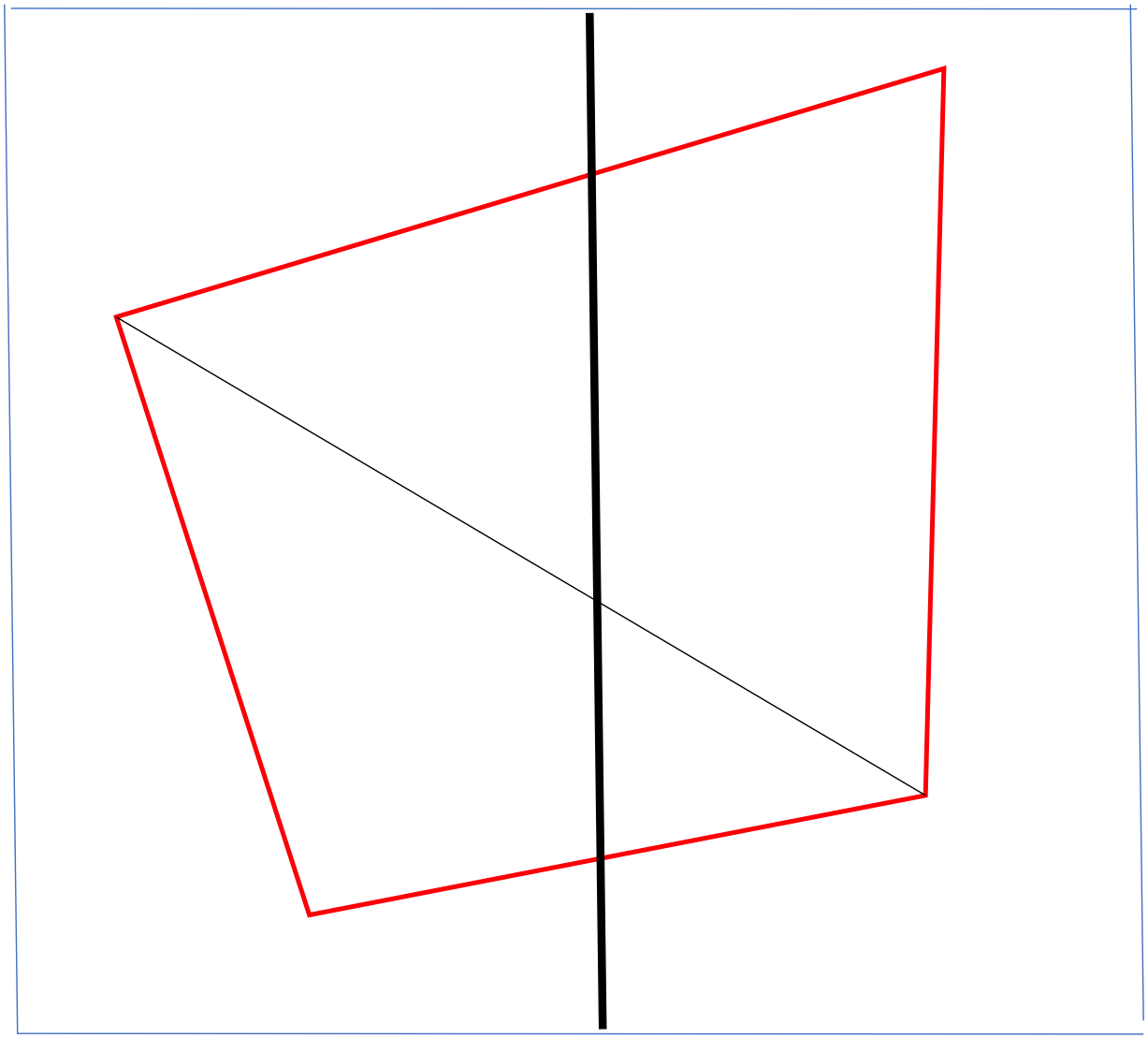
Simplex tessellation



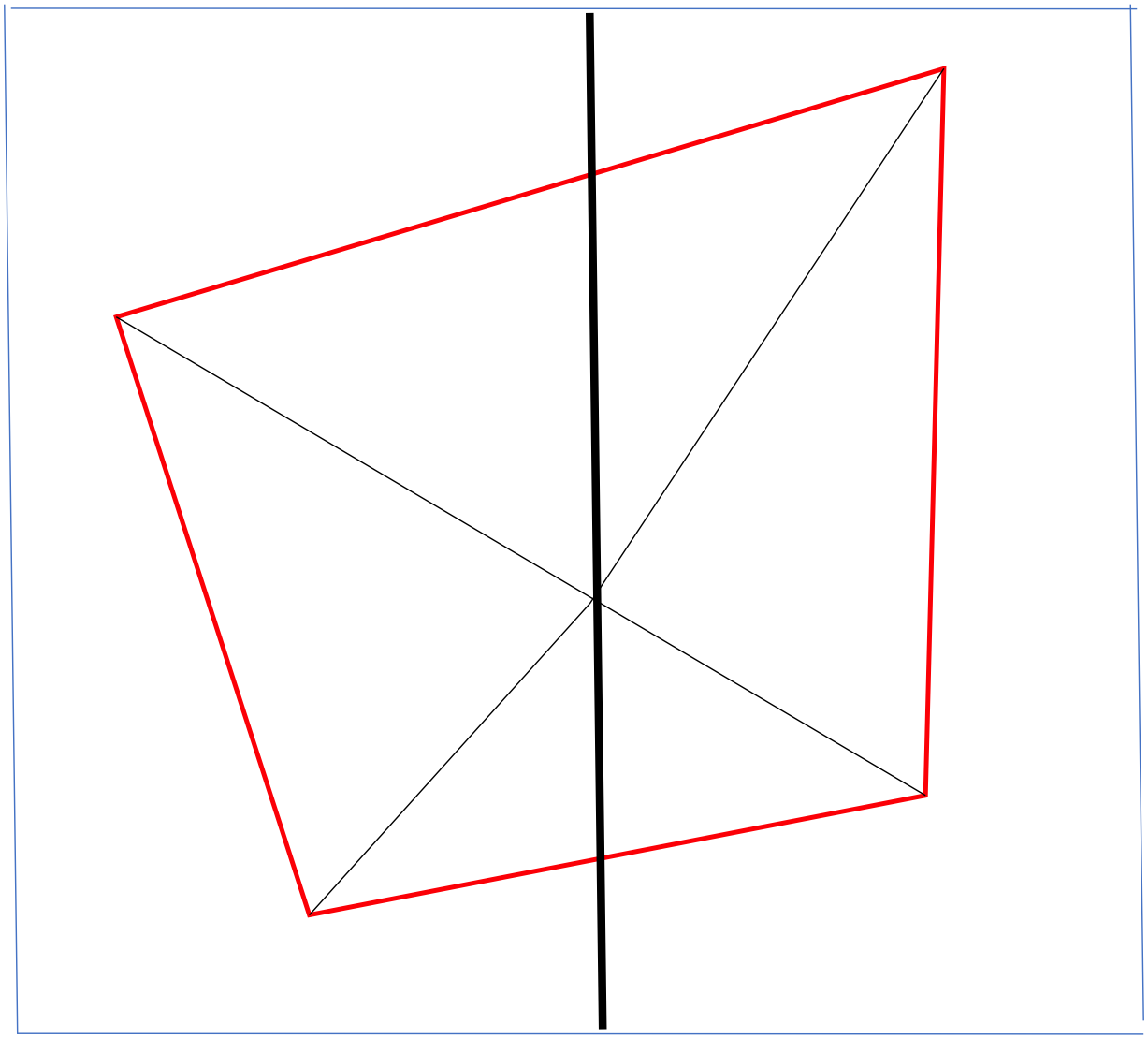
Simplex tessellation



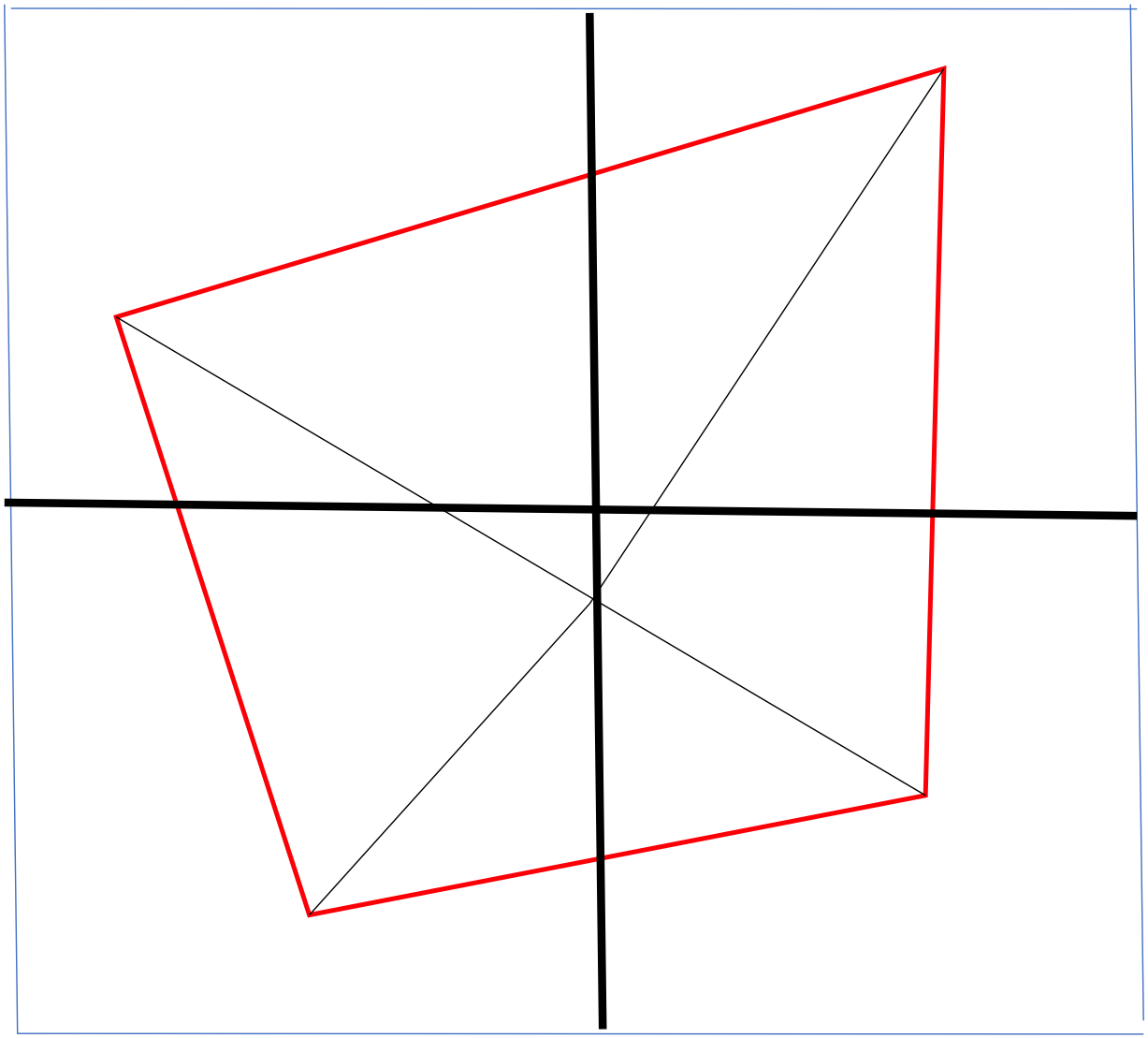
Simplex tessellation



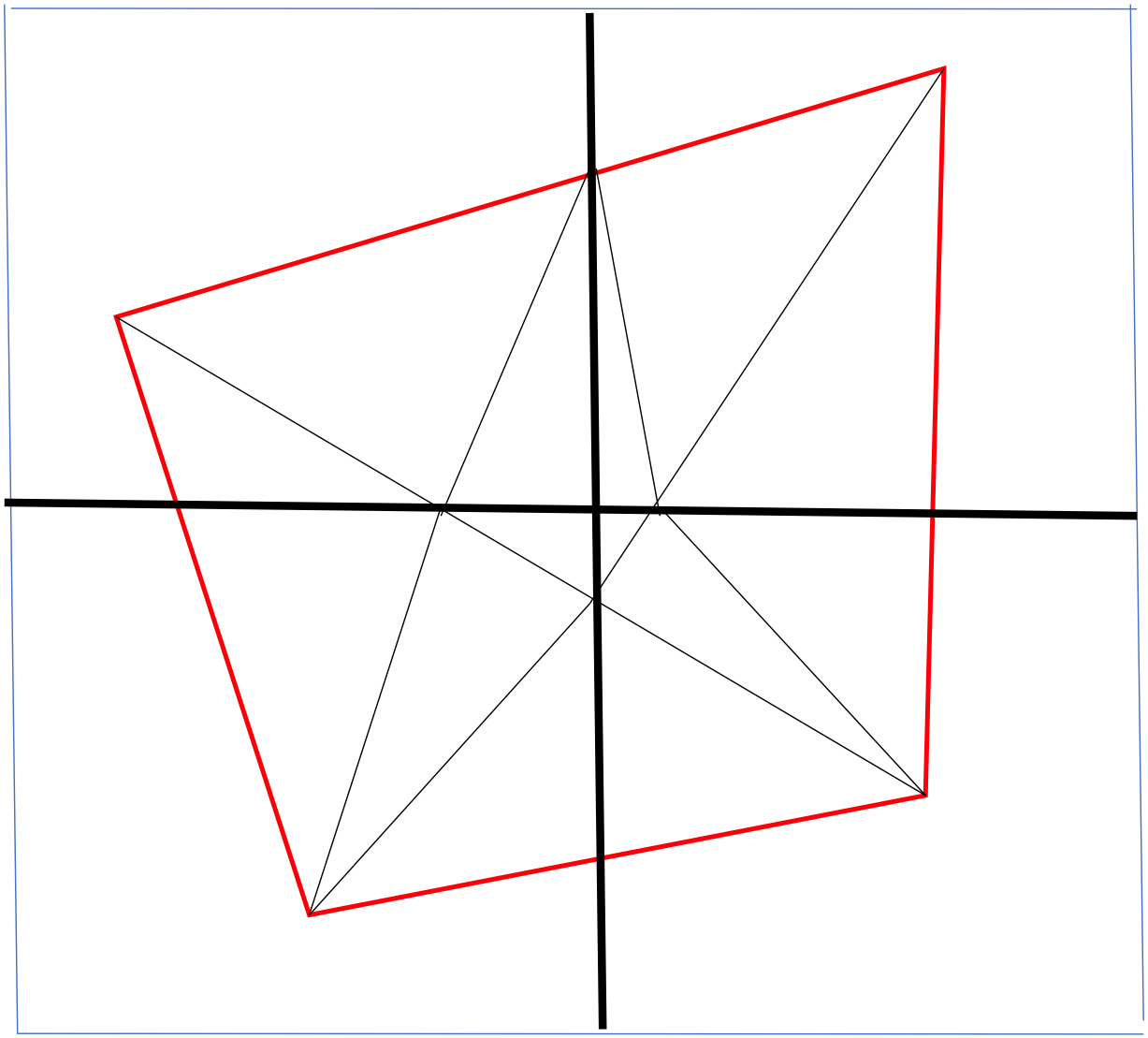
Simplex tessellation



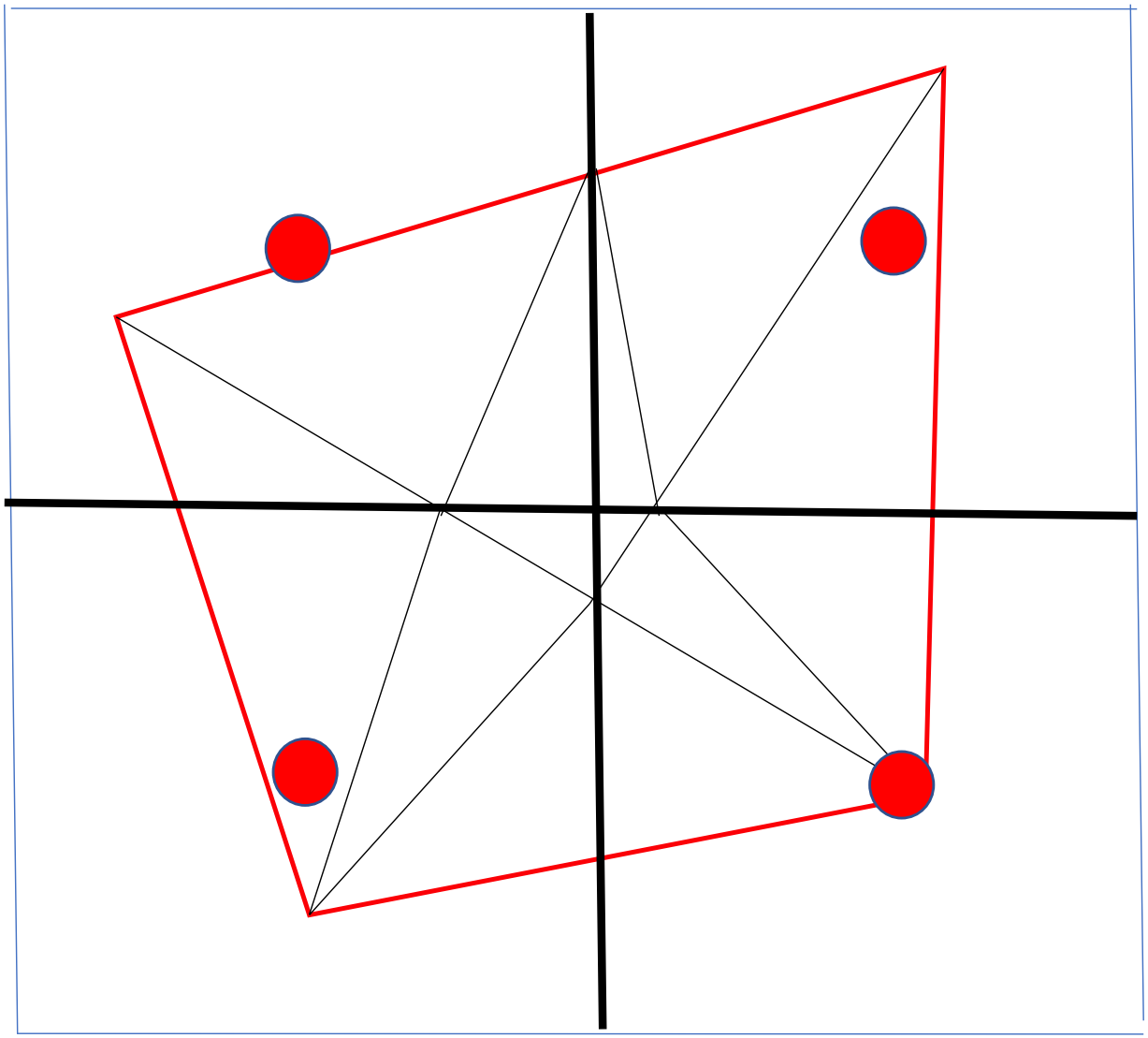
Simplex tessellation



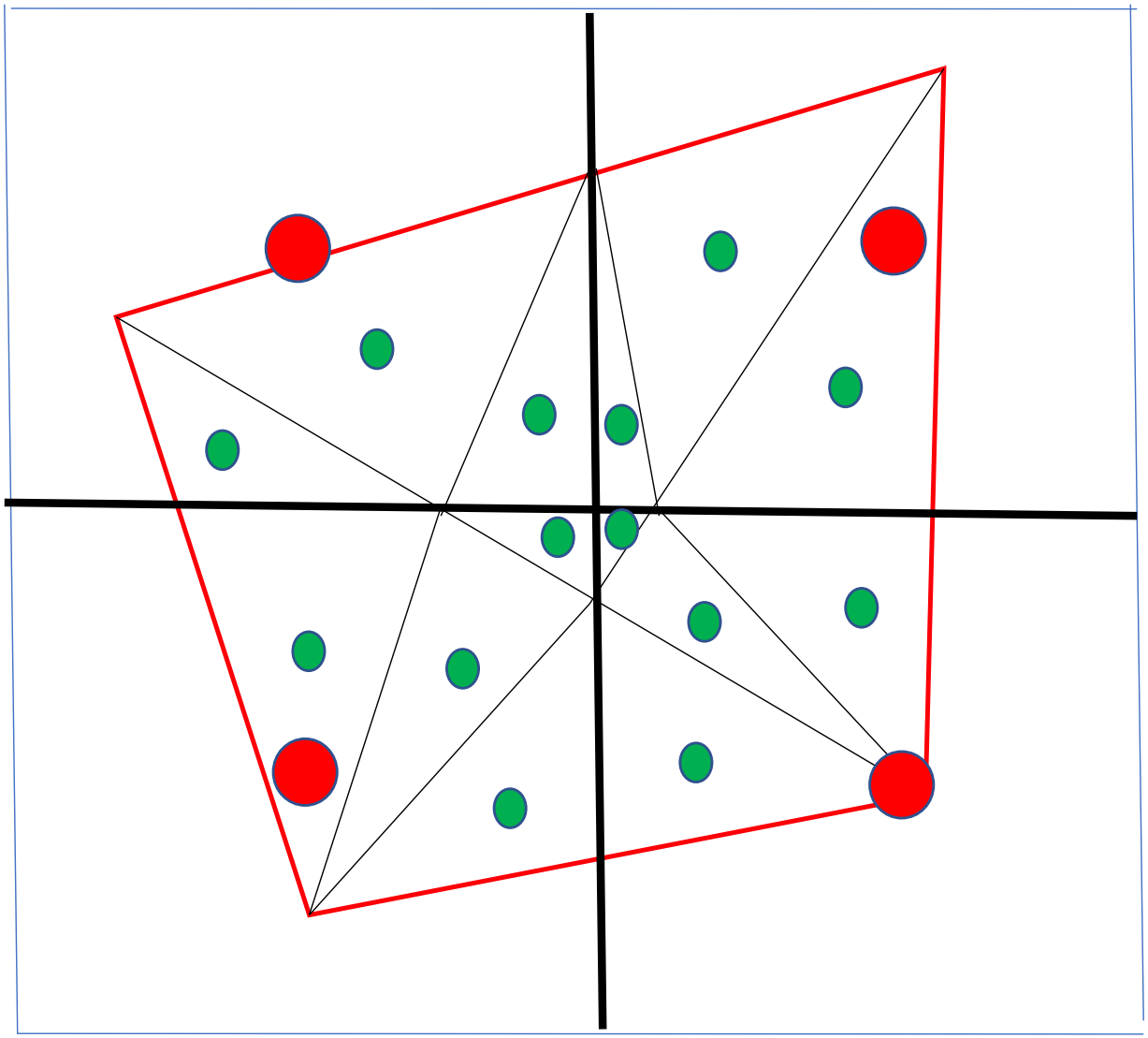
Simplex tessellation



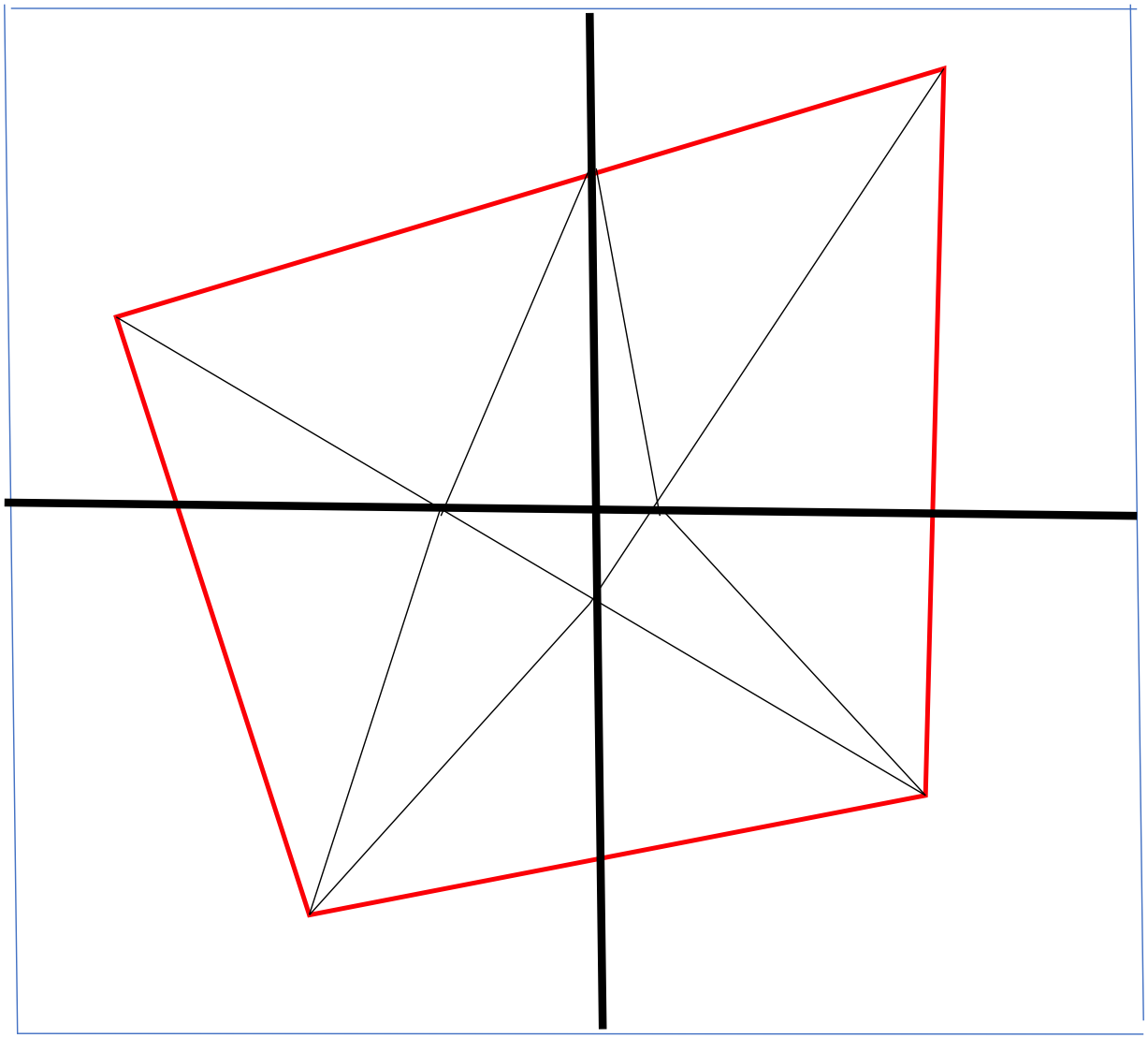
Simplex tessellation



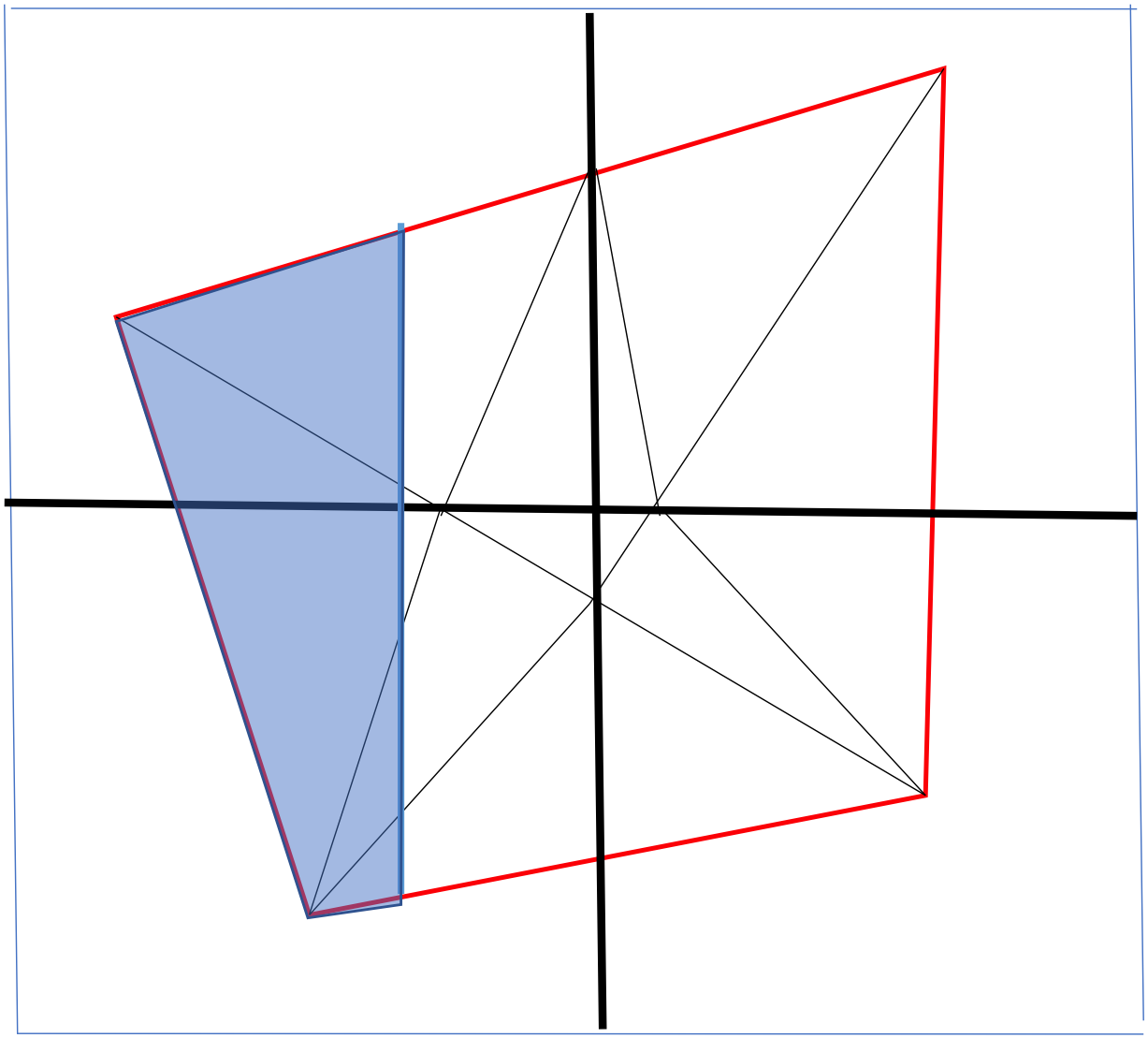
Simplex tessellation



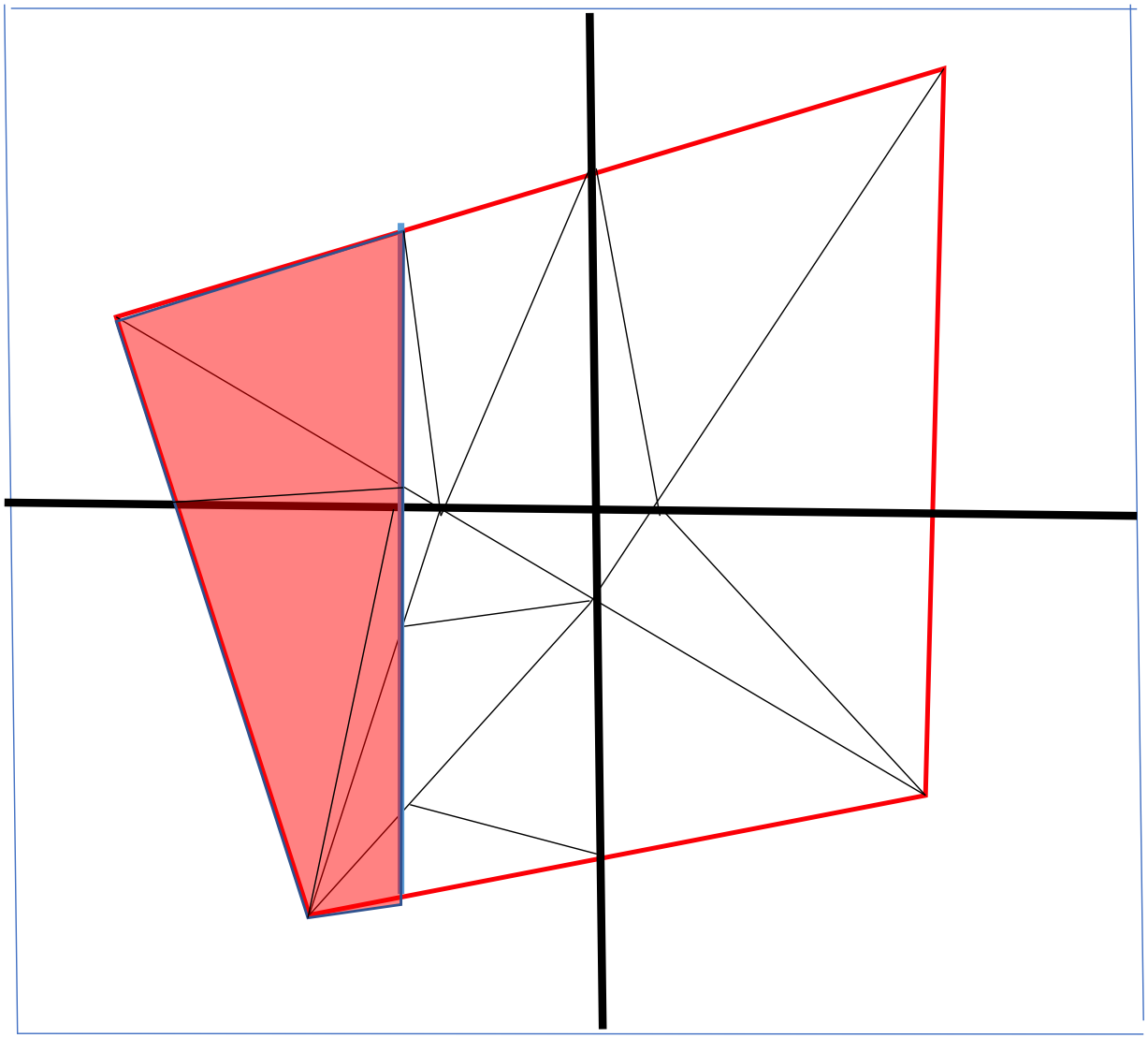
Simplex tessellation



Simplex tessellation



Simplex tessellation



Interface Reconstruction Library (IRL)

- https://gitlab.com/robertchiodi/interfacereconstructionlibrary
- Open-sourced under the MPL-2.0 license
- Interface reconstruction using PLIC
- Normals using ELVIRA, LVIRA
- Provide neighborhood information of mesh and VOF and get the interface plane

```
call reconstructionWithELVIRA3D(neighborhood,liquid_gas_interface(i,j,k))
```

- Simplex tessellation
- Create flux polyhedron, linkage information and get volumes and centroids

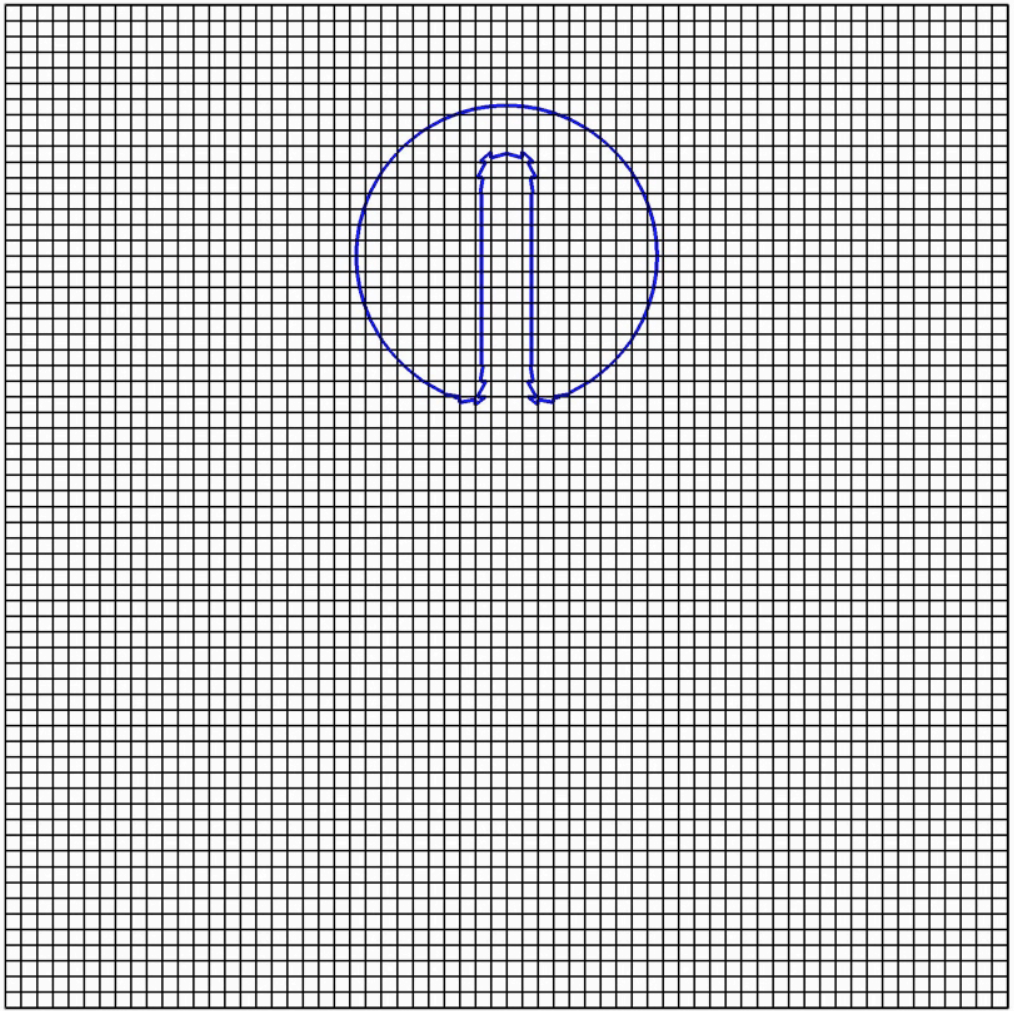
```
call signedGenericCutting(fluxpolyhedron,linkage,volumes_and_centroids)
```

- Multi-plane reconstruction for thin structures

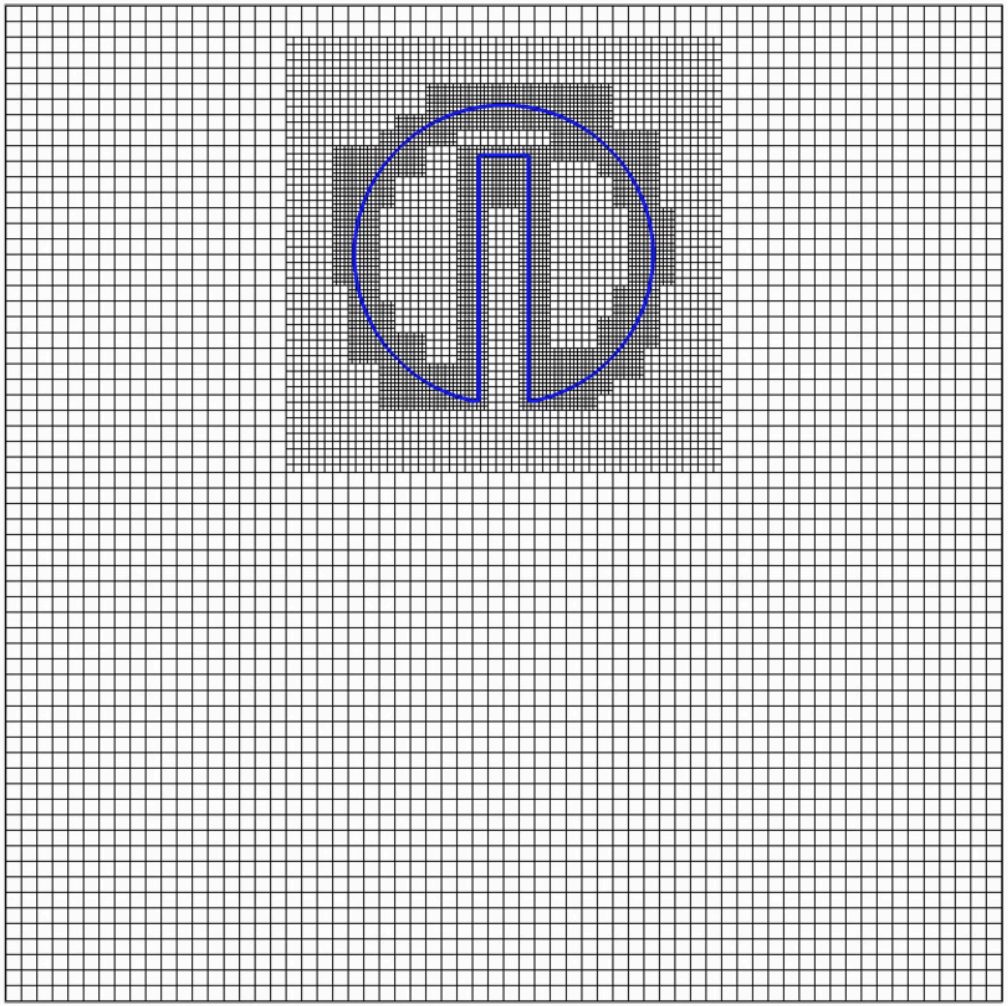
Zalesak's disk

$$\frac{\partial \alpha}{\partial t} + \vec{u} \cdot \nabla \alpha = 0$$

64x64

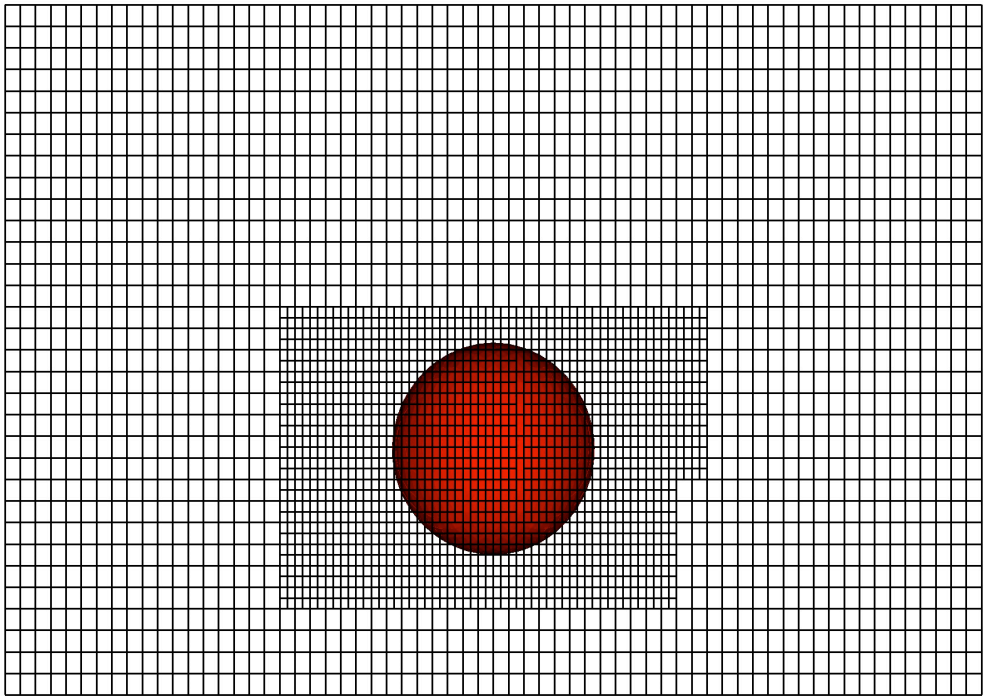


64x64 – 2 level

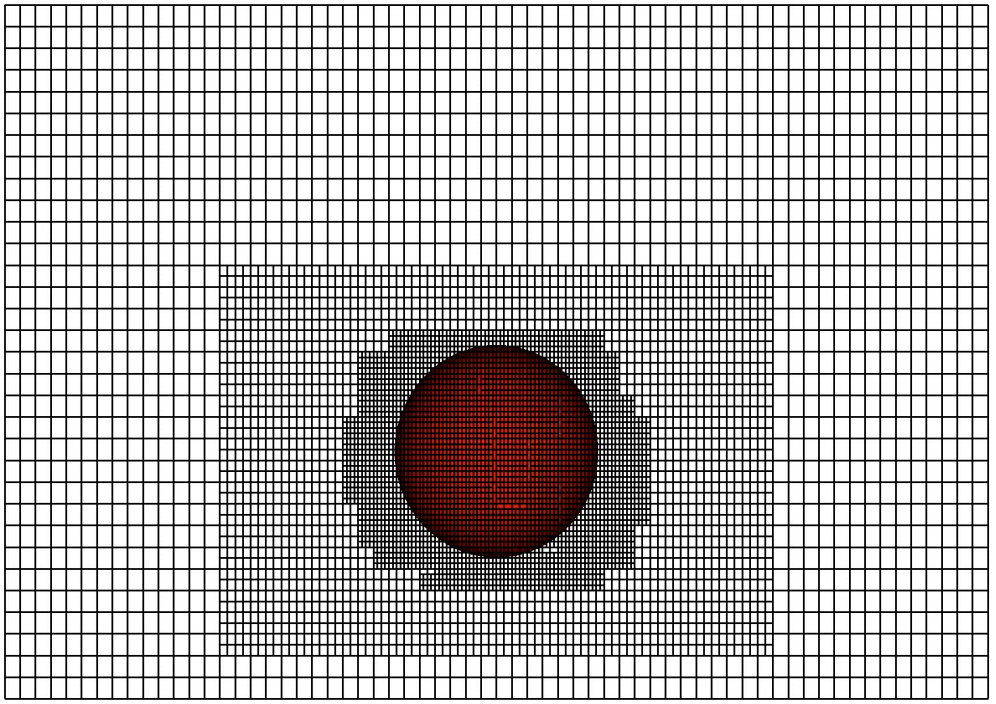


3D Deformation

32x32x32 – 1 level



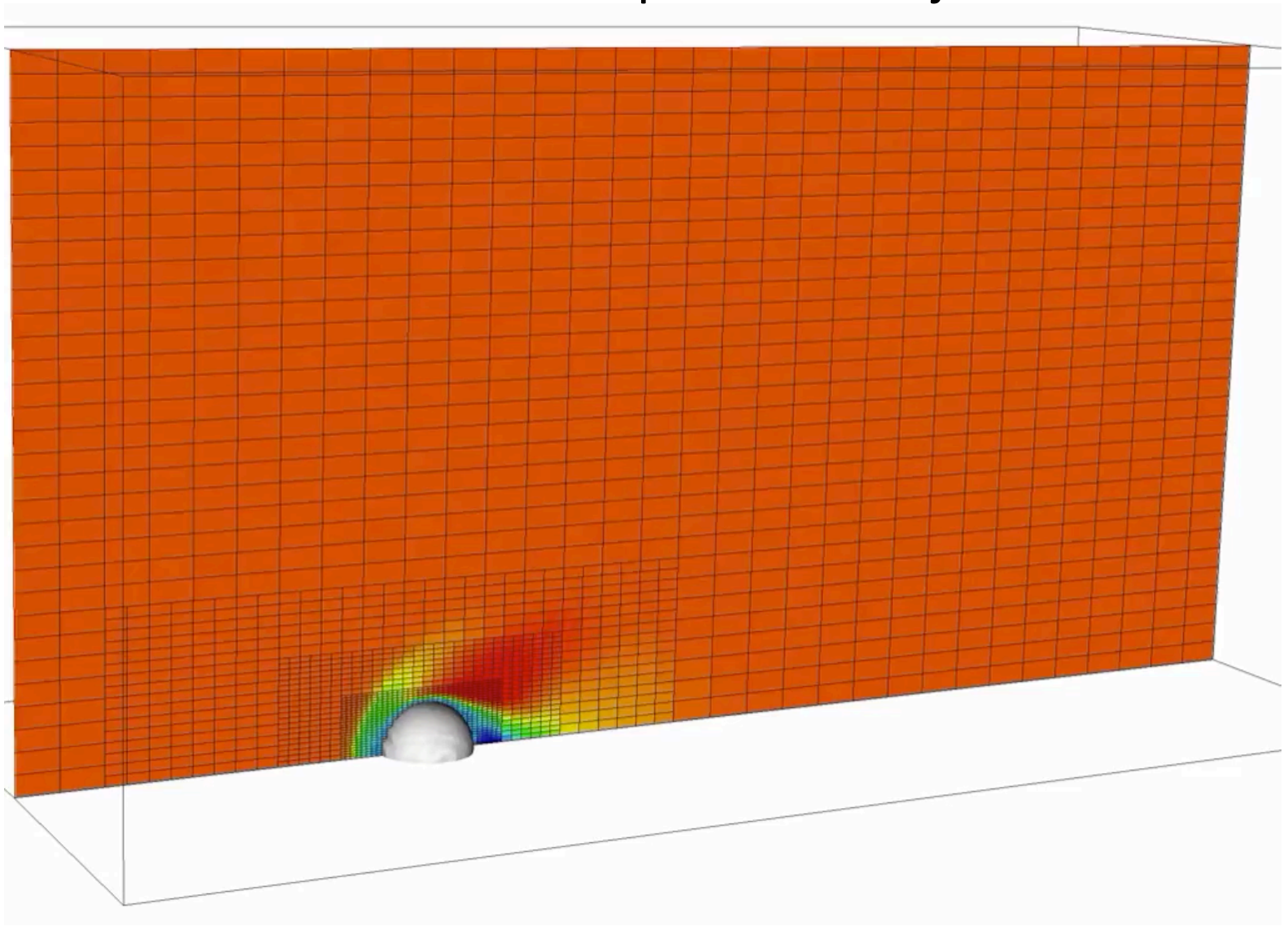
32x32x32 – 2 level



Liquid jet in supersonic crossflow

Fuel atomization in scramjet engines (Funded by AFRL)

- Mach 1.94 crossflow of air with a 1 mm dia., 20 m/s water jet
- 3 levels of refinement – 18 points in the jet diameter



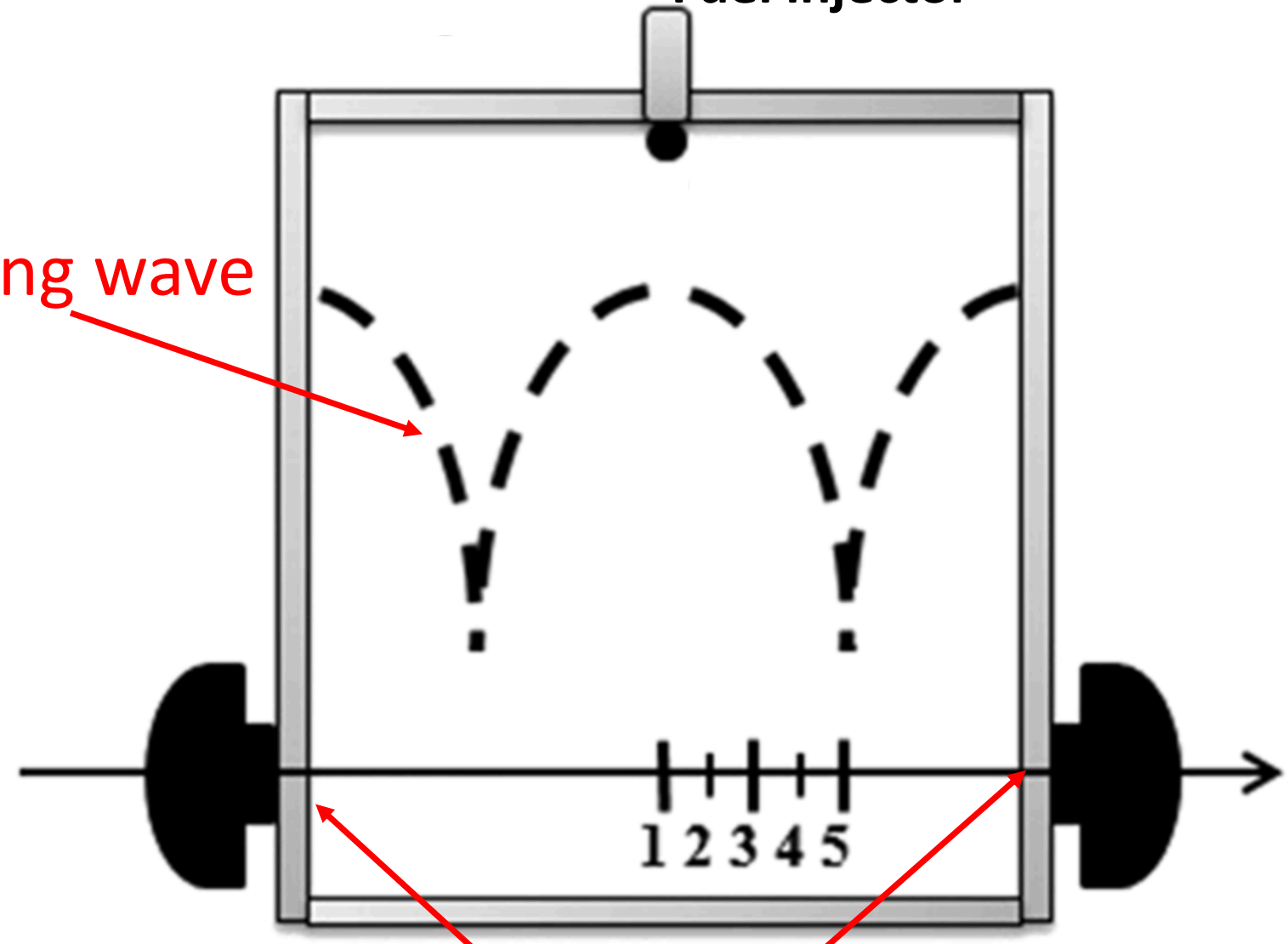
Liquid jet in supersonic crossflow

Fuel atomization in scramjet engines (Funded by AFRL)

- Mach 1.94 crossflow of air with a 1 mm dia., 20 m/s water jet
- 3 levels of refinement – 18 points in the jet diameter



Spray control with acoustic excitation



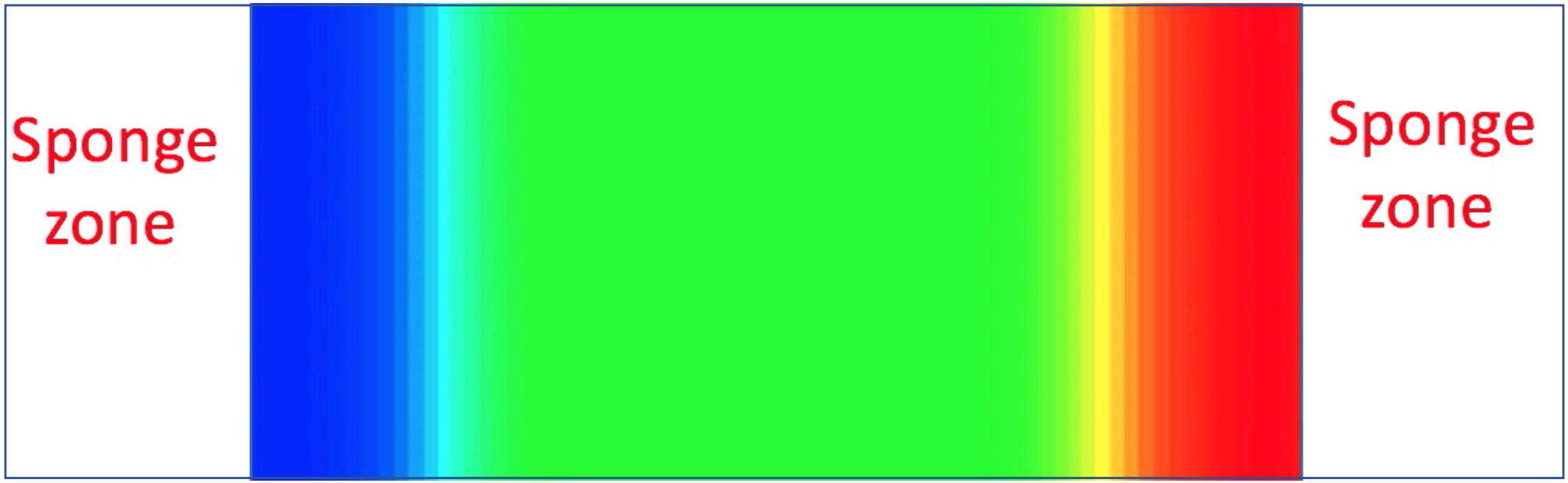
Ficuciello et. al. (2017)

Spray control with acoustic excitation

$$\frac{\partial \mathbf{Q}}{\partial t} = \mathrm{RHS} - A_{\mathrm{sponge}}\xi^2(\mathbf{Q} - \mathbf{Q}_{\mathrm{target}}) \quad \xi \to 0 \text{ to } 1$$

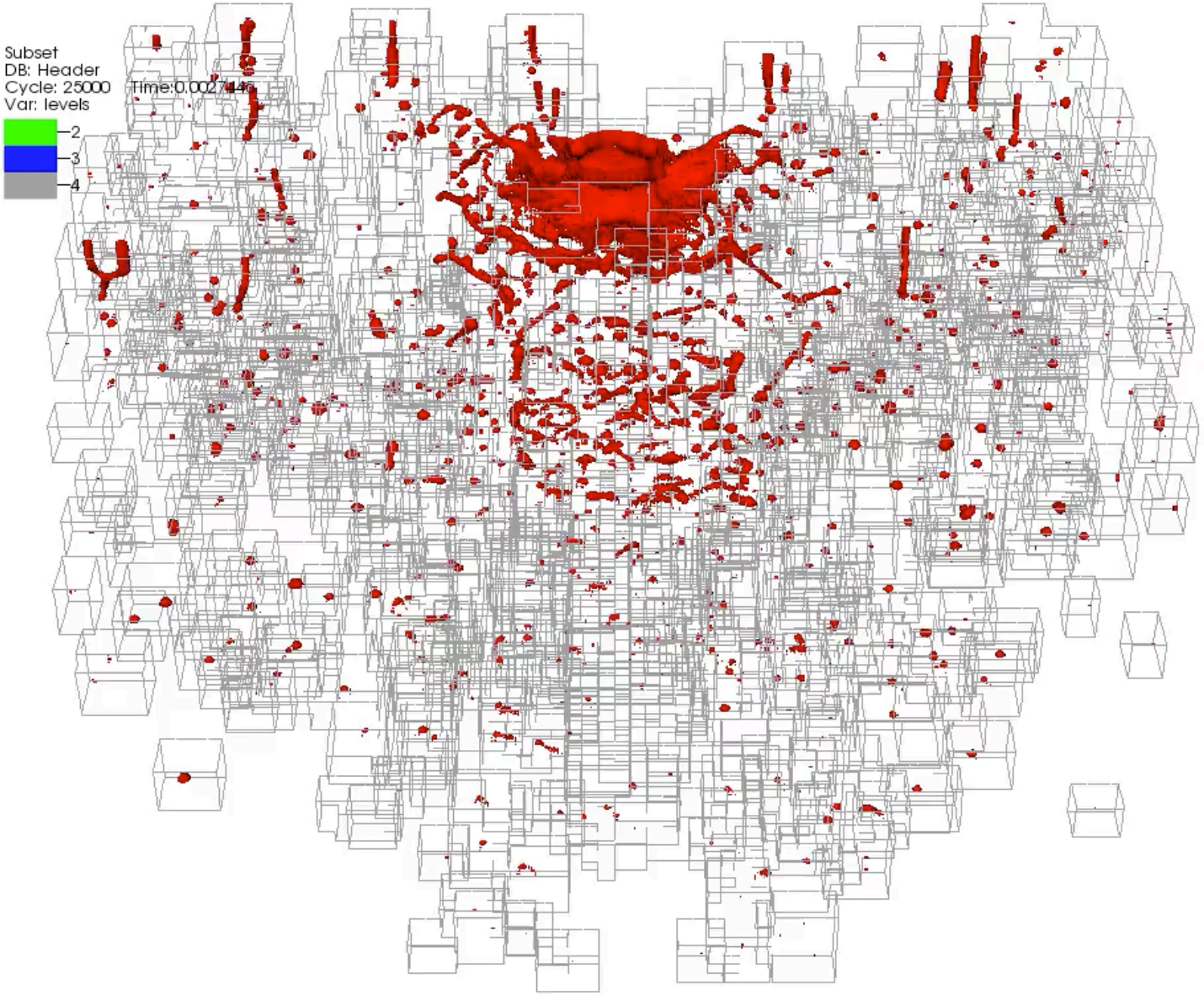
$$(p'_{\mathrm{target}}, \rho'_{\mathrm{target}}, u'_{\mathrm{target}}) = \left(p_{\max} \sin\left(\frac{2\pi}{\lambda} x - \omega t + \phi \right), \frac{p}{c_0^2}, u_0 + \frac{p'}{\rho_0 c_0} \right)$$

- Pmax = 12kPa, corresponds to a sound pressure level of 172 dB
- Non-linear acoustic excitation



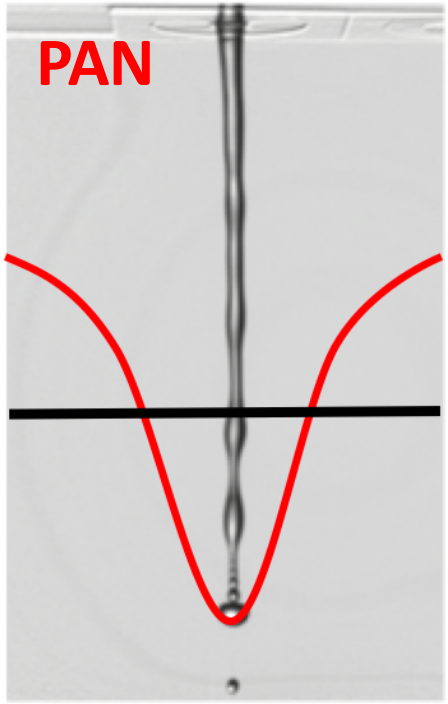
Spray control with acoustic excitation

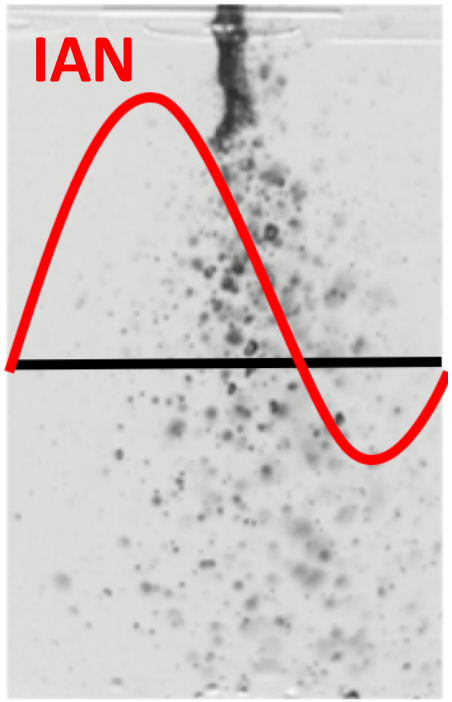
- 3 levels of refinement with all cells with an interface tagged

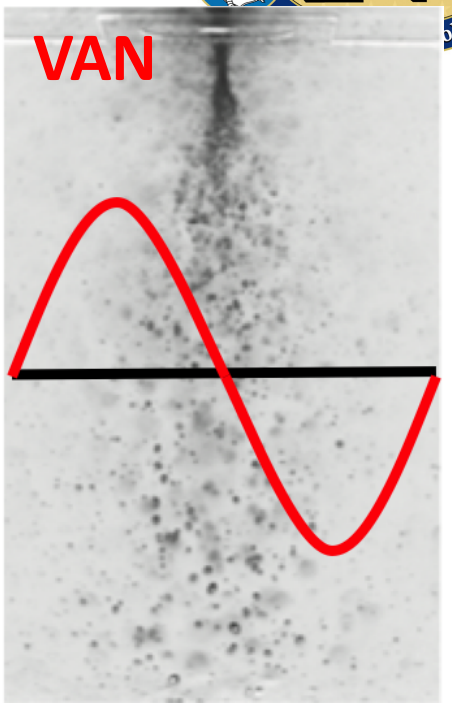


Spray atomization control

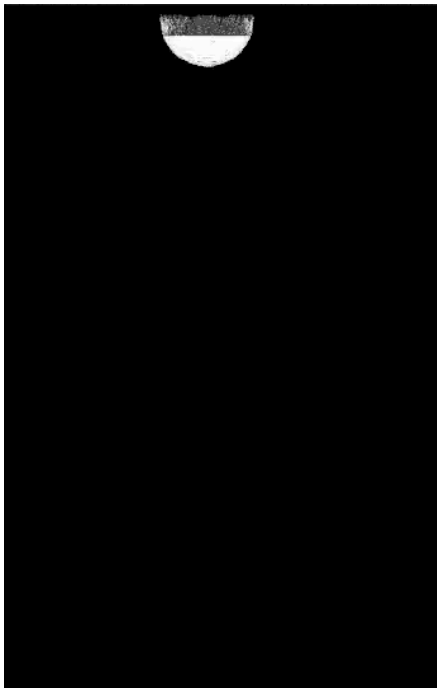
Experiments
(Ficuciello et al.)

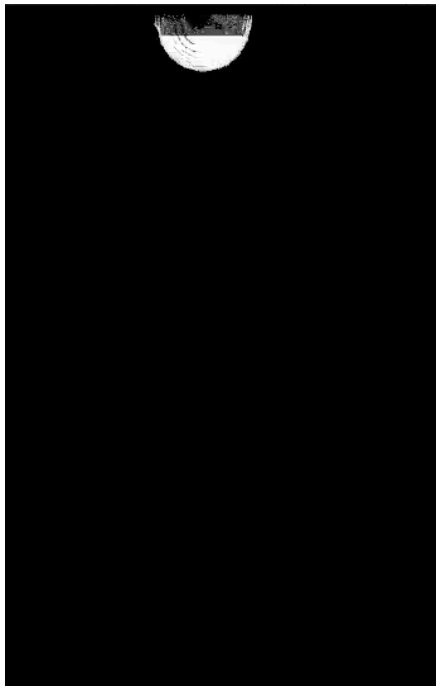


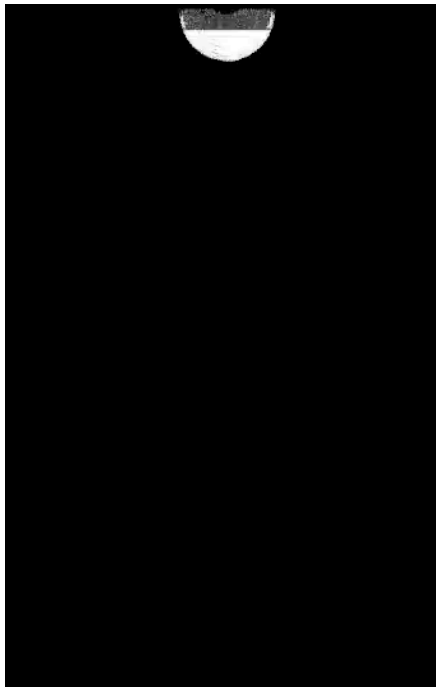




Simulation

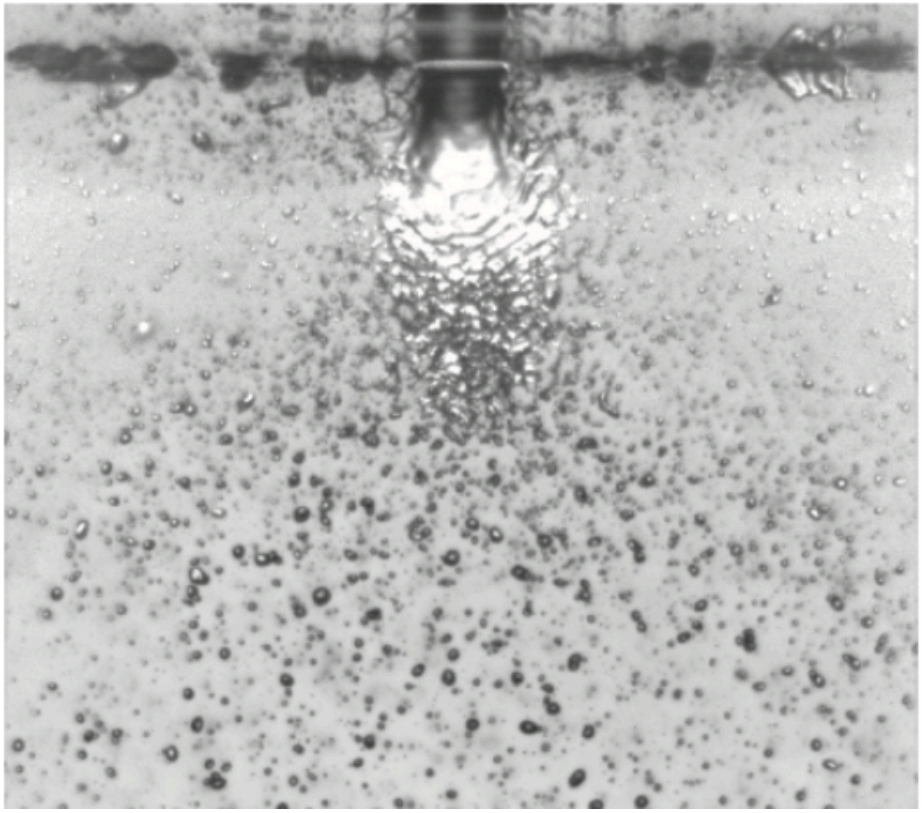




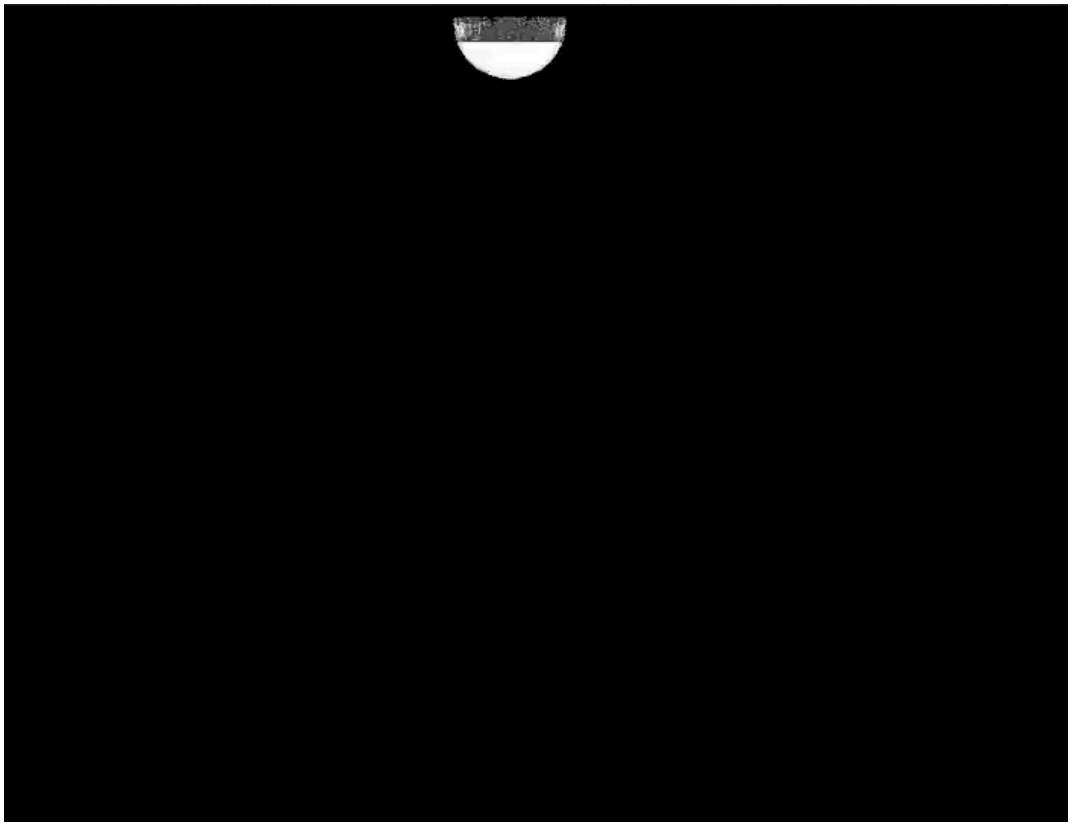


Spray control with acoustic excitation

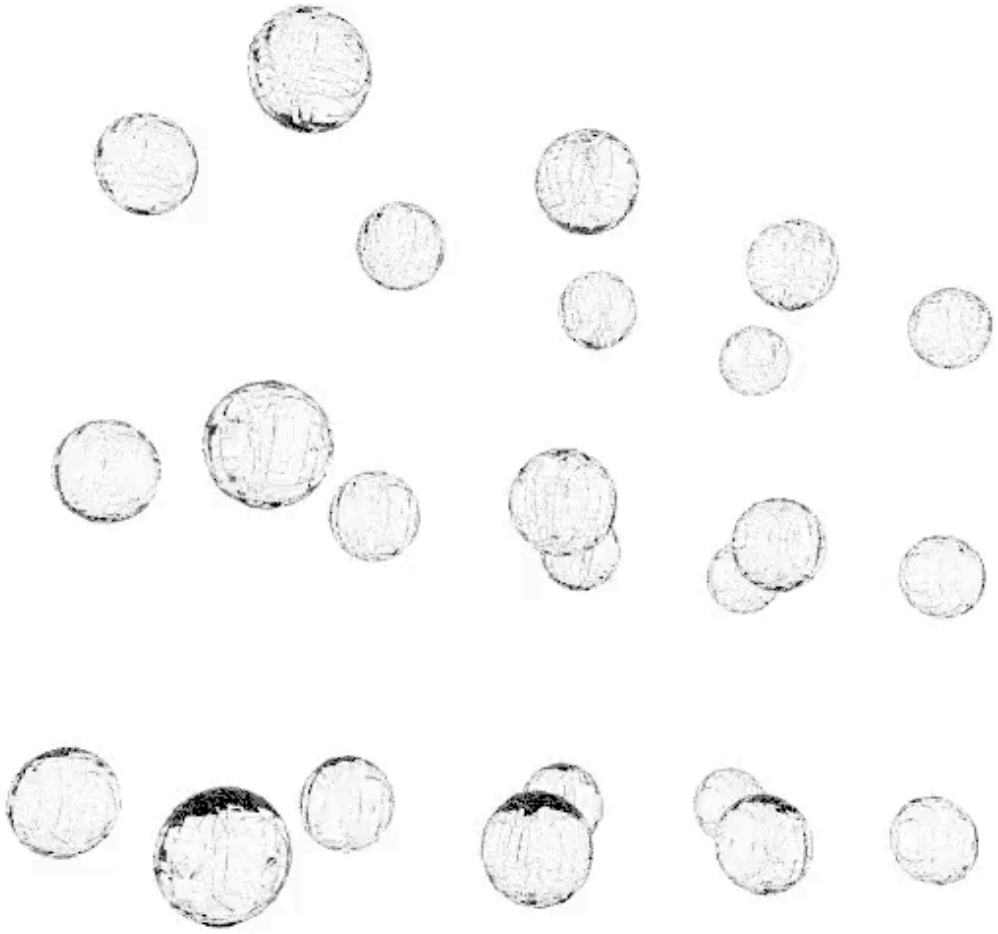
Experiment (Ficuciello et al.)

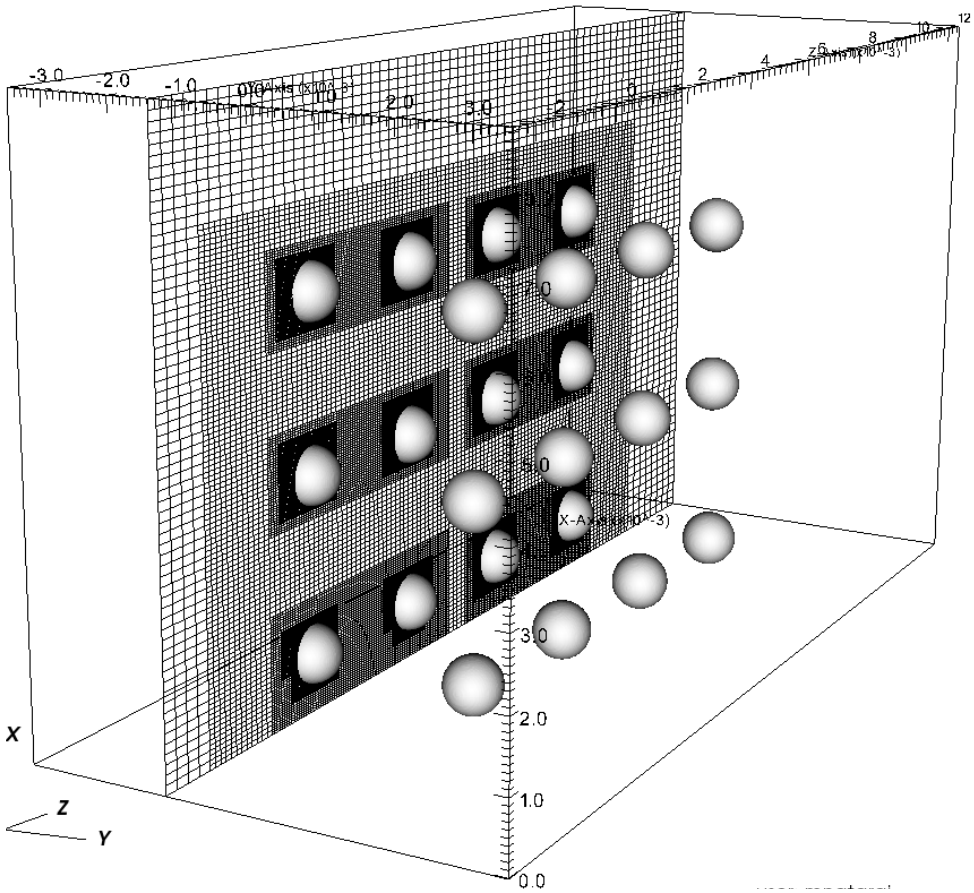


Simulation



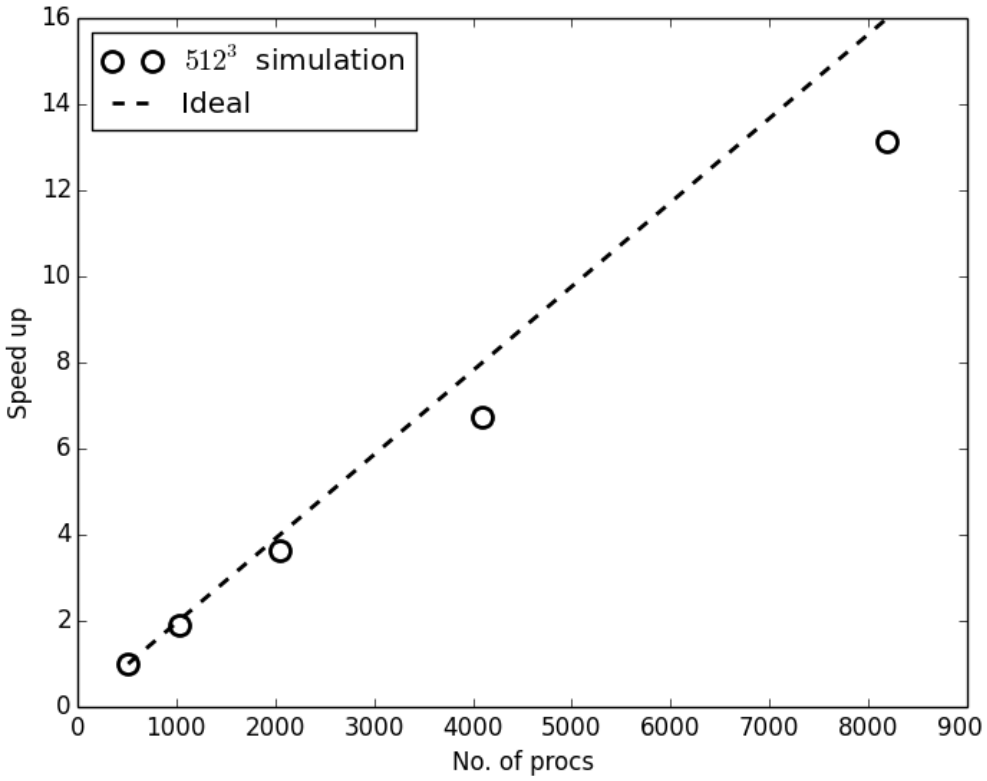
Performance on Stampede2 KNL nodes



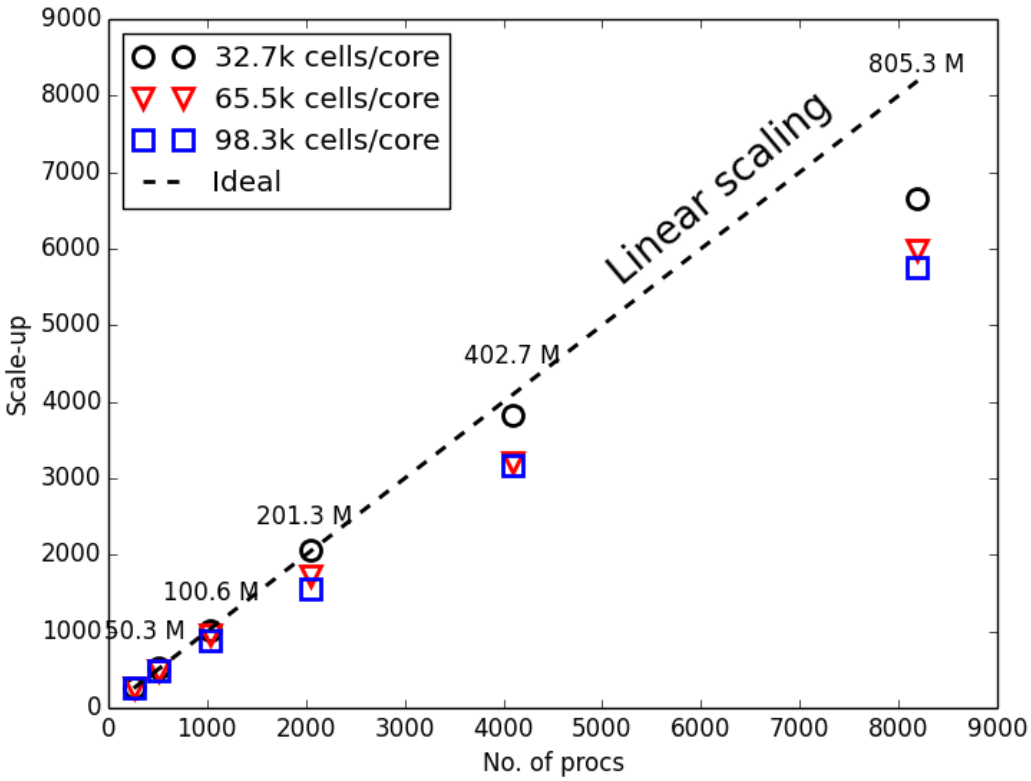


Performance on Stampede2 KNL nodes

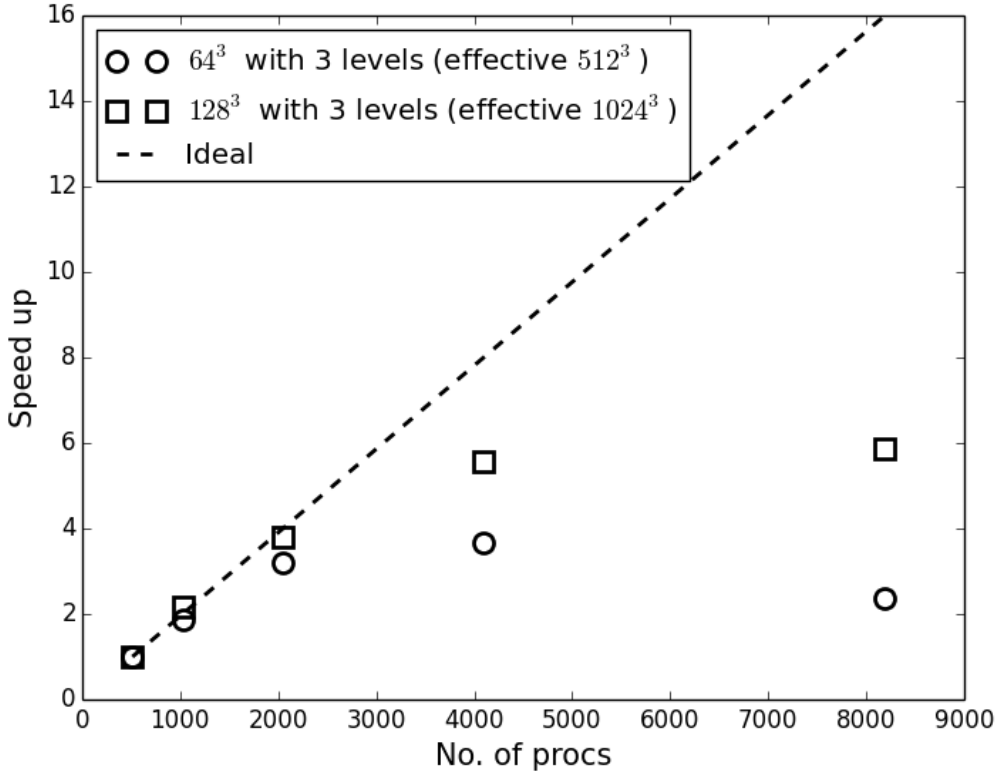
Strong scaling

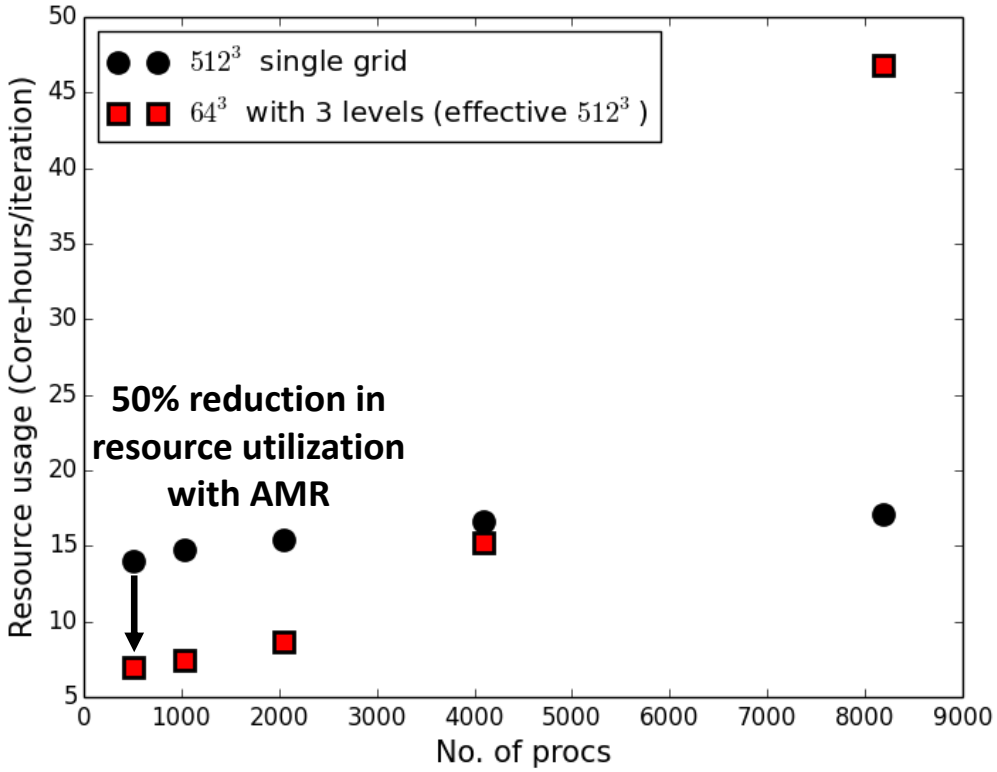


Weak scaling



Performance on Stampede2 KNL nodes









Questions?

This work was sponsored by the Office of Naval Research (ONR) as part of the Multidisciplinary University Research Initiatives (MURI) Program, under grant number N00014-16-1-2617. The views and conclusions contained herein are those of the authors only and should not be interpreted as representing those of ONR, the U.S. Navy or the U.S. Government.